Overcoming and preventing bacterial resistance to antibiotics: The development and characterization of novel RNA polymerase and PqsD inhibitors

Dissertation

zur Erlangung des Grades

des Doktors der Naturwissenschaften

der Naturwissenschaftlich-Technischen Fakultät III

Chemie, Pharmazie, Bio- und Werkstoffwissenschaften

der Universität des Saarlandes

von

Stefan Hinsberger

Saarbrücken

2014

Tag des Kolloquiums:	28.11.2014
Dekan:	Prof. Dr.-Ing. Dirk Bähre
Berichterstatter:	Prof. Dr. Rolf W. Hartmann
	Prof. Dr. Uli Kazmaier
Vorsitz:	Prof. Dr. Claus-Michael Lehr
Akad. Mitarbeiter:	Dr. Jessica Hoppstädter

Die vorliegende Arbeit wurde unter Anleitung von Herrn Prof. Dr. Rolf W. Hartmann in der Fachrichtung 8.2 Pharmazeutische und Medizinische Chemie der Naturwissenschaftlich-Technischen Fakultät III der Universität des Saarlandes von Januar 2011 bis August 2014 angefertigt.

„Thus, the task is, not so much to see what no one has yet seen; but to think what nobody has yet thought, about that which everybody sees.“

Erwin Schrödinger

Summary

The treatment of bacterial infections is seriously hampered by the prevalence of resistance to clinically used antibiotics. Thus, there is an urgent need for the development of novel anti-infectives which are able to overcome existing resistances and do not provoke the quick emergence of new ones.

In this work, an approach comprising a pharmacophore guided virtual screening is applied to identify novel scaffolds inhibiting the validated bacterial target RNA polymerase (RNAP). Structural modifications of the discovered hits result in potent RNAP inhibitors, which are active against Gram-positive pathogens and exhibit significantly lower resistance frequencies compared to clinically used rifampicin. Subsequent investigations concerning the molecular mechanism of RNAP inhibition reveal the compounds as inhibitors of protein-protein interaction between σ^{70} and the RNAP core enzyme and suggest the inhibitors' binding site.

In the second part of this work, the discovered compounds are demonstrated to additionally inhibit PqsD, an attractive target to disrupt cell-to-cell communication of *Pseudomonas aeruginosa*. For this promising anti-virulence concept, which should avoid the occurrence of resistance, bacterial cell death caused by RNAP inhibition is not intended. Thus, the structural requirements needed for PqsD selectivity are elucidated, thereby highlighting the versatility and potential of the discovered benzamidobenzoic acids in the fight against bacterial resistances.

Zusammenfassung

Die Behandlung von bakteriellen Infektionen wird durch Resistenzen gegen klinisch verwendete Antibiotika zunehmend gefährdet. Daher besteht großes Interesse an der Entwicklung neuer Antiinfektiva, die in der Lage sind bestehende Resistenzen zu überwinden und die schnelle Entstehung neuer zu vermeiden.

In der vorliegenden Arbeit wird ein Pharmakophor-basiertes virtuelles Screening verwendet, um neue Inhibitoren des bakteriellen Targets RNA-Polymerase (RNAP) zu finden. Strukturelle Modifikationen der identifizierten Hits führen zu potenten RNAP-Hemmstoffen, die gegen grampositive Bakterien aktiv sind und weniger häufig zu Resistenzen führen als das klinisch eingesetzte Rifampicin. Nachfolgende Untersuchungen des molekularen Mechanismus der RNAP-Inhibition decken auf, dass die Verbindungen Hemmstoffe der Protein-Protein-Interaktion zwischen σ^{70} und dem RNAP Core-Enzym sind, und lassen auf die Bindestelle der Inhibitoren schließen.

Im zweiten Teil der Arbeit wird gezeigt, dass die entdeckten Verbindungen außerdem PqsD hemmen, ein attraktives Target, das für die Zell-Zell-Kommunikation in *Pseudomonas aeruginosa* verantwortlich ist. Da in diesem Antivirulenzkonzept, das das Auftreten von Resistenzen verhindern soll, der bakterielle Zelltod durch RNAP-Hemmung unerwünscht ist, werden die strukturellen Voraussetzungen für PqsD-Selektivität aufgeklärt. Dabei werden die Vielseitigkeit und das Potenzial der entdeckten Benzamidobenzoesäuren im Kampf gegen bakterielle Resistenzen beleuchtet.

Danksagung

Ich möchte mich bei allen Personen, die zum Gelingen dieser Arbeit beigetragen haben, ganz herzlich bedanken.

Ein besonderer Dank gilt Herrn Prof. Dr. Rolf W. Hartmann, der mir ein interessantes und vielseitiges Thema zur Bearbeitung überlassen hat, für die Unterstützung und Betreuung, die Anregungen und Diskussionen, das entgegengebrachte Vertrauen und den Freiraum, den er mir gewährt hat, um meine eigenen Ideen zu entfalten.

Ich danke Prof. Dr. Uli Kazmaier für die Übernahme des Koreferats, Prof. Dr. Claus-Michael Lehr für die Übernahme des Vorsitzes der Prüfungskommission und Dr. Jessica Hoppstädter für die Übernahme des Beisitzes der Prüfungskommission.

Dr. Jörg Haupenthal, Dr. Matthias Groh und Dr. Johannes de Jong danke ich für ihre gute Projektkoordination und dass sie immer ein offenes Ohr für Fragen hatten und mir jederzeit ihre Unterstützung anboten.

Des Weiteren möchte ich allen aktuellen und ehemaligen Mitgliedern des RNAP-Teams meinen Dank aussprechen für die regen wissenschaftlichen Diskussionen und die konstruktive und erfolgreiche Zusammenarbeit.

Bei Dr. Alexander Oster möchte ich mich für die Einführung in die chemische Synthese, für den Spaß und die gute Freundschaft bedanken. Seine ausgezeichnete Betreuung während meiner Diplomzeit, seine dauerhaft gute Laune und Motivation haben unter anderem dazu beigetragen, mich für den Beginn dieser Arbeit zu entscheiden.

Ich danke Juliette Emmerich, Martina Fruth, Sebastian Krug und Michael Storz für die zahlreichen interessanten wissenschaftlichen Diskussionen, die kreativen Kaffeepausen und nicht zuletzt für ihre gute und treue Freundschaft. Juliette gebührt überdies ein Dank für die tollen gemeinsamen Ausflüge und den Konsum meiner schier endlos vielen Kaffeepads, die ich alleine niemals hätte aufbrauchen können. Sebastian und Michael danke ich außerdem für die schöne Zeit als Labor-Dreamteam. Martina möchte ich zudem für die praktische Einweisung in die Geheimnisse der Enzymexpression und ihre dabei (nahezu) unendliche Geduld mit

mir und für die tolle Zeit in Barcelona danken. Sollten wir nicht doch alle gemeinsam eine PostDoc-Stelle in San Diego antreten können, werde ich euch sehr vermissen.

Vielen Dank unserem ganzen TA-Team, insbesondere Jeannine Jung und Jannine Ludwig, für die unkomplizierte Zusammenarbeit und die gute, zuverlässige Arbeit, die sie geleistet haben.

Dr. Ruth Werth, Dr. Claudia Henn, Christine Maurer, Michael Zender und Benjamin Kirsch danke ich für die tolle Zusammenarbeit während der Planung, Gestaltung und Durchführung des Arzneibuch Praktikums. Außerdem bin ich allen dankbar, die uns in diesen Zeiten mit den nötigen Mengen an Kaffee und Süßigkeiten versorgt haben.

Unseren Sekretärinnen Katrin Schmitt und Martina Schwarz und allen technischen Mitarbeitern (ganz besonders Lothar Jager) bin ich für die unkomplizierte Abwicklung von organisatorischen Dingen und die schnellstmögliche Behebung aller technischen Schwierigkeiten zu Dank verpflichtet.

Für ihre praktische Unterstützung danke ich den fleißigen Bienchen Aline Schütz und Isabelle Klein.

Ich danke Dr. Josef Zapp für die Messung der NMR Spektren und Dr. Stefan Boettcher für die Unterstützung bei HPLC-Problemen.

Allen Mitgliedern des Arbeitskreis Hartmann möchte ich danke sagen für die vielen schönen gemeinsam verbrachten Stunden und die gute Arbeitsatmosphäre, durch die sie mir eine unvergesslich schöne Zeit bereitet haben.

Meiner Familie und meinen Freunden danke ich, dass sie mich stets motiviert, aber manchmal auch für die nötigen Ablenkungen gesorgt haben.

Ein besonders großer Dank gilt meinen Eltern, die mir meinen bisherigen Werdegang überhaupt erst ermöglicht haben, für ihre fortwährende Unterstützung.

Nathalie, die jederzeit für mich da war, danke ich, dass sie mich fortdauernd motiviert hat und für ihr großes Verständnis für die vielen Stunden, die ich im Labor verbracht habe.

Zu guter Letzt noch ein Dankeschön an alle die, denen ich zu Dank verpflichtet bin, die ich aber nicht namentlich erwähnen konnte.

Publications included in this thesis

This thesis is divided into three publications numbered with Roman numerals:

I. **Discovery of novel bacterial RNA polymerase inhibitors: Pharmacophore-based virtual screening and hit optimization**
Hinsberger, S.; Hüsecken, K.; Groh, M.; Negri, M.; Haupenthal, J.; Hartmann, R.W. *J. Med. Chem.* **2013**, *56*, 8332–8338.

II. **Surface plasmon resonance – more than a screening technology: Insights in the binding mode of σ^{70}:core RNAP inhibitors**
Hüsecken, K.; Hinsberger, S.; Elgaher, W.A.M.; Haupenthal, J.; Hartmann, R.W. *Future Med. Chem.* **2014**, *6*, 1551–1565.

III. **Benzamidobenzoic acids as potent PqsD inhibitors for the treatment of *Pseudomonas aeruginosa* infections**
Hinsberger, S.; de Jong, J.; Groh, M.; Haupenthal, J.; Hartmann, R.W. *Eur. J. Med. Chem.* **2014**, *76*, 343–351.

Contribution report

Hereby, the author clarifies his contributions to the publications I–III included in this thesis.

I. The author significantly contributed to the design of the study, planned and executed the synthesis and characterization of all compounds. He interpreted the assay results and performed the structure-activity relationship studies. Furthermore, he conceived and wrote the manuscript.

II. The author performed the docking and visualization studies to explain the mutant binding results. Additionally, he contributed by writing parts of the manuscript.

III. The author significantly contributed to the design of the study, planned and executed the synthesis and characterization of compounds **1**–**50**. He interpreted the assay results and performed the structure-activity and structure-selectivity relationship studies. Furthermore, he conceived and wrote the manuscript.

Abbreviations

2-ABA	2-aminobenzoylacetate
AA	anthranilic acid
AHL	*N*-acyl homoserine lactone
AI	autoinducer
β' CC-LRS	β’ coiled-coil and lid-rudder-system
BSA	bovine serum albumin
Cam	chloramphenicol
CC	column chromatography
CD	circular dichroism
CDC	Centers for Disease Control and Prevention
Cer	cerulenin
CF	cystic fibrosis
Cipro	ciprofloxacin
CoA	coenzyme A
DHF	dihydrofolate
DHP	dihydropteroate
DMAP	4-dimethylaminopyridine
DME	dimethoxyethane
DMSO	dimethyl sulfoxide
DTT	dithiothreitol
ELISA	enzyme-linked immunosorbent assay
FabH	β-ketoacyl-acyl carrier protein synthase III
HAQ	4-hydroxy-2-alkylquinoline
HBA	hydrogen bond acceptor
HBD	hydrogen bond donor
HHQ	2-heptyl-4(1*H*)-quinolone
HMA	Heads of Medicines Agencies in Europe
HPLC	high-performance liquid chromatography
IC_{50}	half maximal inhibitory concentration
LB	lysogeny broth
LRET	luminescence resonance energy transfer
MIC	minimum inhibitory concentration
MOA	mode of action
MOE	Molecular Operating Environment

MRSA	methicillin-resistant *Staphylococcus aureus*
MvfR	multiple virulence factor regulator
Myx	myxopyronin B
NADH	reduced form of nicotinamide adenine dinucleotide
NMR	nuclear magnetic resonance
NTP	nucleoside triphosphate
OD_{600}	optical density measured at a wavelength of 600 nm
PBS	phosphate buffered saline
PDB	Protein Data Bank
PPI	protein−protein interaction
PQS	*Pseudomonas* quinolone signal
QS	quorum sensing
Rif	rifampicin
RNAP	RNA polymerase
RPc	RNAP-promoter complex
RPo	RNAP-promoter complex
rt	room temperature
SAR	structure−activity relationship
SD	standard deviation
SI	Supporting Information
SPR	surface plasmon resonance
TCA	trichloroacetic acid
TEA	triethylamine
THF	tetrahydrofolate **or** tetrahydrofuran
TLC	thin-layer chromatography
TT	transcription/ translation
UTP	uridine triphosphate
VS	virtual screening
WHO	World Health Organization

Table of contents

1. Introduction

The different strategies for the treatment of bacterial infections addressed in this work demand a closer look to the definition of “antibiotic”, the modes of action of existing antibiotics, and the problem of bacterial resistance to them.

1.1 Definition of the term “antibiotic”

Originally the term “antibiotic” was introduced by Nobel Prize laureate Selman A. Waksman. It was defined as a natural compound of microbial origin, which can inhibit the growth of or can even destroy other microorganisms [Waksman 1947, Waksman 1952]. Consequently, this definition excluded synthetic molecules on the one hand, but included beside bacteria other microorganisms like for example viruses and fungi. However, this former definition has changed in the last few years due to scientific development and changes in linguistic usage. Nowadays, synthetic agents are included in the definition and “antibiotic” is almost exclusively used as a synonym for “antibacterial” used to treat bacterial infections. This is the way in which the World Health Organization (WHO) as well as the Heads of Medicines Agencies in Europe (HMA) use the term and it is the manner in which it is used in this work [HMA 2012, WHO 2014].

1.2 Antibiotic modes of action

The characteristic of antibiotics is that they act against prokaryotic bacterial cells without seriously affecting eukaryotic organisms including humans. In the majority of cases they induce bacterial growth retardation (bacteriostatic) or cell death (bactericidal) by the inhibition of pivotal enzymes which are exclusively available in bacteria or whose bacterial type considerably differs from its human homolog [Clatworthy *et al.* 2007, Frearson *et al.* 2007].

The five main points of attack of traditional antibiotics are listed below [Greenwood *et al.* 1997] and depicted in Fig. 1:

- Inhibition of cell wall synthesis (e.g., penicillins)
- Inhibition of protein synthesis (e.g., tetracyclins)
- Disruption or alteration of cell membranes (e.g., polymyxins)
- Interference with bacterial metabolism by antimetabolite activity (e.g., sulfonamides)
- Inhibition of nucleic acid synthesis (e.g., quinolones)

In addition to these established modes of action, several ideas for new antibacterial targets, such as the selective inhibition of bacterial cytochrome P450 enzymes, have been discussed in the last few years and will possibly lead to novel antibacterial drugs in the future [McLean *et al.* 2008].

Recently, the intervention with the bacterial cell-to-cell communication system has emerged as a promising alternative strategy. This approach neither kills the bacteria, nor does it inhibit bacterial growth, but it significantly diminishes their pathogenicity [Hentzer *et al.* 2003]. The advantage of this new concept compared to the classic antibiotics will be discussed at a later point (1.4.2.3).

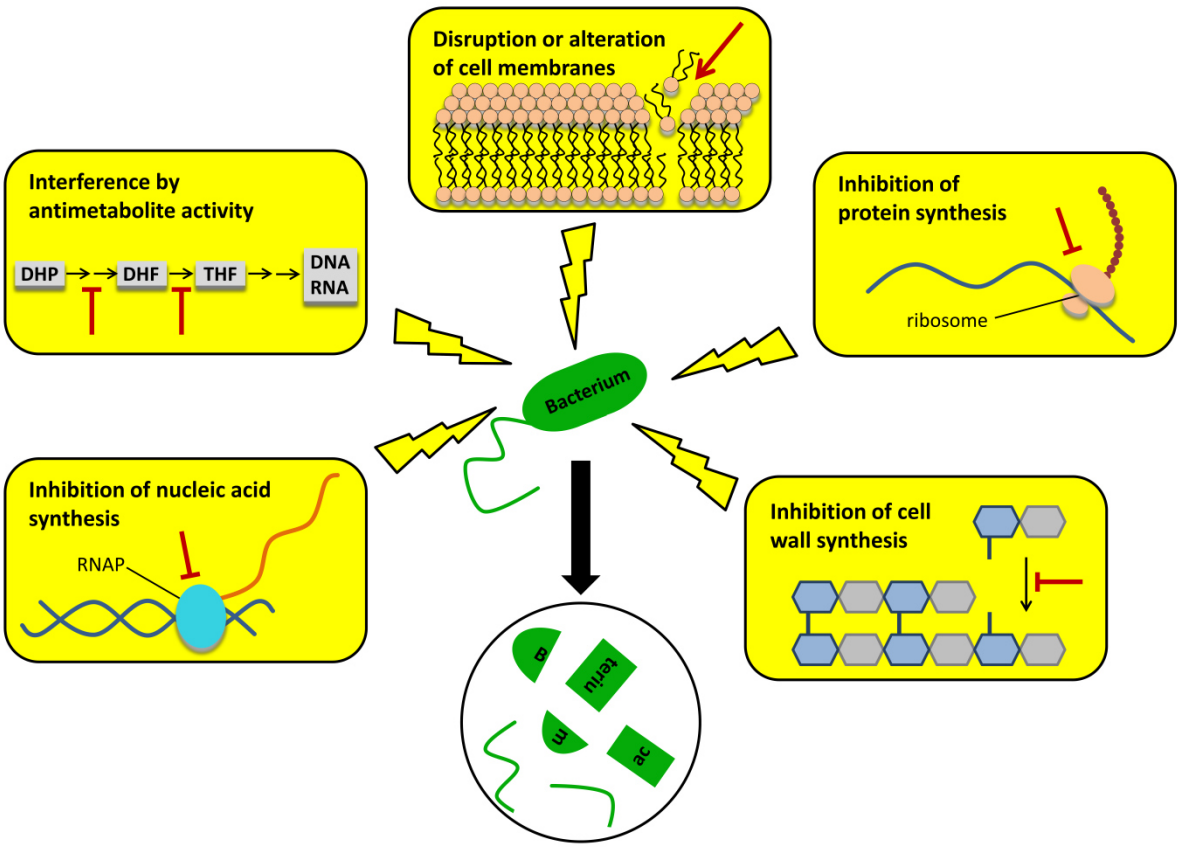

Figure 1. Schematic illustration of the five main points of attack of traditional antibiotics

1.3 Bacterial resistance to antibiotics

Dr. William H. Stewart, US Surgeon General in the 1960s, is often quoted as follows: “It is time to close the book on infectious diseases, and declare the war against pestilence won.” Although there is no evidence that he actually made a statement like this, the content of it probably reflects the view of many people on infections and anti-infectives at that time [Spellberg 2008]. In that so-called “golden era of antibacterial drug discovery” several different antibiotics with diverse modes of action were discovered, enabling a safe and effective treatment of bacterial infections and making people believe the battle against bacteria was won [Baldry 1976, Silver 2011, Chopra 2013].

However, as already Alexander Fleming, the discoverer of penicillin, warned in his Nobel Lecture “it is not difficult to make microbes resistant” [Fleming 1945]. Fatal misuse in public health care and unconscionable abuse in animal feed have led to a situation where resistances progressively render the known antibiotics ineffective and seriously endanger this milestone in modern medical treatment [WHO 2002, Diaz Högberg *et al.* 2010, WHO 2013]. Additionally, in a globalized world with lots of travelers and a rapid exchange of goods newly developed resistances spread all over the globe within a very short time [Butaye *et al.* 2006, WHO 2007, Diaz Högberg *et al.* 2010].

As in the 1980s many pharmaceutical companies abandoned antibiotic research, thinking that no more antibiotics would be needed [Rice 2006], today’s antibiotic research is in the hands of only a few companies [Braine 2011]. Furthermore, even nowadays the financial incentives to readopt the search for new antibacterials are limited. The average duration of treatment is short (compared to indications like hypertension or diabetes), their use is quite restricted and early-rising resistances can make the product developed at great expense useless, not refunding the invested money [Payne *et al.* 2007, Braine 2011]. Due to these reasons, there is the paradoxal situation that resistances are emerging while the number of true antibiotic innovations is decreasing [Diaz Högberg *et al.* 2010]. This shortage of available effective antibiotic treatments is already responsible for many cases of death and dramatically increases the economic burden on the public health sector. For example, the Centers for Disease Control and Prevention (CDC), which are a component of the US Department of Health and Human Services, estimate that in the

US alone every year there are more than 2 million people falling ill due to an infection with antibiotic-resistant pathogens. At least 23,000 of these patients die from their infections. CDC's estimate of additional costs in the US health care system caused by antibiotic resistance ranges as high as $20 billion, and even about $35 billion a year regarding the additional damage to society due to sickness absence and reduced manpower [CDC 2013].

Therefore, especially in these days, the development of new potent antibiotics is an essential field in drug discovery, because "without urgent, coordinated action, the world is heading towards a post-antibiotic era, in which common infections and minor injuries, which have been treatable for decades, can once again kill" [WHO 2014].

1.4 Promising concepts for the treatment of bacterial infections

1.4.1 Inhibition of RNA polymerase (RNAP)

1.4.1.1 RNAP as a drug target

RNAP is crucial for the transcription process, since it catalyzes the formation of RNA from a DNA template [Villain-Guillot *et al.* 2007]. As it is essential for bacterial growth and survival it represents a suitable point of attack for antibacterial drugs [Chopra 2007]. Structural distinction of bacterial RNAP from its eukaryotic complement affords the necessary therapeutic selectivity. Additionally, as RNAP is highly conserved among various bacterial species, the development of broad-spectrum antibiotics is possible making it an ideal target for the treatment of bacterial infections [Ho *et al.* 2009].

1.4.1.2 General RNA polymerase structure

Bacterial RNAP is a large multi-subunit enzyme with an overall shape resembling a crab claw. Its approximately 400 kDa core enzyme consists of five subunits, namely α_I, α_{II}, β, β' and ω (Fig. 2). Whereas the two α chains and ω are primarily required for the assembly of the enzyme, the β and β' subunits build the two pincers of the claw and are responsible for the formation of the Mg^{2+} containing active center, which is located on the bottom of the cleft between the pincers (Fig. 2). The so-called clamp, which is the pincer formed by the β' subunit, is very flexible and can adopt different positions. The “open” conformation allows unhampered entry and exit of template DNA to the active center while the “closed” conformation prevents this step. The whole transcription process can be divided into three sections: initiation, elongation and termination. It has been suggested that the “open” conformation allowing the DNA template to enter the active site is needed for transcription initiation and that the “closed” conformation is required later in the transcription process, especially during the elongation, to keep the DNA in the active center [Ebright 2000, Vassylyev *et al.* 2002, Mukhopadhyay *et al.* 2008, Mariani *et al.* 2009, Murakami 2013].

Although the core enzyme is catalytically active on its own, it associates with one of different σ factors (e.g., σ^{70}, which is the best-studied one, as it is the housekeeping σ factor) to form the RNAP holo enzyme. The interaction with the σ factor is needed

for a specific recognition of the promoter site and an effective transcription initiation [Burgess *et al.* 1969, Villain-Guillot *et al.* 2007].

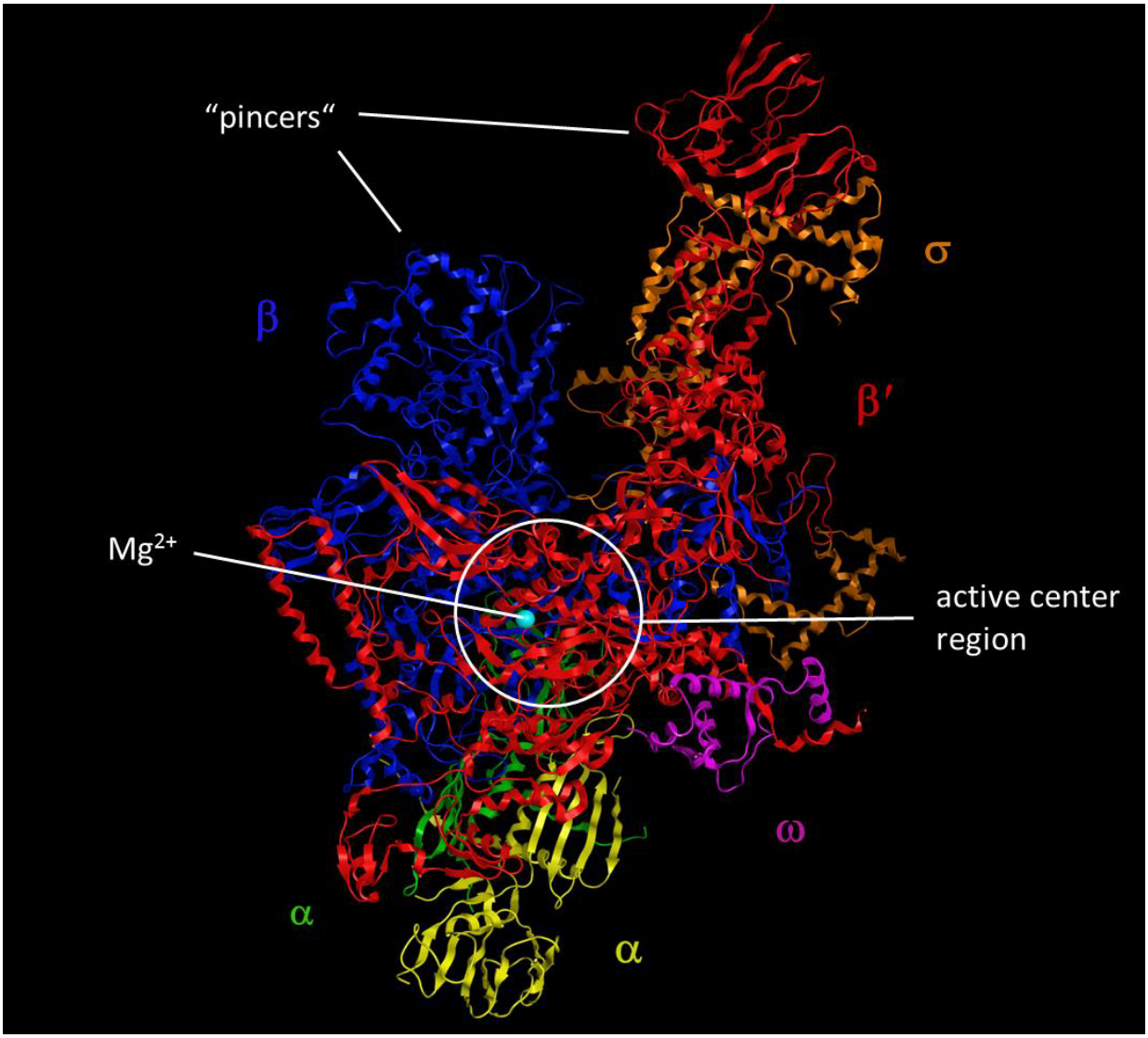

Figure 2. Crystal structure of *T. thermophilus* RNAP (PDB 4MQ9) with highlighted subunits, “pincers”, and active center region containing Mg^{2+}

1.4.1.3 RNAP inhibitors and their binding sites

There are several inhibitors of bacterial RNA polymerase described in literature, ranging from natural products [Margalith *et al.* 1960, Parenti *et al.* 1975, Irschik *et al.* 1983, Irschik *et al.* 1985, Irschik *et al.* 1987, Salomon *et al.* 1992, Ciciliato *et al.* 2004, Kuznedelov *et al.* 2011] to small organic molecules [Artsimovitch *et al.* 2003, André *et al.* 2006, Arhin *et al.* 2006, McPhillie *et al.* 2011, Buurman *et al.* 2012, Yakushiji *et al.* 2013]. The enzyme exhibits a couple of different sites to which known inhibitors bind (Fig. 3):

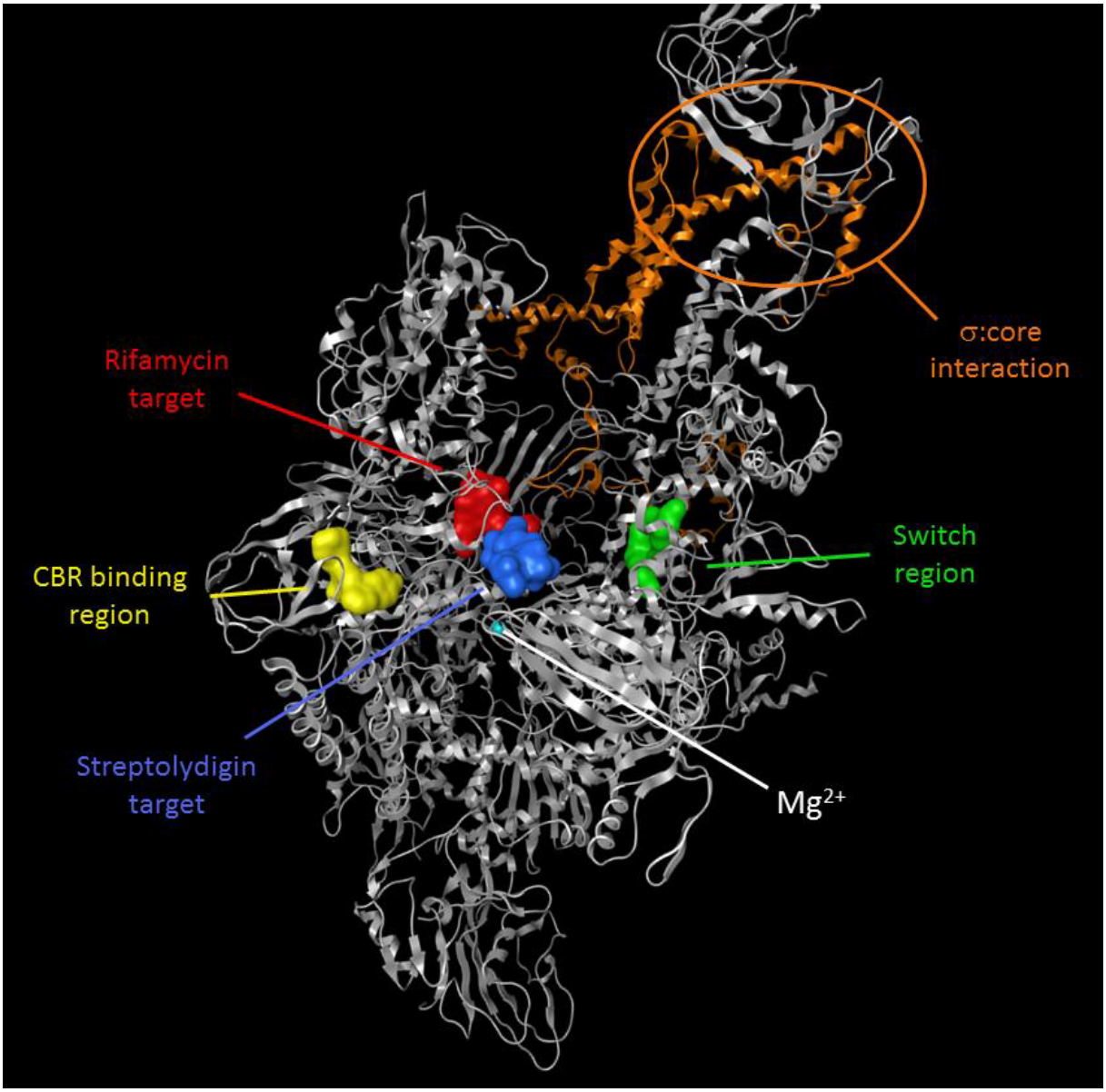

Figure 3. Binding sites of described RNAP inhibitors

a) The most prominent one is the rifamycin binding site. Here, beside other rifamycins, rifampicin, which plays a key role in the first line therapy of tuberculosis, interacts with the enzyme. This pocket is located adjacent to the RNAP active center and binding to it prevents the enzyme from synthesizing RNA products of more than 2–3 nucleotides in length by blocking the formation of the RNA second or third phosphodiester bond [McClure *et al.* 1978, Floss *et al.* 2005]. As rifamycins have been widely used for more than four decades, resistances against this class of antibiotics have arisen. For example the occurrence of single point mutations in the *rpoB* gene encoding for the β subunit of the enzyme makes many bacteria insensitive against rifamycins [Ezekiel *et al.*, 1968, Wehrli *et al.* 1968, Ramaswamy *et al.* 1998], thereby reducing the attractiveness of targeting this binding site.

b) A second RNAP binding site is the so-called “switch region”. It is located at the base of the “clamp” and serves as a hinge enabling the clamp to switch between the “open” and the “closed” conformation [Cramer 2002]. Several known RNAP inhibitors, e.g., the natural products myxopyronin, corallopyronin, ripostatin and fidaxomicin (also referred to as lipiarmycin), but also the squaramides and ureidothiophene carboxylic acids, which are classes of small synthetic molecules, bind to the “switch region” [Mukhopadhyay *et al.* 2008, Srivastava *et al.* 2011, Buurman *et al.* 2012, Sahner *et al.* 2013(A)]. They probably prevent the correct interaction of RNAP with the DNA by blocking the hinge and thus keeping the clamp in the “closed” conformation prohibiting the entry of the DNA template [Mukhopadhyay *et al.* 2008, Srivastava *et al.* 2011]. As the “switch region” is distant from the rifamycin binding site it represents a good drug target avoiding rifampicin cross-resistances [O'Neill *et al.* 2000, Mukhopadhyay *et al.* 2008].

c) A third binding site is targeted by the tetramic acid antibiotic streptolydigin. It binds to a region adjacent to the active center and stabilizes one conformational state by a “straight-bridge helix” [Tuske *et al.* 2005]. As the binding sites of streptolydigin and rifampicin are differing, the two antibiotics only exhibit a limited cross-resistance [Xu *et al.* 2005].

d) A further known binding site is the region where compounds of the CBR series bind. It is located at the surface of the core enzyme opposite the active center. The putative mechanism of action is the allosteric inhibition of nucleotide addition caused

by prevention of the active site movements through a bridge helix [Artsimovitch *et al.* 2003].

e) As the interaction of the core enzyme with the σ factor is required for a specific promoter recognition and effective transcription initiation, it is also a possibility to interfere with the function of the enzyme by disrupting this important interaction [Villain-Guillot *et al.* 2007]. A class of small molecules that is described to act in this way is the SB series discovered by André *et al*. [2006]. The inhibition of σ:core interaction is attractive since the inhibitor-induced occurrence of mutations in the interaction area would also lead to a weaker affinity of the core enzyme to σ [Bergendahl *et al.* 2004].

f) Another possible way of RNAP inhibition, in which the antibacterial peptide microcin J25 acts, is the obstruction of the so-called “secondary channel”, thus hindering NTPs from reaching the active center [Mukhopadhyay *et al.* 2004]

g) Additionally, inhibitors with so far unknown exact modes of action or binding sites have been described, like for example the 2-ureidothiophene-3-carboxylates [Arhin *et al.* 2006] or the pyridyl-benzamides [McPhillie *et al.* 2011].

To date, however, the only clinically used RNAP inhibitors are the rifamycins, whose potency is considerably weakened by resistances [Nachega *et al.* 2003], and fidaxomicin (lipiarmycin), which is approved solely for the treatment of *Clostridium difficile*-associated diarrhea [Hardesty *et al.* 2011]. This shortage of clinically applicable inhibitors is due to the fact that, in spite of the large amount of described compounds, most of them suffer from a decisive drawback. Many of them are natural products, which are often not drug-like and hard to gain [Koehn *et al.* 2005, Haebich *et al.* 2009], others exhibit poor antibacterial activity [Artsimovitch *et al.* 2003] or inadequate physicochemical properties [O'Shea *et al.* 2008]. Hence, there is still an urgent need for novel inhibitors of the underexploited target RNAP [Chopra 2007, Mariner *et al.* 2010].

1.4.2 Interference with the *Pseudomonas* Quorum Sensing (QS) system

1.4.2.1 *Pseudomonas aeruginosa*

P. aeruginosa is a ubiquitous, highly adaptable Gram-negative bacterium responsible for the majority of nosocomial infections in humans [van Delden *et al.* 1998, Khan *et al.* 2010]. Especially in immunocompromised individuals, e.g., patients enfeebled by chemotherapy, organ transplantation or HIV infection, it can cause life-threatening infections [Bodey *et al.* 1983, Asboe *et al.* 1998, Hakki *et al.* 2007]. Additionally, *P. aeruginosa* plays an important role in cystic fibrosis (CF) patients. In these persons a genetic disorder leads to highly viscous mucus in the respiratory tract and diminished mucociliary clearance abetting the colonization by bacteria [Rowe *et al.* 2005]. In 90% of the cases *P. aeruginosa* is the originator of the chronic endobronchial infection in CF patients [Koch *et al.* 1993]. Due to the expression of a large number of virulence factors, which can cause tissue damage and a delayed wound healing, the bacterium is responsible for high rates of illness and death [van Delden *et al.* 1998].

The treatment of *P. aeruginosa* infections is challenging, as the pathogens possess a high level of intrinsic resistance to many antibiotic agents [Okamoto *et al.* 2001]. Beside the limited permeability of the outer membrane, the expression of multidrug efflux pumps and β-lactamases, the formation of biofilms hampers the therapy [Singh *et al.* 2000, Okamoto *et al.* 2001]. Biofilms are the result of a controlled clustering of bacteria, embedded within a matrix of a self-produced polymeric substance, generally composed of extracellular DNA, proteins and polysaccharides [Mann *et al.* 2012]. These components function as protective shield by representing an additional diffusion barrier against antibiotics and counterwork human immune response [Bjarnsholt *et al.* 2010]. Although the exact mechanism of resistance caused by biofilms is still not fully understood, a considerably increased mutation frequency of bacteria in the biofilm [Driffield *et al.* 2008] and an intensified horizontal gene transmission compared to planktonic bacteria [Molin *et al.* 2003] have been shown. Furthermore, gradients of nutrients and oxygen exist in the biofilm and are associated with decreased metabolic activity and increased doubling times of the bacteria. These “dormant” cells are also responsible for the tolerance to antibiotics, especially to the ones exclusively targeting dividing cells [Høiby *et al.* 2010].

1.4.2.2 *P. aeruginosa* Quorum Sensing (QS) system

In *P. aeruginosa* the production of virulence factors and formation of biofilms is regulated by a cell-to-cell communication system known as "*quorum sensing*" (QS) [Fuqua *et al.* 1994, de Kievit 2009]. The functional principle of this system comprises the production and release of hormone-like signal molecules by bacterial cells on the one hand and the detection of these molecules by other bacterial cells within a bacterial community on the other hand [Swift *et al*. 2001]. The extracellular level of signal molecules increases in concentration as a function of cell-density. Once a certain threshold has been reached several transcriptional regulators are activated or repressed resulting in an altered gene expression [McKnight *et al.* 2000, Miller *et al.* 2001]. As this kind of gene activity modulation occurs without "external intervention" and is only induced by the bacteria's own culture supernatants, the molecules are often referred to as autoinducers (AI) [Nealson *et al.* 1970, González *et al.* 2006]. Interestingly, the binding of AIs to their receptor also increases the expression of their own corresponding synthase resulting in a positive feedback mechanism [Engebrecht *et al.* 1983, Engebrecht *et al.* 1984]. This kind of communication system enables bacteria to act as multicellular organism, permitting beneficial behaviors for the entire bacterial population [de Kievit *et al.* 2000].

P. aeruginosa employs three different known QS systems. Two of them, namely the *las* and the *rhl* system, are based on *N*-acyl homoserine lactones (AHLs) [Gambello *et al.* 1991, Pearson *et al.* 1994, Ochsner *et al*. 1994, Pearson *et al*. 1995]. Whereas AHLs are prevalent in many different Gram-negative bacteria [Swift *et al*. 2001], the third QS system, the so-called *pqs* system, can exclusively be found in some *Pseudomonas* and *Burkholderia* spp. [Pesci *et al.* 1999, Diggle *et al.* 2006]. In this system, 4-hydroxy-2-alkylquinolines (HAQs), more precisely *Pseudomonas* quinolone signal (PQS; 2-heptyl-3-hydroxy-4(1*H*)-quinolone) and its precursor 2-heptyl-4(1*H*)-quinolone (HHQ), are used as signal molecules (Scheme 1). PQS as well as, to a lesser extent, HHQ are able to interact with PqsR, also known as multiple virulence factor regulator (MvfR) [Cao *et al.* 2001, Xiao *et al.* 2006]. The activation of PqsR drives the expression of numerous different genes, resulting in the production of virulence determinants such as pyocyanine, lectin A, elastase B, rhamnolipids, and hydrogen cyanide [Déziel *et al.* 2005]. Moreover, biofilm formation and maturation is also controlled by the *pqs* system [Diggle *et al*. 2003].

1.4.2.3 Disruption of the *pqs* QS system as a novel chance for the treatment of *P. aeruginosa* infections

A drawback of the clinically used classical antibiotics is the emergence of resistances in a rather short time [Palumbi 2001]. For the treatment of hazardous *P. aeruginosa* infections a novel strategy overcoming this problem could be the disruption of its QS system. In contrast to the mode of action of traditional antibiotics inducing bacterial growth retardation or cell death, the inhibition of the QS system can lead to reduced pathogenicity without affecting cell viability. This results in the advantage that the pathogen's virulence and biofilm formation, which is a central protective shield against antibiotics [Prince 2002, Bjarnsholt *et al*. 2005], are attenuated without exposing the bacteria to an intense selective pressure, thereby diminishing the probability of the appearance of resistances [Hentzer *et al*. 2003, Rasmussen *et al.* 2006].

Motivated by these benefits several experiments concerning the inhibition of AHL-mediated QS systems were successfully performed in the last decade [Hentzer *et al.* 2002, Hentzer *et al.* 2003, Christensen *et al.* 2012, Jakobsen *et al.* 2012]. Since AHL-mediated QS systems, however, are widespread among Gram-negative bacteria [Swift *et al*. 2001], QS inhibition might not exclusively target the pathogen *P. aeruginosa* but also non-pathogenic bacteria. This shortcoming can be avoided by interfering with the *pqs* system instead of the *las* or the *rhl* systems, as it is solely present in *Pseudomonas* and *Burkholderia* strains [Pesci *et al.* 1999, Diggle *et al.* 2006], thus enabling selective inhibition of the pathogens' QS system. This is further advantageous as the non-pathogenic bacteria of the natural microbial flora, if not affected by the treatment, may repel the attacked *Pseudomonas* exploiting their debility. Moreover, it has been demonstrated that mutations in key enzymes of the *pqs* AI synthesis lead to attenuated virulence [Déziel *et al.* 2005] and altered biofilm formation making the pathogens more vulnerable [Allesen-Holm *et al.* 2006], as the *pqs* system is closely linked to biofilm formation [Yang *et al.* 2009]. Thus, the inhibition of the *pqs* system can be considered as a promising strategy to treat *P. aeruginosa* infections.

1.4.2.4 HAQ biosynthesis and blockade by PqsD inhibition

To disrupt the *pqs* system of *P. aeruginosa* two obvious ways – either antagonizing PqsR or blocking the biosynthesis of *pqs* AIs – are possible. The drawback of a PqsR inhibition is the existence of two additional pathways for PQS-mediated effects independent of PqsR activation, namely PqsE activation and iron chelation [Diggle *et al.* 2007]. Interestingly, it has also been demonstrated that the production of the siderophore pyoverdine is directly linked to the presence of PQS, but is not regulated by PqsR [Diggle *et al.* 2007]. Hence, the interference with the biosynthesis of HAQs seems to be more attractive than a sole inhibition of PqsR, since this strategy results in the avoidance of all HHQ- and PQS-mediated effects.

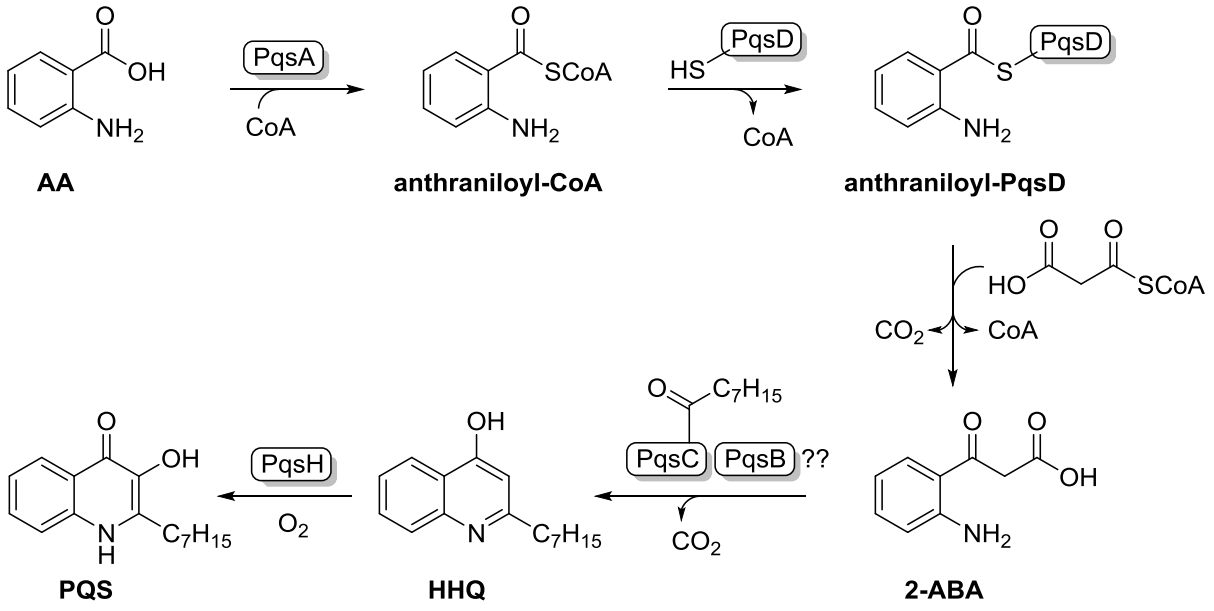

Scheme 1. Proposed biosynthesis cascade for HHQ and PQS (modified from [Dulcey *et al.* 2013])

The supposed biosynthesis cascade for HAQs (Scheme 1) begins with the activation of anthranilic acid (AA) as thioester by PqsA, a coenzyme A (CoA) ligase [Coleman *et al.* 2008]. The activated AA is able to covalently bind to PqsD [Bera *et al.* 2009], which is catalyzing the reaction with malonyl-CoA in a two-step reaction to 2-aminobenzoylacetate (2-ABA) [Dulcey *et al.* 2013]. Subsequently, the decarboxylating coupling of 2-ABA to an octanoate molecule linked to PqsC results in HHQ formation. As it has been shown that the presence of PqsB is required for PqsC to be active and that the two enzymes are closely associated, it is supposed that PqsB is mainly involved in the proper folding of PqsC [Dulcey *et al.* 2013]. HHQ, which is already able to activate PqsR [Xiao *et al.* 2006], can be further converted to the more potent agonist PQS by PqsH [Schertzer *et al.* 2010], a NADH-dependent flavin monooxygenase controlled by the *las* system, thereby representing a link between the *las* and the *pqs* system [Gallagher *et al.* 2002]. In addition to HHQ and PQS, *P. aeruginosa* is able to produce at least 54 further HAQs with varying length and saturation level of the alkyl chain, different substituents in 3-position (hydrogen or hydroxy) or an N-oxide group in place of the quinolone nitrogen [Lépine *et al.* 2004]. While HHQ and PQS are described to participate in *P. aeruginosa* cell-to-cell communication [Pesci *et al*. 1999, Déziel *et al.* 2004], several further HAQs exhibit antimicrobial activities against other bacteria (e.g., *S. aureus*), thus accounting for an advantage in natural selection [Machan *et al.* 1992, Déziel *et al.* 2004].

In summary, this implies that PqsA–D are key enzymes in the biosynthesis of HAQs, thereby representing appropriate targets for the treatment of *P. aeruginosa* infections.

Whereas for PqsA–C no structural information is available, the crystal structure of PqsD has been elucidated [Bera *et al.* 2009] (Fig. 4). *P. aeruginosa* PqsD is a 36 kDa enzyme comprising 337 amino acids. It is composed of two similar domains (residues 1–174 and 175–337) and closely resembles β-ketoacyl-ACP synthase III (FabH), which is involved in fatty acid synthesis (rmsd 1.4 Å for 315 equivalent α-carbon atoms) [Bera *et al.* 2009]. The PqsD active site is located deep in the protein interior at the bottom of a ~15 Å long channel and comprises Cys112, His257 and Asn287 (Fig. 4). The nucleophilic Cys112 is required to capture the anthranilate from anthraniloyl-CoA, enabled by a proton shift from Cys112 to His257, whereas Asn287 is suggested by modeling simulations to be essential for a subsequent reaction step [Hutter *et al.* 2014].

Due to this detailed knowledge concerning protein structure and function of PqsD, we consider the development of drugs inhibiting PqsD as the most promising anti-virulence strategy. Additionally, till this day only few PqsD inhibitors, exclusively developed by our group, have been described in literature [Pistorius *et al.* 2011, Storz *et al.* 2012, Sahner *et al.* 2013(B), Weidel *et al.* 2013, Storz *et al.* 2014].

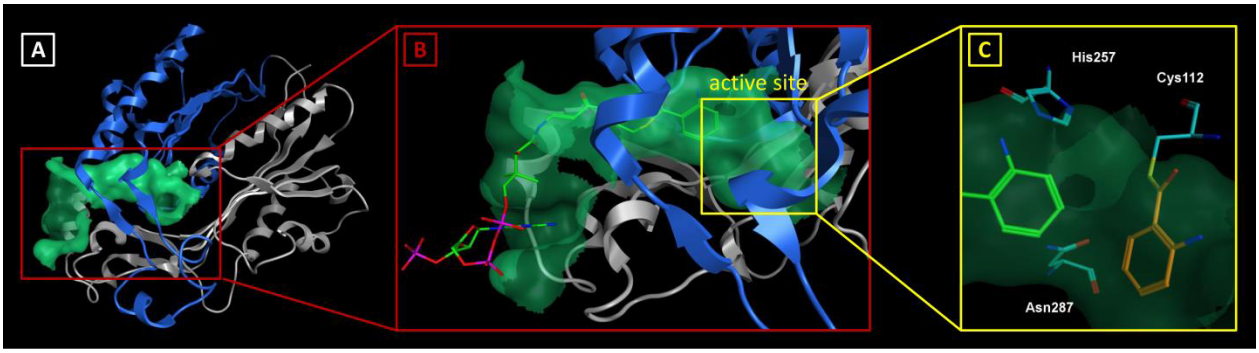

Figure 4. Crystal structure of *P. aeruginosa* PqsD (PDB 3H77). (A) The two similar domains (blue and grey) and highlighted anthraniloyl-CoA channel (green); (B) Orientation of anthraniloyl-CoA (neon green) in the channel to the active site; (C) PqsD active site containing His257, Asn287 and Cys112 (turquois) with covalently bound anthraniloyl (orange)

2. Aim of the Thesis

The alarming emergence of resistances against existing clinically used antibiotics and the deficient research for new antibacterial drugs of the last decades have provoked a situation in which mankind has to deal with inadequate treatment options for multi-drug-resistant bacterial infections. As this situation, coming along with numerous cases of death and a dramatic increase in economic burden, is unacceptable, new potent anti-infectives are urgently needed. Hence, our research group is focused on the development of new drugs for well-established, validated targets as well as novel, so far poorly explored, innovative targets.

The aim of this thesis was the design of novel anti-infectives overcoming existent resistances and avoiding the fast emergence of new ones. RNAP is an attractive and validated target for antibiotics, but the clinical use of rifamycins, the most important RNAP inhibitors, is considerably hampered by resistance. Thus, the intention was the finding of new RNAP inhibiting scaffolds active against rifampicin resistant bacteria. For this purpose, a virtual screening (VS) approach using a pharmacophore model able to identify RNAP inhibitors was pursued. The identified hit compounds had to be biologically evaluated and chemically modified to result in a chemical library suitable for SAR studies in order to determine the best derivatives for further development and to gain intense structural knowledge concerning the novel class of compounds. These efforts were to be followed by mode of action (MOA) studies employing biological, biophysical and computational methods to elucidate the way the inhibitors act in detail and to ascertain their full potential (Publication I + II).

Another promising strategy for innovative anti-infectives with the potential of avoiding the emergence of resistances is the inhibition of PqsD, a key enzyme in the QS system of *P. aeruginosa*. As the novel RNAP inhibitors identified in the VS mentioned above were additionally demonstrated to be potent inhibitors of *P. aeruginosa* PqsD, in the second part of this thesis a synthetic approach aiming at getting an advanced structural insight and resulting in optimized compounds for use as selective PqsD inhibitors is described (Publication III).

Altogether, this thesis dealing with two different approaches to develop novel anti-infectives is intended to be a small contribution to the fight of mankind against bacterial resistance to antibiotics.

3. Results

3.1 Discovery of novel bacterial RNA polymerase inhibitors: Pharmacophore-based virtual screening and hit optimization

Stefan Hinsberger, Kristina Hüsecken, Matthias Groh, Matthias Negri, Jörg Haupenthal, and Rolf W. Hartmann

Reprinted with permission from *J. Med. Chem.* **2013**, *56*, 8332−8338.

Publication I

ABSTRACT

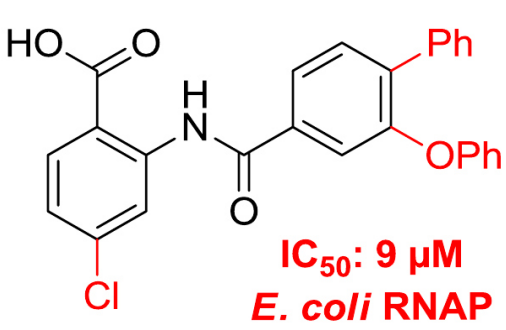

The bacterial RNA polymerase (RNAP) is a validated target for broad spectrum antibiotics. However, the efficiency of drugs is reduced by resistance. To discover novel RNAP inhibitors, a pharmacophore based on the alignment of described inhibitors was used for virtual screening. In an optimization process of hit compounds, novel derivatives with improved *in vitro* potency were discovered. Investigations concerning the molecular mechanism of RNAP inhibition reveal that they prevent the protein−protein interaction (PPI) between σ^{70} and the RNAP core enzyme. Besides of reducing RNA formation, the inhibitors were shown to interfere with bacterial lipid biosynthesis. The compounds were active against Gram-positive pathogens and revealed significantly lower resistance frequencies compared to clinically used rifampicin.

INTRODUCTION

The increasing resistance of bacteria against antibiotics has become a major public health problem.[1] Therefore, new potent antibacterial drugs are required.[2] RNA polymerase (RNAP) catalyzes the formation of RNA from a DNA template[3] and is essential for growth and survival of bacteria. It is highly conserved among various bacterial species but is different in eukaryotes.[4] Hence, inhibiting RNAP is an attractive strategy for the treatment of bacterial infections.[4]

In spite of the fact that several inhibitors of bacterial RNA polymerase are known, only rifamycins and fidaxomicin (lipiarmycin) are currently approved for clinical use.[3,5–7] Because of an increasing amount of bacterial strains resistant to rifamycins, there is an urgent need to discover new RNAP inhibitors for clinical use which should not show cross-resistance to rifamycins, especially rifampicin (Rif).

In this work, a flexible alignment of structurally similar selected synthetic molecules (**I–VII**) that are known to inhibit bacterial RNAP[8–12] was performed (Figure 1). The resulting pharmacophore model was subsequently used to virtually screen an in-house database. Thus, three hit compounds, containing an anthranilic acid core, were identified and experimentally validated. In the following, the compounds were optimized to improve the inhibitory profile and their mode of action was determined. Additionally, the compounds revealed good antibacterial activities.

PHARMACOPHORE-BASED VIRTUAL SCREENING AND HIT COMPOUND DISCOVERY

Seven synthetic bacterial RNAP inhibitors (**I–VII**) that exhibit similar structural features, although belonging to different classes and acting via different binding modes, were retrieved from literature (Figure S1, Supporting Information (SI)).[8–12] Compound **I** inhibits *Staphylococcus aureus* RNAP, but its binding site is not known.[8] **II** and **III** are described as inhibitors of *Escherichia coli* RNAP binding to a surface exposed groove at the junction of the β′-bridge helix and the β-subunit.[9] **IV–VI** are known to prevent the protein–protein interaction (PPI) between σ^{70} and the RNAP core enzyme.[10,11] **VII** shows structural similarity to known RNAP inhibitors but has only been described as an inhibitor of transcription and translation (TT) without any

information about its mode of action.[12] We resynthesized **VII** and were able to demonstrate its inhibition of *E. coli* RNAP *in vitro* (SI).

I–**VII** were employed in a flexible alignment with the aim to identify the common features of these molecules. The alignment with the best similarity score was used to generate an initial pharmacophore model, which was then manually refined. The resulting model derived from these differently acting compounds is not restricted to the identification of hits binding to one special site. It should rather support the discovery of an increased number of RNAP inhibitors independent of their binding mode.

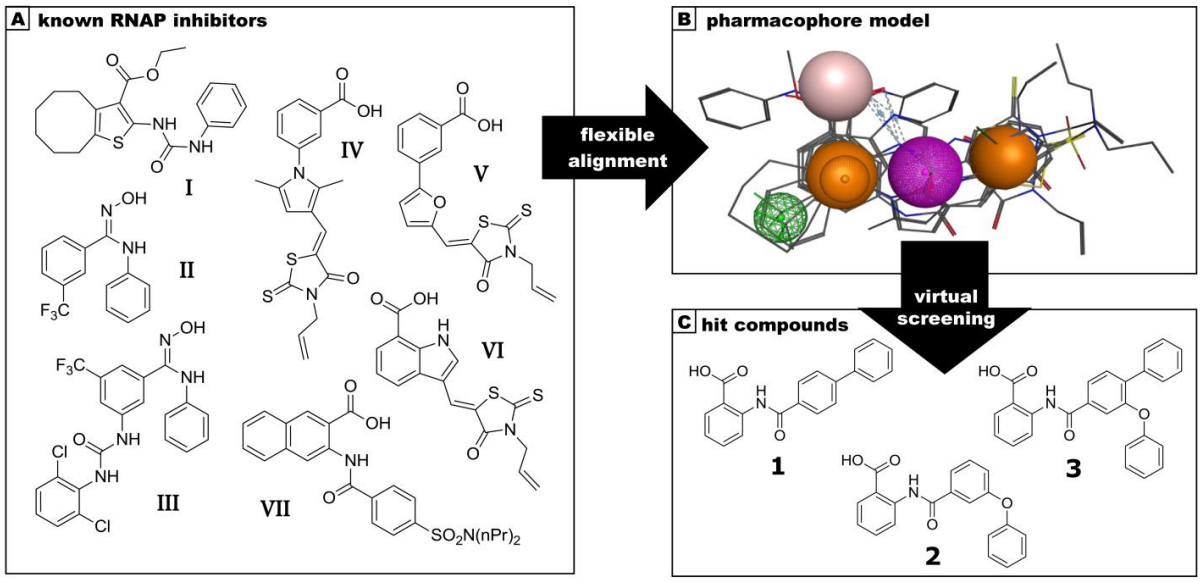

Figure 1. (A) Selected synthetic inhibitors of bacterial RNAP (**I**–**VII**) were used to perform a flexible alignment. (B) A pharmacophore model with four core features (aromatic, orange; HBD/HBA/aromatic, violet; O2/anion, rose), one accessory feature (hydrophobic, green) and two aromatic projections (one hatched orange, one hidden behind a core feature) was created and used for virtual screening. For an overlay of **I**–**VII** with the pharmacophore model see Figure S3 (SI). (C) Validated hit compounds **1**–**3** possessing an RNAP *in vitro* inhibition >20% at a concentration of 200 µM

The final model consisted of four core features (two aromatic, one HBD/HBA/aromatic and one O2/anion). Besides, one accessory feature (hydrophobic) and two aromatic projections were identified (Figure 1, Figure S2, SI). The fit of each inhibitor **I**–**VII** into the pharmacophore model is depicted in Figure S3,

SI. The virtual screening of an in-house database comprising approximately 2000 compounds using this pharmacophore model afforded 64 hits. A virtual hit had to match at least the core features and the aromatic projections, while the presence of the accessory feature was not mandatory.

Eleven of these hit compounds originating from five different structural classes were experimentally confirmed to be active in our *in vitro* transcription assay[13] (>20% inhibition at 200 µM) (Figure S4, SI). Out of these, three promising compounds (**1**−**3**), containing an anthranilic acid core, were chosen for further optimization. They displayed 31% (**1**), 23% (**2**), and 100% (**3**, IC_{50} 20 µM) inhibition at 200 µM, respectively.

CHEMISTRY

The synthesis of the target compounds was carried out starting from the appropriate anthranilic acids. The methyl 2-benzamidobenzoate intermediates **1a**−**34a** were synthesized via coupling reaction with the benzoyl chloride derivatives (Scheme 1).

Scheme 1. Synthetic Route to Compounds 1−34

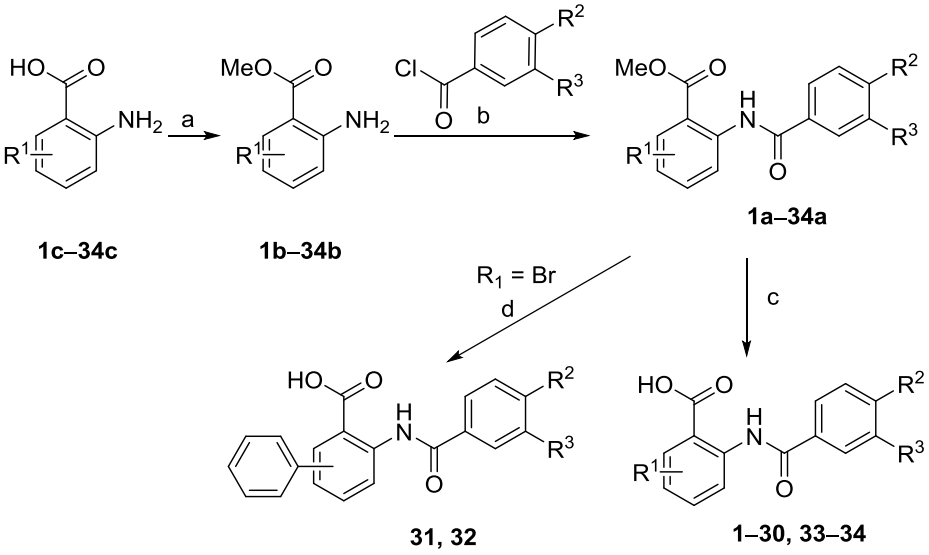

Reagents and conditions: (a) $SOCl_2$, MeOH, reflux; (b) pyridine, DMAP, rt or TEA, CH_2Cl_2, rt or toluene, reflux; (c) NaOH, THF/MeOH/H_2O, rt; (d) $PhB(OH)_2$, $Pd(PPh_3)_4$, Cs_2CO_3, DME/H_2O, reflux.

The methyl esters were hydrolyzed to yield the target compounds. A Suzuki coupling with phenylboronic acid was performed with the appropriate brominated intermediates to obtain compounds **31** and **32**. The hydroxy substituted compound **24** was obtained from the methoxy intermediate **24a** by ether cleavage using boron tribromide.

RESULTS AND DISCUSSION

Compounds **1**–**3** contain a 2-benzamidobenzoic acid partial structure which perfectly fits into the pharmacophore model. In addition, the structures contain a phenyl ring in *para*- and/ or a phenoxy substituent in *meta*-position, respectively, which does not correspond to any feature of the pharmacophore model. Hence, the hit compounds were reduced in size to investigate whether these lipophilic residues are necessary for activity. Although the unsubstituted 2-benzamidobenzoic acid (**4**) fits the pharmacophore model, no activity was observed for this compound. This resulted in the conclusion that the features included in the first pharmacophore model are insufficient to differentiate between active and inactive substances. To provide a remedy, two new accessory hydrophobic/ aromatic features were added on the eastern side of the pharmacophore model (representing the phenyl and the phenoxy substituents) (Figure S5, SI). Using this extended model, a compound will be defined as a hit if, beside the four core features, at least one of the new accessory features is present. As the extended model is more limiting, its use should improve efficacy and reduce the occurrence of false positives in future screenings. An overlay of inhibitors with the extended pharmacophore model can be found in Figure S6, SI.

To explore the structure–activity relationship (SAR) around the anthranilic acid core, substituents were introduced in 4- and 5-position where the pharmacophore model contains a lipophilic accessory feature. As the most potent hit compound **3** has a relatively high molecular weight, optimization efforts were started modifying the two smaller hits **1** and **2**. For each hit, a small series was synthesized introducing 4-Cl (**6** and **7**), 5-F (**11** and **12**), 5-Br (**16** and **17**), and 4,5-dimethoxy (**19** and **20**) substituents. The introduction of these substituents resulted in an increased *in vitro* activity, especially for the compounds with 4-Cl (**6** and **7**) and 5-Br (**16** and **17**) substituents. Aside from that, most 4-phenyl and 3-phenoxy compounds displayed

very similar activities. To investigate whether the oxygen of the phenylether group has a beneficial effect as HBA, we synthesized compound **18** containing a 3-benzyl instead of the 3-phenoxy substituent. The removal of the oxygen did not affect the potency, indicating that a HBA is not necessary for *in vitro* activity. Therefore we regarded it as sufficient to continue the SAR studies introducing further substituents into the 4-phenyl series.

To determine which kind of substituents could improve activity, substituents differing in electronic properties and lipophilicity were introduced in 5-position. The incorporation of the lipophilic, electron withdrawing chloro substituent resulted in the most potent compound **8** while a hydrophilic and electron donating hydroxy group (**24**) decreased activity in comparison to **1**. Introduction of a lipophilic and electron donating substituent (**30**, CH_3) or a hydrophilic electron withdrawing substituent (**26**, CN) was tolerated and led to moderately active compounds.

In a next step, the best position for a substitution at the anthranilic acid moiety was determined. Considering the good activity of chloro compound **8**, especially lipophilic, electron withdrawing substituents in different positions of the anthranilic acid moiety were introduced. A chloro substituent in 3-position (**5**) led to a total loss of activity. Similar results were found for the chloro, fluoro, and methoxy substituents in 6-position (**9**, **13**, **23**) (Table 1). As expected, the introduction of an electron donating methoxy substituent in 4- and 5-position afforded only a moderate improvement of activity. In contrast all the compounds bearing a lipophilic, electron withdrawing substituent in 4- or 5-position (**6**, **8**, **10**, **11**, **14**, **16**, **25**, **27−29**) possess a highly improved *in vitro* potency. Especially the introduction of a large lipophilic phenyl substituent in 4- or 5-position generated very potent inhibitors of RNAP (**31**, 14 µM; **32**, 13 µM). Interestingly, almost no difference in activity was observed between compounds with a substituent in 4-position and compounds with the same substituent in 5-position (**6** and **8**, **10** and **11**, **14** and **16**, **27**, and **28**).

From these results, it is obvious that especially lipophilic electron withdrawing substituents attached to the anthranilic acid core in 4- or 5-position are favorable, whereas substituents in 3- or 6-position strongly reduce the *in vitro* activity.

Table 1. Inhibitory Activity against *E. coli* RNA Polymerase *in Vitro* and Antibacterial Activity

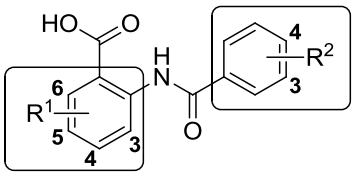

Cpd	R^1	R^2	IC_{50} or % inhib. of *E. coli* RNAP[a]	MIC *E. coli* TolC [µg/mL][b]	Cpd	R^1	R^2	IC_{50} or % inhib. of *E. coli* RNAP[a]	MIC *E. coli* TolC [µg/mL][b]
1	H	4-Ph	31%	13	**19**	4-,5-OMe	4-Ph	35%	19
2	H	3-OPh	23%	9	**20**	4-,5-OMe	3-OPh	154 µM	6
3	H	3-OPh, 4-Ph	20 µM	13	**21**	4-OMe	4-Ph	162 µM	9
4	H	H	n.i.	>100	**22**	5-OMe	4-Ph	52%	8
5	3-Cl	4-Ph	n.i.	55	**23**	6-OMe	4-Ph	n.i.	58
6	4-Cl	4-Ph	37 µM	3	**24**	5-OH	4-Ph	17%	31
7	4-Cl	3-OPh	44 µM	3	**25**	4-NO_2	4-Ph	36 µM	>25
8	5-Cl	4-Ph	46 µM	2	**26**	5-CN	4-Ph	23% @ 50 µM	7
9	6-Cl	4-Ph	n.i.	57	**27**	4-CF_3	4-Ph	27 µM	5
10	4-F	4-Ph	98 µM	4	**28**	5-CF_3	4-Ph	28 µM	2
11	5-F	4-Ph	138 µM	7	**29**	5-OCF_3	4-Ph	31 µM	4
12	5-F	3-OPh	98 µM	5	**30**	5-Me	4-Ph	139 µM	7
13	6-F	4-Ph	14%	34	**31**	4-Ph	3-OPh	14 µM	8
14	4-Br	4-Ph	28 µM	2	**32**	5-Ph	3-OPh	13 µM	2
15	4-Br	3-OPh	34 µM	3	**33**	4-F	3-OPh, 4-Ph	13 µM	>25
16	5-Br	4-Ph	31 µM	3	**34**	4-Cl	3-OPh, 4-Ph	9 µM	>25
17	5-Br	3-OPh	34 µM	3	Rif	-	-	0.03 µM	10
18	5-Br	3-CH_2Ph	37 µM	2	Myx[c]	-	-	0.35 µM	1

[a] IC_{50} value (SD <20%) or percentage inhibition at 200 µM (SD <40%); Data represent the mean values of at least three experiments.
[b] Minimum inhibitory concentration; data represent the mean values of at least two independent experiments (three for MIC <10 µg/mL).
[c] Myx: myxopyronin B.
n.i.: no inhibition

After all, the acquired SAR information of the anthranilic acid core was used for the optimization of **3**. As it was not eligible to make the compounds too large and lipophilic, only F and Cl were introduced (**33** and **34**). As expected, these modifications had a beneficial effect on the activity and afforded the best *in vitro* compound of this series (**34**, 9 µM).

As the pharmacophore model is not restricted to one special binding site, it remains to be clarified where our compounds bind to RNAP. Comparing the structures of the optimized hit compounds and the inhibitors **I**–**VII**, used to create the pharmacophore model, it becomes apparent that the new compounds are very similar to **VII**. This suggests that **VII** and our compounds are likely to interact with the same RNAP site. However, the binding mechanism of **VII** is not known.

Table 2. Results of the ELISA-Based Assembly Inhibition Assay and the Core/Holo Transcription Assay

compd	assembly inhibition σ^{70}/ RNAP core (ELISA) (IC_{50})[a]	inhibition of RNAP holo (IC_{50})[a]	inhibition of RNAP core (IC_{50})[a]	ratio[b]
Rif[c]	n.i.	27 nM	16 nM	1
V[c]	30 µM	38 µM	57 µM	2.6
VII	97 µM	52 µM	81 µM	2.6
3	41 µM	20 µM	36 µM	3.0
9	n.i.	n.d.	n.d.	-
14	68 µM	27 µM	39 µM	3.0
28	60 µM	28 µM	67 µM	4.0
32	47 µM	16 µM	27 µM	2.8
34	33 µM	7 µM	12 µM	2.9

[a] IC_{50} value (SD <20%); Data represent the mean values of at least two experiments. n.i.: no inhibition; for **9** inhibition <10% at 50 µM; for Rif inhibition <5% at 10 µM. n.d.: not determined.
[b] (IC_{50} core:$holo_{compd}$/IC_{50} core:$holo_{Rif}$). The core:holo IC_{50} ratios were related to the Rif core:holo ratio.
[c] Inhibition values of core/holo transcription assay by Hüsecken et al.[14]

One possible mechanism of action could be the inhibition of the PPI between σ^{70} and the RNAP core enzyme because this has been demonstrated to be the way compounds **IV**–**VI** function.[10,11] Hence, selected compounds (**3**, **9**, **14**, **28**, **32**, **34**) as

well as TT inhibitor **VII** were tested in an ELISA-based RNAP assembly assay.[14] Rif and **V** were used as negative and positive controls, respectively. In contrast to Rif and inactive compound **9**, inhibitors **3**, **14**, **28**, **32**, **34**, and **VII**, which had been active in the transcription assay, inhibit PPI between σ^{70} and the RNAP core enzyme to a similar extent as positive control **V** (Table 2).

Inhibitors acting via such a mechanism would be expected to show a stronger effect in a σ^{70}-dependent transcription assay using holo enzyme than in a σ^{70}-independent transcription assay with core enzyme. To further confirm PPI interruption as RNAP inhibitory mechanism, we tested our compounds in both assays in parallel. Indeed, **3**, **14**, **28**, **32**, **34**, and **VII** were found to be more active in the assay using holo enzyme than in the core enzyme assay (Table 2). To normalize interassay conditions, ratios of IC_{50} values (core:holo) were calculated in relation to IC_{50} ratio (core:holo) of Rif, which was used as negative control not acting via PPI inhibition. The calculated IC_{50} ratios (core:holo) of the tested compounds are within the range of 2−4, comparable or even higher than the ratio of described PPI inhibitor **V** (Table 2). These results confirm the assumption that the mechanism of action of our compounds and TT inhibitor **VII** is the interference with the interaction between σ^{70} and RNAP core enzyme.

ANTIBACTERIAL ACTIVITY

For investigation of antibacterial activity, minimum inhibitory concentration (MIC) values were determined for all compounds. Two described RNAP inhibitors were used as references: Rif, which reveals a good antibacterial activity against Gram-positive and negative strains,[15−18] and the natural product myxopyronin B, only active against Gram-positive bacteria.[19] To evade effects associated with drug efflux, initial MIC tests were performed using *E. coli* TolC mutant, deficient in the AcrAB−TolC multidrug efflux system. There are several compounds possessing high antibacterial activity comparable to the reference compounds, especially **6−8**, **14−18**, **28**, and **32**, with MIC values in the range of 2−3 μg/mL. For most compounds, antibacterial activity roughly correlates with *in vitro* RNAP inhibition. However, for some highly potent inhibitors, compounds **25**, **33**, and **34**, bacterial growth inhibition was less than expected, a finding which possibly was caused by permeability problems.

Table 3. Minimum Inhibitory Concentration (MIC) for Selected Compounds

compd	MIC [µg/mL][a]			
	E. coli K12	*PA*01[b]	*B. subtilis*	*S. aureus*
Rif[c]	7	13	5	0.02
Myx[c]	>25	>25	0.9	0.5
6	>50	>50	2	24
7	>50	>50	3	14
12	>100	>100	4	48
15	>25	>25	3	8
28	>50	>50	4	5
32	>25	>25	3	6
33	>25	>25	>25	17

[a] Minimum inhibitory concentration; Data represent the mean values of at least two independent experiments (three for MIC <10 µg/mL).
[b] *P. aeruginosa*.
[c] Rif, rifampicin; Myx, myxopyronin B.

To further explore the antibacterial profile, MIC values for *E. coli* K12, *Pseudomonas aeruginosa*, *Bacillus subtilis*, and *Staphylococcus aureus* were determined for selected compounds (**6**, **7**, **12**, **15**, **28**, **32**, **33**; Table 3). None of the tested inhibitors reduced the growth of Gram-negative strains (*E. coli* K12 and *P. aeruginosa*). These results suggest that the compounds are either not able to penetrate the cell membranes of the Gram-negative bacteria or are discharged by efflux pumps. The latter mechanism is more probable considering the differences between the MIC values for *E. coli* K12 and *E. coli* TolC. On the other hand, the inhibitors were in general effective against Gram-positive bacteria; especially against *Bacillus subtilis* excellent MIC values were determined.

It is striking that our compounds show very low MIC values comparable to the reference compounds although their RNAP inhibitory activities are less pronounced than those of the references.

To confirm the mechanism of antibacterial activity, the impact on macromolecular biosynthesis in *E. coli* TolC was examined. While exerting no appreciable effect on DNA and protein synthesis at 4 x MIC, **32** displayed an inhibition of RNA formation

comparable to the clinically used RNAP inhibitor Rif (Figure 2). In addition, a strong decrease in lipid biosynthesis was observed (Figure 2). In this regard, it is also of interest that benzamidobenzoic acids, including compounds **2** and **3**, have been described in the context of anti-infective research. While compound **3** was shown to inhibit PqsD, an enzyme associated with the *Pseudomonas* quorum sensing system,[20] compounds **2** and **3** have been published as inhibitors of FabH, an enzyme involved in fatty acid synthesis.[21] Therefore, it can be supposed that the good antibacterial activity is due to an additional FabH inhibition.

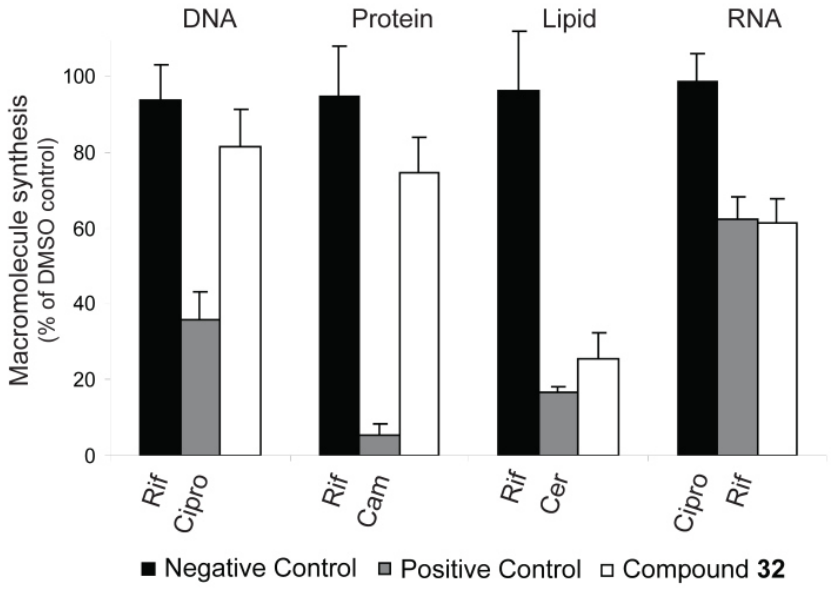

Figure 2. Effects of **32** at 4 x MIC on macromolecular synthesis in *E. coli* TolC. Controls: cerulenin (Cer), chloramphenicol (Cam), ciprofloxacin (Cipro), and rifampicin (Rif)

As it is our aim to develop compounds which are less susceptible to bacterial resistance development, the spontaneous resistance frequencies in *E. coli* TolC were determined *in vitro* for compounds **28** and **32** at 2 x MIC. Importantly, a lower resistance frequency ($<4.5 \times 10^{-11}$) of both novel compounds compared to Rif (8.3×10^{-8}) was observed. One explanation for this remarkable observation could be the dual target effects of our compounds.

CONCLUSION

RNAP is an attractive antibacterial target, but due to emerging resistance, new types of RNAP inhibitors are urgently needed. For the discovery of those, we performed a flexible alignment with a series of selected RNAP inhibitors[8−12] and developed a pharmacophore model which is not focused on one particular binding site. Using this model, a virtual screening was performed, hit compounds were identified, and 11 of those subsequently experimentally validated. On the basis of three hits of one structural class, an optimization approach was performed, resulting in enhanced inhibitory potencies. Concerning the mechanism of RNAP inhibition, we could demonstrate that the new inhibitors prevent the PPI between σ^{70} and the RNAP core enzyme.

Determination of MIC values revealed that the best compounds are highly active against *E. coli* TolC and the Gram-positive pathogens *B. subtilis* as well as the clinically relevant *S. aureus*. The wild-type Gram-negative strains *P. aeruginosa* and *E. coli* K12 were not affected, probably due to pharmacokinetic reasons.

Regarding the effects of our compounds on macromolecule synthesis in *E. coli* TolC, an inhibition of bacterial lipid biosynthesis was observed beside the reduced RNA formation. This highly interesting dual target effect could explain the good MIC values and the significantly lower resistance rate compared to the clinically used inhibitor Rif. These findings are presently further elucidated. In conclusion, we consider the new compounds promising for further development.

EXPERIMENTAL SECTION

Chemistry. All tested compounds have >95% chemical purity as measured by HPLC. Spectroscopic data for all compounds are provided in the SI.

Procedure for the Synthesis of the Acyl Chlorides Used for Amide Coupling Reaction. Benzoyl chlorides, if not commercially available, were obtained from the corresponding carboxylic acid via reaction with thionyl chloride (2.5 equiv) in CH_2Cl_2 in the presence of catalytic amounts of dimethylformamide (4 h reflux).

General Procedure for the Synthesis of Methyl 2-Aminobenzoates ***5b, 21b−23b, 25b, 27b, 29b,*** *and* ***30b****. Method A.* A solution of the appropriate 2-aminobenzoic acid (1 equiv) in

MeOH was cooled to 0 °C followed by a dropwise addition of thionyl chloride (2.5 equiv). The mixture was refluxed for 24 h. After evaporation of the solvent and neutralization by addition of a saturated aqueous $NaHCO_3$ solution, the mixture was extracted with EtOAc and the combined organic layers were dried over $MgSO_4$. Purification by CC (*n*-hexane/EtOAc) provided the title compounds (yields, physical, and spectral data are reported in SI).

*General Procedure for the Synthesis of Methyl 2-Benzamidobenzoate Derivatives **1a−34a** (Amide Coupling Reaction). Method B.* Three different procedures were used to obtain the title compounds:

BI. The appropriate methyl 2-aminobenzoate (1 equiv) was added to a solution of the acyl chloride (1.2 equiv) in CH_2Cl_2 under a N_2 atmosphere. After the addition of TEA (2 equiv), the reaction mixture was stirred for 18 h at room temperature.

BII. The appropriate methyl 2-aminobenzoate (1 equiv) and a catalytic amount of DMAP were added to a suspension of the acyl chloride (1.5 equiv) in pyridine under a N_2 atmosphere. The reaction mixture was stirred for 18 h at room temperature, and 2 M HCl was added. The mixture was extracted with EtOAc, and the combined organic layers washed with saturated $NaHCO_3$ and dried over $MgSO_4$.

BIII. The appropriate methyl 2-aminobenzoate (1 equiv) and the acyl chloride (1.2 equiv) were dissolved in toluene and refluxed for 4 h (except for **5a** and **33a−34a**, which were refluxed for 18 or 72 h).

For purification, the solvent was removed under reduced pressure and the remaining solid suspended in MeOH (except for **5a** and **31a−32a**). After filtration, the precipitate was washed with MeOH to yield the pure compound.

For compounds **5a** and **31a−32a**, the purification step was performed by CC or preparative TLC.

*General Procedure for the Synthesis of 2-Benzamidobenzoate Derivatives **1−34**. Method C.* The methyl esters of the title compounds (**1a−34a**) were hydrolyzed with 5 M NaOH in THF/MeOH (2:1) at room temperature (18 h). The mixture was acidified by the addition of 1 M HCl and filtered, and the precipitate was washed with 1 M HCl to provide the title compounds. If the compound was not pure at this stage of the procedure, it was washed with MeOH and CH_2Cl_2 or was purified by CC or preparative TLC.

General Procedure for Suzuki Coupling. Method D. A mixture of the appropriate methyl bromo-2-benzamidobenzoate (1 equiv), phenylboronic acid (1.5 equiv), Cs_2CO_3 (3 equiv), and tetrakis(triphenylphosphine)palladium (0.01 equiv) in a degassed DME/water (1:1) solution was refluxed under a nitrogen atmosphere for 4 h. The reaction mixture was cooled to room temperature. The mixture was extracted with EtOAc. The combined organic layers were washed with 1 M HCl and dried over $MgSO_4$. The product was purified by CC or preparative TLC.

General Procedure for Ether Cleavage Using Boron Tribromide. Method E. To a solution of the appropriate methoxy substituted methyl 2-benzamidobenzoate derivative (1 equiv) in anhydrous CH_2Cl_2 at −78 °C (dry ice/acetone bath), boron tribromide (1 M in CH_2Cl_2, 6 equiv) was

added dropwise. The reaction mixture was stirred for 18 h at room temperature under a nitrogen atmosphere. Water was added, and the aqueous layer was extracted with EtOAc. The combined organic layers were washed with brine and dried over $MgSO_4$. The product was purified by CC followed by preparative TLC.

Biology.

Transcription Assay. Transcription assay was performed as described previously.[13,22] During the transcription time of 10 min, the substrate concentration as well as the enzyme activity were not limiting the transcription reaction. Consequently, the reaction process in our assay was linear.

Determination of IC_{50} Values. For the determination of IC_{50} values, three different concentrations of a compound were chosen (duplicate determination) in the linear range of the log dose response curve (20−80% inhibition) including concentrations above and below the IC_{50} value. The calculation of the IC_{50} value was performed by plotting the percent inhibition versus the concentration of inhibitor on a semilog plot. From this, the molar concentration causing 50% inhibition was calculated. At least three independent determinations were performed for each compound. Standard deviation was less than 20%.

Minimal Inhibitory Concentration (MIC) Determinations. These experiments were performed as described recently.[22] Given MIC values are means of two independent determinations (three if MIC <10 µg/mL) and are defined as the lowest concentration of compounds that reduced OD_{600} by ≥95%.

Determination of Resistance Frequencies. Defined amounts of *E. coli* TolC cells were incubated in LB in presence of the 2 x MIC of compounds **28** and **32** in parallel (16 h, 37 °C, 50 rpm, 0.5% DMSO). On each of the three following days, a fraction of each of the samples was supplemented with fresh compound containing LB followed by recultivation (conditions as before). The final cultures were plated on LB agar to select spontaneous resistant mutants. The bacterial start concentration which was needed to yield at least one colony on the plates was determined. The reciprocal value of this threshold was defined to be the resistance frequency. For **28** and **32**, no colonies were detected at the highest possible bacterial start concentration, resulting in a resistance frequency $<4.5 \times 10^{-11}$.

Macromolecular Biosynthesis Assay. E. coli TolC was cultured in lysogeny broth (LB) medium. ^3H labeled precursors (1−1.25 µCi/mL) were added during the logarithmic growth phase and several min (3 min for uridine and thymidine, 5 min for acetic acid, 12 min for glutamine) before the addition of compound **32** and the controls chloramphenicol (Cam), cerulenin (Cer), ciprofloxacin (Cipro), and rifampicin (Rif) at four times their MICs. For DNA, RNA, and protein synthesis, 300 µL of the cultured bacteria were harvested 0 and 30 min after addition of the inhibitors and supplemented with 2 volumes of 10% TCA. After 45 min at 4 °C, the precipitates were collected and washed using 96-well glass fiber filter plates (Multiscreen GFB) (Millipore, Billerica, MA). After adding Optiphase Supermix (Perkin-

Elmer, Waltham, MA), the quantification of radioactivity was performed using a Wallac MicroBeta TriLux system (Perkin-Elmer). For determination of lipid synthesis, cells were treated with $CHCl_3$/MeOH (1:1) and water, subsequently. The organic phase was collected, evaporated, redissolved in cyclohexane, and supplemented with Opti-Fluor O (Perkin-Elmer) before measuring the radioactivity in the MicroBeta TriLux.

ELISA-Based RNAP Assembly Assay. The procedure was performed as described by Hüsecken et al.[14]

Core/Holo Transcription Assay. The procedure was performed as described by Hüsecken et al.[14]

ACKNOWLEDGMENTS

We thank Jeannine Jung for determination of RNAP IC_{50} values and Jannine Ludwig for determination of MIC values.

REFERENCES

1. Hooper, D. C.; DeMaria, A.; Limbago, B. M.; O'Brien, T. F.; McCaughey, B. Antibiotic resistance: How serious is the problem, and what can be done? *Clin. Chem.* **2012**, *58*, 1182−1186.

2. Chopra, I. The 2012 Garrod Lecture: Discovery of antibacterial drugs in the 21st century. *J. Antimicrob. Chemother.* **2013**, *68*, 496−505.

3. Villain-Guillot, P.; Bastide, L.; Gualtieri, M.; Leonetti, J.-P., Progress in targeting bacterial transcription. *Drug Discov. Today* **2007**, *12*, 200−208.

4. Ho, M. X.; Hudson, B. P.; Das, K.; Arnold, E.; Ebright, R. H. Structures of RNA polymerase-antibiotic complexes. *Curr. Opin. Struc. Biol.* **2009**, *19*, 715−723.

5. Hardesty, J. S.; Juang, P. Fidaxomicin: A macrocyclic antibiotic for the treatment of *Clostridium difficile* infection. *Pharmacotherapy* **2011**, *31*, 877−886.

6. Mariani, R.; Maffiolo, S. I. Bacterial RNA polymerase inhibitors: An organized overview of their structure, derivatives, biological activity and current clinical development status. *Curr. Med. Chem.* **2009**, *16*, 430−454.

7. Chopra, I. Bacterial RNA polymerase: A promising target for the discovery of new antimicrobial agents. *Curr. Opin. Invest. Dr.* **2007**, *8*, 600−607.

8. Arhin, F.; Bélanger, O.; Ciblat, S.; Dehbi, M.; Delorme, D.; Dietrich, E.; Dixit, D.; Lafontaine, Y.; Lehoux, D.; Liu, J.; McKay, G. A.; Moeck, G.; Reddy, R.; Rose, Y.; Srikumar, R.; Tanaka, K. S. E.; Williams, D. M.; Gros, P.; Pelletier, J.; Parr Jr, T. R.; Far, A. R. A new

class of small molecule RNA polymerase inhibitors with activity against Rifampicin-resistant *Staphylococcus aureus*. *Bioorg. Med. Chem.* **2006**, *14*, 5812−5832.

9. Artsimovitch, I.; Chu, C.; Lynch, A. S.; Landick, R. A new class of bacterial RNA polymerase inhibitor affects nucleotide addition. *Science* **2003**, *302*, 650−654.

10. André, E.; Bastide, L.; Michaux-Charachon, S.; Gouby, A.; Villain-Guillot, P.; Latouche, J.; Bouchet, A.; Gualtiéri, M.; Leonetti, J.-P. Novel synthetic molecules targeting the bacterial RNA polymerase assembly. *J. Antimicrob. Chemoth.* **2006**, *57*, 245−251.

11. Villain-Guillot, P.; Gualtieri, M.; Bastide, L.; Roquet, F. o.; Martinez, J.; Amblard, M.; Pugniere, M.; Leonetti, J.-P. Structure-Activity Relationships of phenyl-furanyl-rhodanines as inhibitors of RNA polymerase with antibacterial activity on biofilms. *J. Med. Chem.* **2007**, *50*, 4195−4204.

12. Larsen, S. D.; Hester, M. R.; Craig Ruble, J.; Kamilar, G. M.; Romero, D. L.; Wakefield, B.; Melchior, E. P.; Sweeney, M. T.; Marotti, K. R. Discovery and initial development of a novel class of antibacterials: Inhibitors of *Staphylococcus aureus* transcription/translation. *Bioorg. Med. Chem. Lett.* **2006**, *16*, 6173−6177.

13. Haupenthal, J.; Hüsecken, K.; Negri, M.; Maurer, C. K.; Hartmann, R. W. Influence of DNA template choice on transcription and inhibition of *Escherichia coli* RNA polymerase. *Antimicrob. Agents Ch.* **2012**, *56*, 4536−4539.

14. Hüsecken, K.; Negri, M.; Fruth, M.; Boettcher, S.; Hartmann, R. W.; Haupenthal, J. Peptide-based investigation of the *Escherichia coli* RNA polymerase σ^{70}: Core interface as target site. *ACS Chem. Biol.* **2013**, *8*, 758−766.

15. Thornsberry, C.; Hill, B. C.; Swenson, J. M.; McDougal, L. K. Rifampin: Spectrum of antibacterial activity. *Rev. Infect. Dis.* **1983**, *5*, 412−417.

16. Bandow, J. E.; Brötz, H.; Hecker, M. *Bacillus subtilis* Tolerance of moderate concentrations of Rifampin involves the sigma(B)-dependent general and multiple stress response. *J. Bacteriol.* **2002**, *184*, 459−467.

17. Fowler, C. E.; Soothill, J. S.; Oakes, L. MICs of rifampicin and chloramphenicol for mucoid *Pseudomonas aeruginosa* strains are lower when human lactoferrin is present. *J. Antimicrob. Chemoth.* **1997**, *40*, 877−879.

18. Williams, K. J.; Piddock, L. J. Accumulation of rifampicin by *Escherichia coli* and *Staphylococcus aureus*. *J. Antimicrob. Chemoth.* **1998**, *42*, 597−603.

19. Irschik, H.; Gerth, K.; Höfle, G.; Kohl, W.; Reichenbach, H. The myxopyronins, new inhibitors of bacterial RNA synthesis from *Myxococcus fulvus* (*Myxobacterales*). *J. Antibiot.* **1983**, *36*, 1651−1658.

20. Pistorius, D.; Ullrich, A.; Lucas, S.; Hartmann R.W.; Kazmaier, U.; Müller R. Biosynthesis of 2-alkyl-4(1H)-quinolones in *Pseudomonas aeruginosa*: Potential for therapeutic interference with pathogenicity. ChemBioChem **2011**, *12*, 850−853.

21. Nie, Z.; Perretta, C.; Lu, J.; Su, Y.; Margosiak, S.; Gajiwala, K. S.; Cortez, J.; Nikulin, V.; Yager, K. M.; Appelt, K.; Chu, S. Structure-based design, synthesis, and study of potent

inhibitors of β-ketoacyl-acyl carrier protein synthase III as potential antimicrobial agents. *J. Med. Chem.* **2005**, *48*, 1596−1609.

22. Sahner, J. H.; Groh, M.; Negri, M.; Haupenthal, J.; Hartmann, R. W. Novel small molecule inhibitors targeting the “switch region” of bacterial RNAP: Structure-based optimization of a virtual screening hit. *Eur. J. Med. Chem.* **2013**, *65*, 223−231.

3.2 Surface plasmon resonance – more than a screening technology: Insights in the binding mode of σ^{70}:core RNAP inhibitors

Kristina Hüsecken, Stefan Hinsberger, Walid A. M. Elgaher, Joerg Haupenthal, and Rolf W. Hartmann

Future Med. Chem. **2014**, *6*, 1551–1565. doi:10.4155/fmc.14.105

Publication II

ABSTRACT

Background: Antibiotic resistance has become a major health problem. The σ^{70}:core interface of bacterial RNA polymerase is a promising drug target. Recently, the coiled-coil and lid-rudder-system of the β' subunit has been identified as an inhibition hot spot. **Results/Methodology:** By using surface plasmon resonance-based assays, inhibitors of the protein-protein interaction were identified and competition with σ^{70} was shown. Effective inhibition was verified in an *in vitro* transcription and a σ^{70}:core assembly assay. For one hit series we found a correlation between activity and affinity. Mutant interaction studies suggest the inhibitors' binding site. **Conclusion:** Surface plasmon resonance is a valuable technology in drug design, that has been used in this study to identify and evaluate σ^{70}:core RNA polymerase inhibitors.

3.3 Benzamidobenzoic acids as potent PqsD inhibitors for the treatment of *Pseudomonas aeruginosa* infections

Stefan Hinsberger, Johannes C. de Jong, Matthias Groh, Jörg Haupenthal, and Rolf W. Hartmann

Reprinted with permission from *Eur. J. Med. Chem.* **2014,** *76*, 343–351.

Publication III

ABSTRACT

Targeting PqsD is a promising novel approach to disrupt bacterial cell-to-cell-communication in *Pseudomonas aeruginosa*. In search of selective PqsD inhibitors, two series of benzamidobenzoic acids – one published as RNAP inhibitors and the other as PqsD inhibitors – were investigated for inhibitory activity toward the respective other enzyme. Additionally, novel derivatives were synthesized and biologically evaluated. By this means, the structural features needed for benzamidobenzoic acids to be potent and, most notably, selective PqsD inhibitors were identified. The most interesting compound of this study was the 3-Cl substituted compound **5** which strongly inhibits PqsD (IC_{50} 6.2 µM) while exhibiting no inhibition of RNAP.

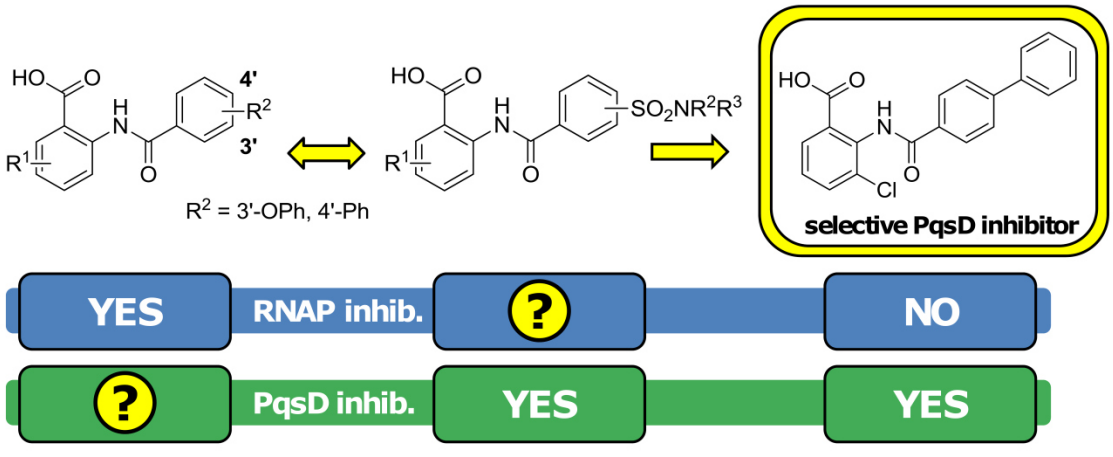

1. INTRODUCTION

Increasing resistance of bacteria against clinically used antibiotics provoke an urgent need for new antibacterial drugs and innovative therapeutic options [1, 2]. An established method is the induction of bacterial growth retardation or cell death by inhibiting pivotal enzymes [3]. A disadvantage of this therapy is selective pressure causing rapid emergence of resistance [3, 4]. This should be different in a more recent approach to combat bacterial infections [5]. By intervening with the bacterial cell-to-cell-communication system the production of virulence factors and the biofilm formation can be reduced [5]. A newly described strategy to interfere with the *Pseudomonas* Quinolone Signal (PQS) communication system in *Pseudomonas aeruginosa*, is the inhibition of PqsD, which is responsible for the biosynthesis of the important signal molecule 2-heptyl-4-quinolone (HHQ) [6].

Recently, we described a series of potent novel RNA polymerase (RNAP) inhibitors [7] derived from a known inhibitor of PqsD [6]. These compounds containing a benzamidobenzoic acid core were shown to inhibit RNAP *in vitro* in the low micromolar range (IC_{50} around 10 µM) [7]. Due to their origin and their structural similarity to the PqsD inhibitors recently published by Weidel et al. [8], we expected this new class of RNAP inhibitors also to inhibit PqsD and tested the compounds in our PqsD *in vitro* assay for inhibitory activity (Fig. 1). Indeed, we found most of them to be very potent.

As bacterial cell death caused by potent RNAP inhibition provoking selective pressure is not intended for an anti-virulence concept [3], it is of special interest to look for structural modifications that lead to an increased selectivity of PqsD inhibitors.

In this work we want to elucidate which structural features in the former class of RNAP inhibitors are beneficial for potent PqsD inhibition and which are needed to afford selectivity over RNAP. To make the SAR complete the compounds published by Weidel et al. are tested for RNAP inhibition (Fig. 1). For getting an extended insight into this important class of benzamidobenzoic acids and for extension of their structure-activity and structure-selectivity profile regarding both enzymes several new benzamidobenzoic acid analogs were synthesized and biologically evaluated.

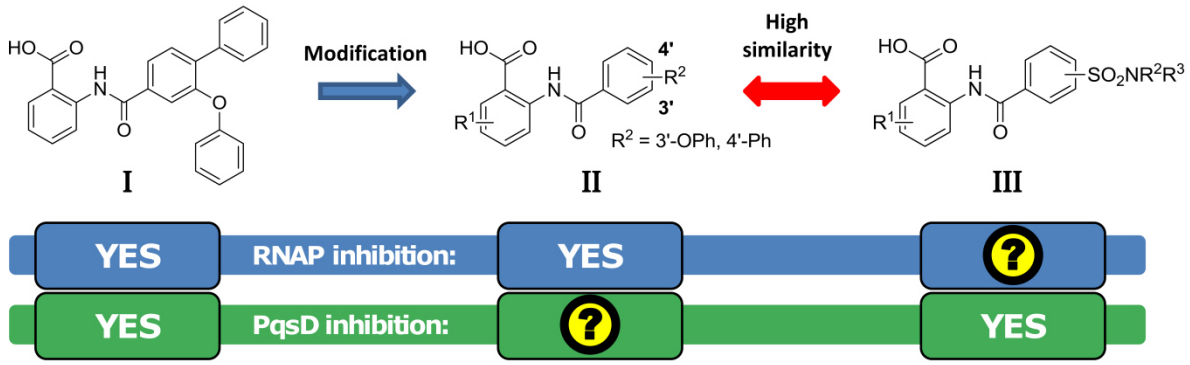

Figure 1. A recently described series of potent novel RNA polymerase (RNAP) inhibitors (II) [7] was derived from a known PqsD inhibitor (I) [6]. The compounds consisting of a benzamidobenzoic acid core are structurally very similar to the class of PqsD inhibitors (III) published by Weidel et al. [8]. This raised the question about selectivity: Do the compounds from class II also inhibit PqsD and are the molecules from class III inhibitors of RNAP?

2. CHEMISTRY

Compounds **1**–**34** and **51**–**86** were prepared as described earlier [7, 8].

As outlined in Scheme 1 the synthesis of the 6-OH substituted anthranilic acid derivative **35** started from 2-amino-6-methoxybenzoic acid **35c**, which was converted into the corresponding hydroxy substituted benzoic acid **35b** by reaction with boron tribromide. Subsequently **35b** was coupled with [1,1'-biphenyl]-4-carbonyl chloride refluxing in toluene to obtain **35a**, which was hydrolyzed with a mixture of 5N LiOH (aq.) and THF, yielding the target compound **35**.

Scheme 1. Synthetic route to compound 35

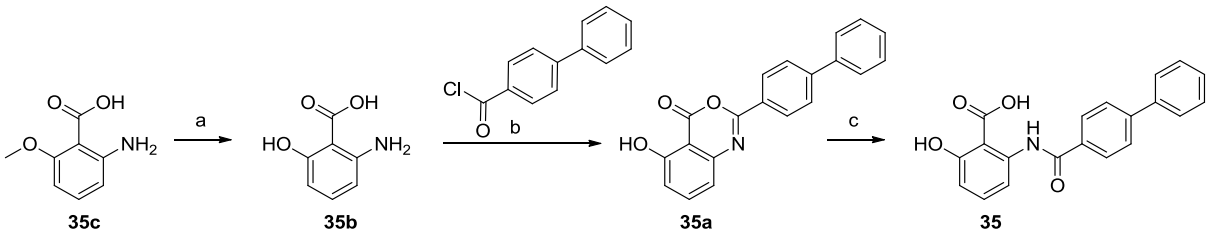

Reagents and conditions: (a) BBr_3, CH_2Cl_2, –78°C → rt; (b) toluene, reflux; (c) LiOH, THF/H_2O, rt.

Scheme 2. Synthetic route to compounds 36−37

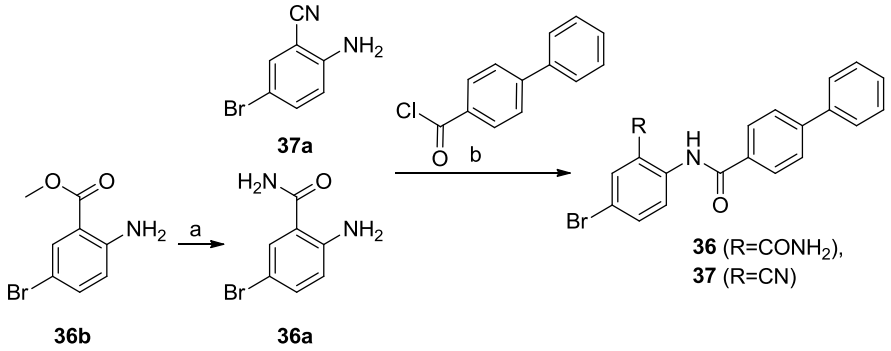

Reagents and conditions: (a) NH_3, MeOH, rt; (b) pyridine, DMAP, rt or toluene, reflux.

Reaction of bromo substituted methyl anthranilate **36b** with ammonia in MeOH at room temperature afforded the benzamide **36a**. The latter and **37a** were coupled with [1,1'-biphenyl]-4-carbonyl chloride in pyridine and catalytic amounts of DMAP at room temperature to obtain products **36** and **37** (Scheme 2).

Scheme 3. Synthetic route to compounds 38−50

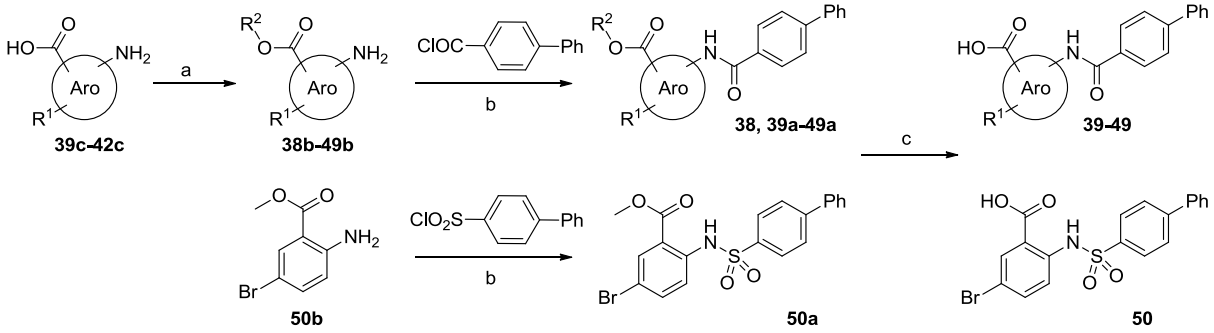

Reagents and conditions: (a) $SOCl_2$, MeOH, reflux; (b) pyridine, DMAP, rt or TEA, CH_2Cl_2, rt or toluene, reflux; (c) NaOH, THF/MeOH/H_2O, rt or KOH, THF/MeOH/H_2O, rt or LiOH, THF/MeOH/H_2O, reflux.

Compounds **38**–**50** were obtained as depicted in Scheme 3. For the synthesis of derivatives containing a carboxylic acid group in *meta* or *para* position to the amino group (**39**–**42**), the methyl esters (**39b**–**42b**) were gained by reaction of the starting compounds (**39c**–**42c**) with thionyl chloride and MeOH under reflux conditions. The other methyl or ethyl esters used were commercially available or were synthesized as

described earlier [9]. A coupling reaction of **38b**–**49b** with [1,1'-biphenyl]-4-carbonyl chloride and **50b** with [1,1'-biphenyl]-4-sulfonyl chloride was performed in pyridine with catalytic amounts of DMAP at room temperature, in CH_2Cl_2 with triethylamine at room temperature or in toluene under reflux conditions. The resulting intermediate esters **39a**–**50a** were cleaved with a mixture of MeOH/THF and 1N NaOH (aq.) or 1N KOH (aq.) or 1N LiOH (aq.) to get the free carboxylic acids **39**–**50**.

3. BIOLOGICAL RESULTS

The inhibitory activities of compounds **1**–**50** against RNAP and PqsD are displayed in Table 1 and 2.

The unsubstituted anthranilic acid **1** has already been described as a potent inhibitor of PqsD [6] and RNAP [7]. Removal of the 3'-OPh or 4'-Ph part of the compound led to **2** and **3**, which only moderately inhibited the two enzymes. Removal of both moieties resulted in the completely inactive compound **4**. In the following, different substituents were introduced into the free positions of the anthranilic acid substructure of **2** or **3**. A chloro substituent in 3-position (**5**) caused a nearly tenfold improvement of PqsD inhibitory activity and a total loss of RNAP inhibition. Lipophilic electron withdrawing substituents in 4-position (**6**–**14**) led to an increased inhibition of both enzymes. Compound **15** bearing a phenyl ring in 4-position is slightly more potent against RNAP, but not against PqsD. A 4-methoxy substituent (**16**) slightly increased activity for both enzymes compared to the unsubstituted compound **2**, whereas a 4-,5-dimethoxy substitution (**17**, **18**) even decreased PqsD inhibition. A shift of the lipophilic electron withdrawing substituents from 4- to 5-position (**19**–**26**) resulted in no substantial changes. The same effect was observed for the phenyl substituent (**27**). The 5-methyl and the 5-cyano compounds **28** and **29** showed a slightly increased inhibition of RNAP. With respect to PqsD inhibition, this is only true for compound **29**. A methoxy substituent in 5-position (**30**) did not relevantly change the activity compared to the unsubstituted compound **2** for both enzymes. Interestingly, **31**, which contains a hydrophilic electron donating hydroxy group in 5-position, that is unfavorable for RNAP inhibition, is a very potent PqsD inhibitor.

Table 1. Inhibitory activities of 1−35 against *E. coli* RNA polymerase and PqsD *in vitro*

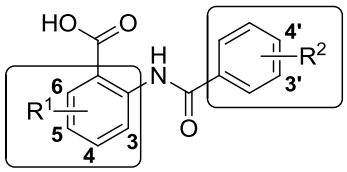

Cpd	R^1	R^2	RNAP inhib.[a,b]	PqsD inhib.[c]	Cpd	R^1	R^2	RNAP inhib.[a,b]	PqsD inhib.[c]
1	H	3'-OPh, 4'-Ph	20 µM	6.6 µM	**19**	5-F	4'-Ph	138 µM	15.2 µM
2	H	4'-Ph	31%	55%	**20**	5-F	3'-OPh	98 µM	57%
3	H	3'-OPh	23%	37%	**21**	5-Cl	4'-Ph	46 µM	3.8 µM
4	H	H	n.i.	n.i.	**22**	5-Br	4'-Ph	31 µM	3.2 µM
5	3-Cl	4'-Ph	n.i.	6.2 µM	**23**	5-Br	3'-OPh	34 µM	4.4 µM
6	4-F	4'-Ph	98 µM	18.2 µM	**24**	5-Br	3'-CH_2Ph	37 µM	5.0 µM
7	4-F	3'-OPh, 4'-Ph	13 µM	6.0 µM	**25**	5-OCF_3	4'-Ph	31 µM	4.0 µM
8	4-Cl	4'-Ph	37 µM	8.7 µM	**26**	5-CF_3	4'-Ph	28 µM	3.4 µM
9	4-Cl	3'-OPh	44 µM	5.7 µM	**27**	5-Ph	3'-OPh	13 µM	7.7 µM
10	4-Cl	3'-OPh, 4'-Ph	9 µM	~5 µM[d]	**28**	5-Me	4'-Ph	139 µM	42%
11	4-Br	4'-Ph	28 µM	3.2 µM	**29**	5-CN	4'-Ph	23% @ 50 µM	8.6 µM
12	4-Br	3'-OPh	34 µM	5.1 µM	**30**	5-OMe	4'-Ph	52%	46%
13	4-NO_2	4'-Ph	36 µM	3.3 µM	**31**	5-OH	4'-Ph	17%	4.2 µM
14	4-CF_3	4'-Ph	27 µM	4.9 µM	**32**	6-F	4'-Ph	14%	21%
15	4-Ph	3'-OPh	14 µM	6.6 µM	**33**	6-Cl	4'-Ph	n.i.	20%
16	4-OMe	4'-Ph	162 µM	43% @ 25 µM	**34**	6-OMe	4'-Ph	n.i.	n.i.
17	4-,5-OMe	4'-Ph	35%	27%	**35**	6-OH	4'-Ph	74 µM	1.3 µM
18	4-,5-OMe	3'-OPh	154 µM	27%					

[a] IC_{50} value (SD <20%) or percentage inhibition at 200 µM (SD <40%) for *E. coli* RNAP; Data represent the mean values of at least three experiments.
[b] RNAP inhibition values originally published by Hinsberger et al. [7] except for **35**
[c] IC_{50} value (SD <23%, except for **10**) or percentage inhibition at 50 µM (SD <40%); Data represent the mean values of at least two experiments.
[d] could not be determined exactly due to high SD
n.i.: no inhibition

The introduction of electron withdrawing lipophilic substituents to the 6-position of the anthranilic acid core (**32**, **33**) and also the introduction of a methoxy group in this position (**34**) led to a drop or even a complete loss of inhibitory activity for both

enzymes. By contrast, 6-hydroxy substitution (**35**) appreciably improved RNAP inhibition and simultaneously led to the most potent PqsD inhibitor of this series (IC_{50} 1.3 µM).

Motivated by these initial interesting results several new analogs with further modifications were synthesized and evaluated. In a first step the carboxylic acid group of compound **22**, which is a very potent inhibitor of both enzymes, was exchanged by $CONH_2$ (**36**), CN (**37**) or COOMe (**38**). As these modifications led to severe solubility problems, no further COOH-replacements were performed. Shifting the carboxylic acid group of **2** to *meta* position (**39**) resulted in a slight increase of activity for RNAP inhibition. However, introduction of a bromo substituent in 4- or 5-position of **39** leading to compounds **40** and **41** reduced inhibitory activity for both enzymes compared to the brominated compounds with the carboxylic acid group in *ortho* position (**11**, **12** and **22**–**24**). A shift of the carboxylic acid group of **2** to the *para* position (**42**) resulted in a hardly soluble compound with a weak RNAP inhibition.

In the next step a bioisosteric replacement of the anthranilic acid phenyl ring by differently substituted thiophenes was performed. The unsubstituted thiophene compounds **43**–**45** showed a considerably improved PqsD inhibitory potency, especially **43**, whereas only for **45** a slightly improved RNAP inhibition was found. Interestingly, adding substituted and unsubstituted phenyl rings to the free positions of the thiophene (**46**–**49**) strongly enhanced RNAP inhibition while PqsD inhibitory activity was concurrently diminished.

Finally, we replaced the phenyl rings connecting amide function of highly potent **22** by a sulfonamide linker. The resulting compound **50** exhibited a reasonable increase of PqsD inhibition while the RNAP inhibitory potency was retained.

To make the SAR complete, the potent PqsD inhibitors published by Weidel et al. [8] (**51**–**86**, SI) were tested for RNAP inhibition. Interestingly, most of the compounds were found not to inhibit RNAP at a concentration of 200 µM or at their highest soluble concentration (SI). Only some compounds containing a 5-NO_2 substituent (**64**), a substituted phenyl ring in 5-position (**74**–**77**), a 3'-SO_2NEtBenzyl (**86**) or a 4'-SO_2NEt_2 moiety (**65**) show a weak to moderate inhibition of RNAP (SI).

Table 2. Inhibitory activities of 36−50 against *E. coli* RNA polymerase and PqsD *in vitro*

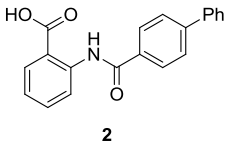
2

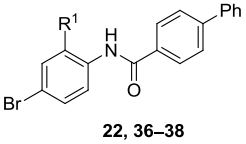
22, 36–38

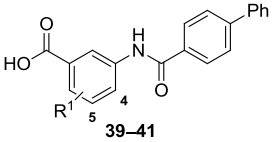
39–41

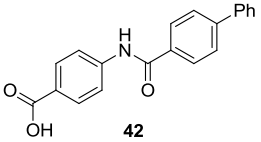
42

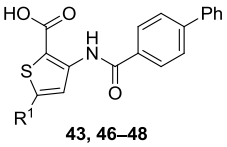
43, 46–48

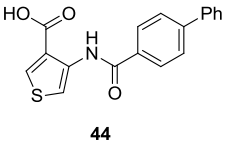
44

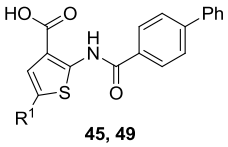
45, 49

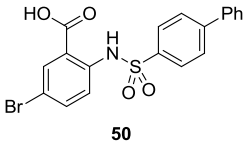
50

Cpd	R^1	RNAP inhibition[a]	PqsD inhibition[b]
2	–	31%	55%
22	COOH	31 µM	3.2 µM
36	$CONH_2$	n.i.[c]	n.i.[c]
37	CN	n.i.[c]	n.i.[c]
38	COOMe	n.i.[c]	n.i.[c]
39	H	31% @ 100 µM	25% @ 25 µM
40	4-Br	25%	n.i.
41	5-Br	110 µM	32.6 µM
42	–	15% @ 100 µM	n.i. @ 10 µM
43	H	28%	5.2 µM
44	–	33%	19.5 µM
45	H	161 µM	15.7 µM
46	Ph	10 µM	9.8 µM
47	*p*-Cl-Ph	13 µM	35%
48	*p*-OMe-Ph	9 µM	45%
49	Ph	33% @ 50 µM	28%
50	–	35 µM	1.3 µM

[a] IC_{50} value (SD <20%) or percentage inhibition at 200 µM (SD <40%) for *E. coli* RNAP; Data represent the mean values of at least three experiments.
[b] IC_{50} value (SD <20%) or percentage inhibition at 50 µM (SD <40%); Data represent the mean values of at least two experiments.
[c] low solubility: no inhibition in saturated solution
n.i.: no inhibition

4. DISCUSSION

In this paper we could demonstrate that it is possible to convert the unsubstituted benzamidobenzoic acid **4** into potent PqsD inhibitors by structural modifications. As already shown for RNAP [7] substituents in 3'- or 4'-position are also a minimum requirement for a moderate inhibition of PqsD (**2**, **3**). The combination of substituents in both positions, however, results in very potent PqsD inhibitor **1** [6]. Another very effective way to increase potency of **2** and **3** is the introduction of lipophilic electron withdrawing substituents or phenyl rings in 4- or 5-position of the anthranilic acid core (**6**–**15**, **19**–**27**). The same phenomenon has already been described for the sulfamoylbenzamidobenzoic acids [8].

However, the disadvantage all described modifications have in common is that they do not selectively enhance the inhibitory potency for PqsD, but also for RNAP. This is an unwanted effect of the inhibitors, as antibacterial activity caused by potent RNAP inhibition would provoke selective pressure [3], which is in contradiction with the anti-virulence concept by PqsD inhibition. Therefore it is of particular interest that the presented series of compounds also contain structural modifications which selectively enhance PqsD inhibitory potency and do not affect or even decrease RNAP inhibition (Fig. 2).

For example the introduction of a 3-Cl substituent (**5**), which strongly increases PqsD inhibition, leads to a total loss of activity for RNAP. A similar observation is made for the introduction of a 5-OH group (**31**), which also results in a very potent and highly PqsD selective compound. The introduction of a OH group in 6-position (**35**) causes a slight increase in RNAP inhibition, however, improvement of PqsD inhibitory activity is much stronger leading to a compound which is about 50 times more potent on PqsD than on RNAP. Apart from introduction of substituents into the anthranilic acid core, selectivity can be gained by bioisosteric replacement. Via exchange of the anthranilic acid phenyl ring by a thiophene, potent and selective PqsD inhibitors can be obtained without affecting the moderate RNAP inhibitory activity (esp. **43**). However, the introduction of a phenyl substituent into **43** should be avoided, as this modification results in a loss or even an inversion of selectivity. A further option to gain selectivity is the replacement of the amide function by a sulfonamide. This slightly increases PqsD inhibition without affecting RNAP activity.

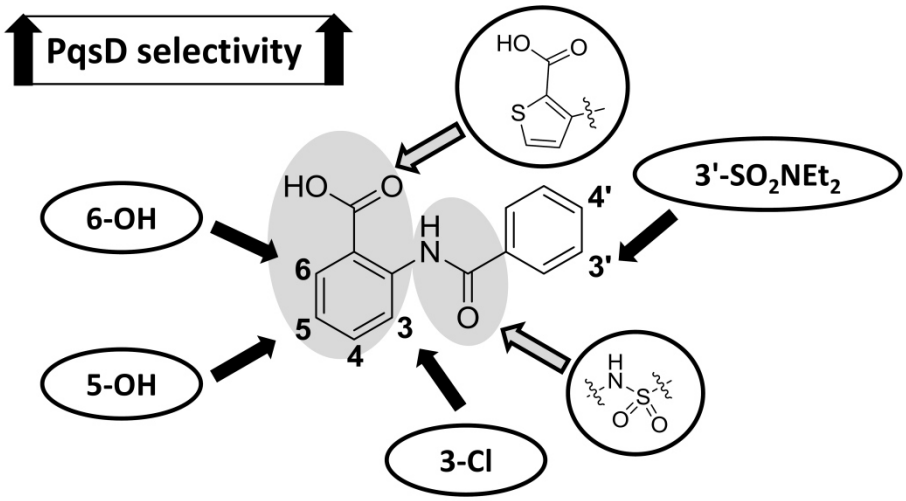

Figure 2. Structural modifications generating selectivity in favor of PqsD inhibition over RNAP inhibition in the class of benzamidobenzoic acids

Regarding the recently published PqsD inhibitors [8] (**51**–**86**, SI) it is striking that most of these compounds do not contain any of the structural features that we identified in this study to be causing PqsD selectivity. Instead, many of them contain substituents that are also beneficial for RNAP inhibition in the class of benzamidobenzoic acids, as described earlier [7] (e.g., Br, Cl, CF_3). This raised the question whether these sulfamoylbenzamidobenzoic acids are, beside their strong inhibition of PqsD, also selective. Interestingly, only few of them slightly or moderately inhibit RNAP. This reveals that in the class of benzamidobenzoic acids selectivity between PqsD and RNAP can also be gained by variation of R^2. Apart from a few exceptions, all aliphatically substituted sulfonamide substituents (e.g., SO_2NEt_2, $SO_2N(n\text{-}Pr)_2$) in 3' position are suitable to obtain selectivity over RNAP.

As the compounds containing a further substituted 5-Ph or a 5-NO_2 substituent moderately inhibit RNAP, despite of the aliphatically substituted sulfonamide substituent in 3'-position, these RNAP inhibition favoring moieties should be avoided. Compound **86**, containing a 3'-SO_2NEtBenzyl rest, inhibits RNAP to a similar extent as **2** and **3**, indicating that in general aromatics in this part of the compound are crucial for RNAP inhibition and therefore should not be used as R^2. Another PqsD inhibitor of the sulfamoylbenzamidobenzoic acid series which shows an RNAP inhibitory activity is compound **65** bearing the SO_2NEt_2 substituent not in 3'- but in 4'-position. Actually, this was not an unexpected observation as earlier we have been

able to demonstrate that a very similar inhibitor of transcription/translation (TT) carrying a 4'-$SO_2N(n\text{-}Pr)_2$ substituent is a quite potent RNAP inhibitor [7]. This results in the conclusion that a 4'-sulfonamide substituent is not suitable for selective PqsD inhibition.

5. CONCLUSION

As emergence of bacterial resistance against clinically used antibiotics is becoming a major public health problem [1], the novel anti-virulence concept by PqsD inhibition is of special interest [10]. For following this strategy and avoiding selective pressure it is important that PqsD inhibitors do not cause bacterial cell death by inhibition of pivotal enzymes [3] like RNAP. In this work we presented a series of new potent PqsD inhibitors of the benzamidobenzoic acid class and identified the structural modifications that are necessary to convert potent RNAP inhibitors into selective PqsD inhibitors. It is striking that already simple bioisosteric replacements led to a notable gain of selectivity. For further optimization of potency and selectivity it is conceivable to combine some of these modifications into one structure. As the *in vitro* PqsD inhibitory activities of our compounds are promising, they will be further evaluated *in vivo*.

6. EXPERIMENTAL SECTION

6.1 General Directions

Chemical names follow IUPAC nomenclature. Starting materials were purchased from Sigma-Aldrich, Acros, Maybridge, Combi Blocks, Fluka, ABCR, Alfa Aesar, Apollo and were used without purification.

Column chromatography (CC) was performed on silica gel (63–200 µm), preparative thin layer chromatography (TLC) on 1 mm SIL G-100 UV254 glass plates (Macherey-Nagel), and reaction progress was monitored by TLC on Alugram SIL G UV254 (Macherey-Nagel).

^1H NMR and ^{13}C NMR spectra were recorded on a Bruker AM500 spectrometer (500 MHz and 125 MHz) at 300 K in $CDCl_3$ or CD_3SOCD_3. Chemicals shifts are reported in δ values (ppm), the

hydrogenated residues of deuterated solvent were used as internal standard ($CDCl_3$: δ = 7.27 ppm in ^{1}H NMR and δ = 77.0 ppm in ^{13}C NMR, CD_3SOCD_3: δ = 2.50 ppm in ^{1}H NMR and δ = 39.5 ppm in ^{13}C NMR). Signals are described as s, d, t, dd, ddd, dt and m for singlet, doublet, triplet, doublet of doublet, doublet of doublet of doublet, doublet of triplet and multiplet, respectively. Coupling constants (*J*) are given in Hertz (Hz).

The reported yields are the isolated yields of purified material and are not optimized.

Purity of compounds **35**–**50** was determined using LC/MS as follows:

The SpectraSystems®-LC-system consisted of a pump, an autosampler, and a UV detector. Mass spectrometry was performed on a MSQ® electro spray mass spectrometer (Thermo Fisher, Dreieich, Germany). The system was operated by the standard software Xcalibur®. A RP C18 NUCLEODUR® 100-5 (125 x 3 mm) column (Macherey-Nagel GmbH, Duehren, Germany) was used as stationary phase. All solvents were HPLC grade.

Solvent system: In a gradient run the percentage of acetonitrile (containing 0.1% triflouro-acetic acid) in 0.1% triflouro-acetic acid was increased from an initial concentration of 0% at 0 min to 100% at 15 min and kept at 100% for 5 min.

The injection volume was 10 µL and flow rate was set to 800 µL/min. MS analysis was carried out at a spray voltage of 3800 V, a capillary temperature of 350 °C and a source CID of 10 V. Spectra were acquired in positive mode from 100 to 1000 m/z and at 254 nm for the UV trace.

All tested compounds have >95% chemical purity as measured by HPLC.

Melting points were determined on a Stuart Scientific melting point apparatus SMP3 and are uncorrected.

6.2 Chemistry

6.2.1 General Procedure for the synthesis of methyl aminobenzoates 39b–42b.

A solution of the appropriate 2-aminobenzoic acid (1 equiv) in MeOH was cooled to 0 °C followed by a dropwise addition of thionyl chloride (2.5 equiv). The mixture was refluxed for 24 h. After evaporation of the solvent and neutralization by addition of a saturated aqueous $NaHCO_3$ solution, the mixture was extracted with EtOAc and the combined organic layers were dried over $MgSO_4$. Purification by CC (*n*-hexane/EtOAc) provided the title compounds.

Methyl 3-aminobenzoate (**39b**)

yellow oil, yield: 100%. ^{1}H NMR (500 MHz, $CDCl_3$) δ = 7.45–7.41 (m, 1 H) 7.38–7.33 (m, 1 H), 7.24–7.19 (m, 1 H), 6.86 (ddd, *J* = 8.0, 2.4, 0.9 Hz, 1 H), 3.89 (s, 3 H, OCH_3), 3.78 (br. s., 2 H, NH_2)

ppm. ^{13}C NMR (125 MHz, $CDCl_3$) δ = 167.3, 146.4, 131.1, 129.2, 119.7, 119.4, 115.7, 52.0 (OCH_3) ppm. LC/MS: m/z = 193 [M + H^+ + CH_3CN]; t_R = 3.44 min; > 99.9% pure (UV).

Methyl 3-amino-4-bromobenzoate (**40b**)

brown solid, yield: 83%. ^{1}H NMR (500 MHz, $CDCl_3$) δ = 7.47 (d, *J* = 8.3 Hz, 1 H), 7.43 (d, *J* = 2.0 Hz, 1 H), 7.26 (dd, *J* = 8.3, 2.0 Hz, 1 H), 4.23 (br. s., 2 H, NH_2), 3.89 (s, 3 H, OCH_3) ppm. ^{13}C NMR (125 MHz, $CDCl_3$) δ = 166.7, 144.1, 132.6, 130.3, 120.0, 116.3, 114.2, 52.2 (OCH_3) ppm. LC/MS: m/z = 230 and 232 [M + H^+], 271 and 273 [M + H^+ + CH_3CN]; t_R = 10.13 min; 98.8% pure (UV).

Methyl 3-amino-5-bromobenzoate (**41b**)

yellow solid, yield: 91%. ^{1}H NMR (500 MHz, $CDCl_3$) δ = 7.54–7.52 (m, 1 H), 7.26 (dd, *J* = 2.2, 1.3 Hz, 1 H), 6.99 (dd, *J* = 2.2, 1.6 Hz, 1 H), 3.89 (s, 3 H, OCH_3), 3.86 (br. s., 2 H, NH_2) ppm. ^{13}C NMR (125 MHz, $CDCl_3$) δ = 166.0, 147.7, 132.6, 122.9, 122.2, 121.6, 114.6, 52.3 (OCH_3) ppm. LC/MS: m/z = 230 and 232 [M + H^+], 271 and 273 [M + H^+ + CH_3CN]; t_R = 9.22 min; 97.0% pure (UV).

Methyl 4-aminobenzoate (**42b**)

yellow solid, yield: 99%. ^{1}H NMR (500 MHz, $CDCl_3$) δ = 7.89–7.81 (m, 2 H), 6.66–6.60 (m, 2 H), 4.10 (br. s., 2 H, NH_2), 3.85 (s, 3 H, OCH_3) ppm. ^{13}C NMR (125 MHz, $CDCl_3$) δ = 167.1, 150.8, 131.5, 119.6, 113.7, 51.6 (OCH_3) ppm. LC/MS: m/z = 193 [M + H^+ + CH_3CN]; t_R = 5.21 min; > 99.9% pure (UV).

6.2.2 General Procedures for the synthesis of methyl benzamidobenzoate or methyl benzamidothiophenecarboxylate derivatives 36–38, 39a–49a (amide coupling reactions).

Three different amide coupling procedures were used to obtain the title compounds:

6.2.2.1 General Procedure for the synthesis of 38, 39a, 41a–43a.

The appropriate alkyl aminobenzoate or alkyl aminothiophenecarboxylate (1 equiv) was added to a solution of the acyl chloride (1.2 equiv) in CH_2Cl_2 under a N_2 atmosphere. After the addition of TEA (2 equiv) the reaction mixture was stirred for 18 h at room temperature. For purification the solvent was evaporated and the remaining solid was suspended in MeOH. After filtration the precipitate was washed with MeOH to provide the pure compound.

Methyl 2-([1,1'-biphenyl]-4-ylcarboxamido)-5-bromobenzoate (**38**)

slightly yellow solid, yield: 26%. ^{1}H NMR (500 MHz, $CDCl_3$) δ = 12.01 (br. s, 1 H, NH), 8.91 (d, *J* = 9.1 Hz, 1 H), 8.22 (d, *J* = 2.5 Hz, 1 H), 8.15–8.08 (m, 2 H), 7.79–7.74 (m, 2 H), 7.71 (dd, *J* = 9.1, 2.5 Hz, 1 H), 7.68–7.62 (m, 2 H), 7.54–7.46 (m, 2 H), 7.45–7.38 (m, 1 H), 4.00 (s, 3 H, OCH_3) ppm. ^{13}C NMR (125 MHz, $CDCl_3$) δ = 168.0, 165.4, 144.9, 141.0, 139.9, 137.5, 133.5, 133.1, 128.9, 128.1, 127.9, 127.5, 127.2, 122.1, 116.6, 115.0, 52.8 (OCH_3) ppm. LC/MS: m/z = 410 and 412 [M + H^+], 821 and 823 [2M + H^+]; t_R = 16.41 min; 98.4% pure (UV).

Methyl 3-([1,1'-biphenyl]-4-ylcarboxamido)benzoate (**39a**)

white solid, yield: 62%. ^{1}H NMR (500 MHz, DMSO-d_6) δ = 10.51 (s, 1 H, NH), 8.50 (s, 1 H), 8.13–8.07 (m, 3 H), 7.85 (d, *J* = 8.3 Hz, 2 H), 7.77 (d, *J* = 7.3 Hz, 2 H), 7.74–7.68 (m, 1 H), 7.55–7.48 (m, 3 H), 7.47–7.41 (m, 1 H), 3.88 (s, 3 H, OCH_3) ppm. ^{13}C NMR (125 MHz, DMSO-d_6) δ = 166.1, 165.3, 143.3,

139.6, 139.0, 133.3, 130.0, 129.1, 129.1, 128.4, 128.2, 126.9, 126.6, 124.7, 124.2, 120.8, 52.2 (OCH_3) ppm. LC/MS: m/z = 332 [M + H^+], 373 [M + H^+ + CH_3CN], 663 [2M + H^+]; t_R = 12.50 min; 97.7% pure (UV).

Methyl 3-([1,1'-biphenyl]-4-ylcarboxamido)-5-bromobenzoate (**41a**)
beige solid, yield: 51%. ^{1}H NMR (500 MHz, $CDCl_3$) δ = 8.37–8.33 (m, 1 H), 8.23 (s, 1 H, NH), 8.12–8.07 (m, 1 H), 7.99–7.92 (m, 3 H), 7.72–7.69 (m, 2 H), 7.64–7.61 (m, 2 H), 7.50–7.45 (m, 2 H), 7.45–7.38 (m, 1 H), 3.91 (s, 3 H, OCH_3) ppm. ^{13}C NMR (125 MHz, $CDCl_3$) δ = 165.5, 165.5, 145.1, 139.6, 139.4, 132.6, 132.3, 129.0, 128.3, 128.2, 127.7, 127.5, 127.3, 127.2, 122.9, 119.7, 52.5 (OCH_3) ppm. LC/MS: m/z = 410 and 412 [M + H^+], 451 and 453 [M + H^+ + CH_3CN], 821 and 823 [2M + H^+]; t_R = 14.91 min; 97.5% pure (UV).

Methyl 4-([1,1'-biphenyl]-4-ylcarboxamido)benzoate (**42a**)
slightly yellow solid, yield: 43%. ^{1}H NMR (500 MHz, DMSO-d_6) δ = 10.61 (s, 1 H, NH), 8.08 (d, *J* = 8.3 Hz, 2 H), 7.98 (s, 4 H), 7.86 (d, *J* = 8.3 Hz, 2 H), 7.81–7.74 (m, 2 H), 7.55–7.48 (m, 2 H), 7.47–7.40 (m, 1 H), 3.84 (s, 3 H, OCH_3) ppm. ^{13}C NMR (125 MHz, DMSO-d_6) δ = 165.8, 165.6, 143.7, 143.4, 139.0, 133.3, 130.1, 129.1, 128.5, 128.2, 126.9, 126.6, 124.3, 119.6, 51.9 (OCH_3) ppm. LC/MS: m/z = 332 [M + H^+], 373 [M + H^+ + CH_3CN], 663 [2M + H^+]; t_R = 12.59 min; > 99.9% pure (UV).

Methyl 3-([1,1'-biphenyl]-4-ylcarboxamido)thiophene-2-carboxylate (**43a**)
beige solid, yield: 19%. ^{1}H NMR (500 MHz, $CDCl_3$) δ = 11.25 (s, 1 H, NH), 8.34 (d, *J* = 5.5 Hz, 1 H), 8.13–8.08 (m, 2 H), 7.78–7.72 (m, 2 H), 7.67–7.64 (m, 2 H), 7.55 (d, *J* = 5.5 Hz, 1 H), 7.52–7.46 (m, 2 H), 7.45–7.37 (m, 1 H), 3.95 (s, 3 H, OCH_3) ppm. ^{13}C NMR (125 MHz, $CDCl_3$) δ = 165.2, 163.9, 145.3, 145.1, 139.9, 132.3, 131.9, 128.9, 128.1, 128.0, 127.5, 127.2, 122.4, 110.4, 52.1 (OCH_3) ppm. LC/MS: m/z = 338 [M + H^+], 379 [M + H^+ + CH_3CN], 675 [2M + H^+]; t_R = 14.87 min; 94.9% pure (UV).

6.2.2.2 General Procedure for the synthesis of 37, 40a, 44a–47a, 49a. The appropriate alkyl aminobenzoate or alkyl aminothiophenecarboxylate (1 equiv) and a catalytic amount of DMAP were added to a suspension of the acyl chloride (1.5 equiv) in pyridine under a N_2 atmosphere. The reaction mixture was stirred for 18 h at room temperature and 2 M HCl was added. The mixture was extracted with EtOAc, the combined organic layers washed with saturated $NaHCO_3$ and dried over $MgSO_4$. For purification the solvent was evaporated and the remaining solid was suspended in MeOH. After filtration the precipitate was washed with MeOH (and EtOAc in case of **45a**) to provide the pure compound.

N-(4-Bromo-2-cyanophenyl)-[1,1'-biphenyl]-4-carboxamide (**37**)
white solid, yield: 35%. Mp: 232–233 °C. ^{1}H NMR (500 MHz, DMSO-d_6) δ = 10.72 (s, 1 H, NH), 8.19 (d, *J* = 2.3 Hz, 1 H), 8.12–8.08 (m, 2 H), 7.95 (dd, *J* = 8.8, 2.3 Hz, 1 H), 7.91–7.86 (m, 2 H), 7.80–7.75 (m, 2 H), 7.58 (d, *J* = 8.8 Hz, 1 H), 7.55–7.49 (m, 2 H), 7.47–7.40 (m, 1 H) ppm. ^{13}C NMR (125 MHz, DMSO-d_6) δ = 165.2, 143.8, 139.9, 138.9, 136.8, 135.2, 132.0, 129.1, 128.6, 128.4, 128.3, 127.0, 126.8, 117.9, 115.6, 111.0 ppm. LC/MS: m/z = 377 and 379 [M + H^+]; t_R = 13.63 min; 98.0% pure (UV).

Methyl 3-([1,1'-biphenyl]-4-ylcarboxamido)-4-bromobenzoate (**40a**)
white solid, yield: 71%. ^{1}H NMR (500 MHz, $CDCl_3$) δ = 9.21 (d, *J* = 2.2 Hz, 1 H), 8.53 (s, 1 H, NH), 8.05–8.02 (m, 2 H), 7.77–7.64 (m, 6 H), 7.52–7.47 (m, 2 H), 7.45–7.40 (m, 1 H), 3.95 (s, 3 H, OCH_3) ppm. ^{13}C NMR (125 MHz, $CDCl_3$) δ = 166.2, 164.9, 145.3, 139.7, 136.0, 132.8, 132.3, 130.7, 129.0,

128.2, 127.7, 127.6, 127.2, 126.2, 122.5, 118.7, 52.4 (OCH_3) ppm. LC/MS: m/z = 410 and 412 [M + H^+], 451 and 453 [M + H^+ + CH_3CN], 821 and 823 [2M + H^+]; t_R = 14.62 min; 99.0% pure (UV).

Methyl 4-([1,1'-biphenyl]-4-ylcarboxamido)thiophene-3-carboxylate (**44a**)
beige solid, yield: 58%. ^{1}H NMR (500 MHz, $CDCl_3$) δ = 11.06 (s, 1 H, NH), 8.24 (d, *J* = 3.5 Hz, 1 H), 8.12 (d, *J* = 3.5 Hz, 1 H), 8.10–8.07 (m, 2 H), 7.76–7.74 (m, 2 H), 7.67–7.64 (m, 2 H), 7.51–7.47 (m, 2 H), 7.44–7.38 (m, 1 H), 3.97 (s, 3 H, OCH_3) ppm. ^{13}C NMR (125 MHz, $CDCl_3$) δ = 164.9, 164.4, 144.7, 140.0, 136.7, 132.6, 128.9, 128.0, 127.7, 127.5, 127.2, 121.6, 110.8, 52.1 (OCH_3) ppm. LC/MS: m/z = 338 [M + H^+], 379 [M + H^+ + CH_3CN], 675 [2M + H^+]; t_R = 15.41 min; 94.2% pure (UV).

Ethyl 2-([1,1'-biphenyl]-4-ylcarboxamido)thiophene-3-carboxylate (**45a**)
brown solid, yield: 42%. ^{1}H NMR (500 MHz, $CDCl_3$) δ = 12.09 (br. s., 1 H, NH), 8.15–8.09 (m, 2 H), 7.79–7.74 (m, 2 H), 7.68–7.63 (m, 2 H), 7.53–7.47 (m, 2 H), 7.45–7.39 (m, 1 H), 7.29 (d, *J* = 5.7 Hz, 1 H), 6.81 (d, *J* = 5.7 Hz, 1 H), 4.42 (q, *J* = 7.2 Hz, 2 H, OCH_2), 1.44 (t, *J* = 7.2 Hz, 3 H, CH_3) ppm. ^{13}C NMR (125 MHz, $CDCl_3$) δ = 166.1, 163.3, 149.3, 145.4, 139.7, 130.7, 129.0, 128.2, 128.0, 127.6, 127.2, 123.9, 116.2, 113.3, 60.8 (OCH_2), 14.4 (CH_3) ppm. LC/MS: m/z = 352 [M + H^+], 393 [M + H^+ + CH_3CN], 703 [2M + H^+]; t_R = 16.46 min; 97.2% pure (UV).

Methyl 3-([1,1'-biphenyl]-4-ylcarboxamido)-5-phenylthiophene-2-carboxylate (**46a**)
beige solid, yield: 43%. ^{1}H NMR (500 MHz, $CDCl_3$) δ = 11.28 (s, 1 H, NH), 8.60 (s, 1 H), 8.15–8.09 (m, 2 H), 7.78–7.73 (m, 4 H), 7.68–7.64 (m, 2 H), 7.52–7.39 (m, 6 H), 3.97 (s, 3 H, OCH_3) ppm. ^{13}C NMR (125 MHz, $CDCl_3$) δ = 165.2, 164.0, 150.2, 145.7, 145.1, 139.9, 133.2, 132.3, 129.3, 129.1, 129.0, 128.2, 128.0, 127.6, 127.2, 126.2, 118.1, 109.1, 52.1 (OCH_3) ppm. LC/MS: m/z = 414 [M + H^+], 827 [2M + H^+]; t_R = 17.93 min; 97.1% pure (UV).

Methyl 3-([1,1'-biphenyl]-4-ylcarboxamido)-5-(4-chlorophenyl)thiophene-2-carboxylate (**47a**)
beige solid, yield: 28%. ^{1}H NMR (500 MHz, $CDCl_3$) δ = 11.26 (s, 1 H, NH), 8.58 (s, 1 H), 8.13–8.09 (m, *J* = 8.2 Hz, 2 H), 7.78–7.75 (m, *J* = 8.5 Hz, 2 H), 7.68–7.62 (m, 4 H), 7.52–7.48 (m, 2 H), 7.46–7.38 (m, 3 H), 3.97 (s, 3 H, OCH_3) ppm. ^{13}C NMR (125 MHz, $CDCl_3$) δ = 165.1, 164.0, 148.6, 145.7, 145.2, 139.8, 135.3, 132.1, 131.7, 129.3, 129.0, 128.2, 128.0, 127.6, 127.4, 127.2, 118.4, 109.3, 52.2 (OCH_3) ppm. LC/MS: m/z = 448 and 450 [M + H^+], 895 and 899 [2M + H^+]; t_R = 18.42 min; 99.1% pure (UV).

Ethyl 2-([1,1'-biphenyl]-4-ylcarboxamido)-5-phenylthiophene-3-carboxylate (**49a**)
yellow solid, yield: 40%. ^{1}H NMR (500 MHz, $CDCl_3$) δ = 12.10 (s, 1 H, NH), 8.16–8.10 (m, 2 H), 7.80–7.77 (m, 2 H), 7.68–7.62 (m, 4 H), 7.52–7.48 (m, 3 H), 7.46–7.38 (m, 3 H), 7.33–7.28 (m, 1 H), 4.45 (q, *J* = 7.3 Hz, 2 H, OCH_2), 1.47 (t, *J* = 7.3 Hz, 3 H, CH_3) ppm. ^{13}C NMR (125 MHz, $CDCl_3$) δ = 166.0, 163.3, 148.6, 145.5, 139.7, 134.0, 133.8, 130.7, 129.0, 129.0, 128.3, 128.1, 127.6, 127.5, 127.3, 125.5, 119.3, 114.1, 61.0 (OCH_2), 14.4 (CH_3) ppm. LC/MS: m/z = 428 [M + H^+], 469 [M + H^+ + CH_3CN], 855 [2M + H^+]; t_R = 18.34 min; > 99.9% pure (UV).

6.2.2.3 General Procedure for the synthesis of 36 and 48a. The appropriate alkyl aminobenzoate or alkyl aminothiophenecarboxylate (1 equiv) and the acyl chloride (1.2 equiv) were dissolved in toluene and refluxed for 4 h (**36**) or 18 h (**48a**). For purification the solvent was removed under reduced pressure and the remaining solid suspended in MeOH. After filtration the precipitate was washed with MeOH to yield the pure compound.

N-(4-Bromo-2-carbamoylphenyl)-[1,1'-biphenyl]-4-carboxamide (**36**)
white solid, yield: 79%. Mp: 254–256 °C. ^{1}H NMR (500 MHz, DMSO-d_6) δ = 12.93 (s, 1 H, NH), 8.68 (d, J = 9.1 Hz, 1 H), 8.54 (br. s., 1 H), 8.11 (d, J = 2.5 Hz, 1 H), 8.04–7.97 (m, 3 H), 7.90–7.86 (m, 2 H), 7.79–7.74 (m, 3 H), 7.54–7.48 (m, 2 H), 7.46–7.41 (m, 1 H) ppm. ^{13}C NMR (125 MHz, DMSO-d_6) δ = 169.8, 164.2, 143.7, 139.4, 138.9, 135.2, 133.1, 131.2, 129.1, 128.3, 127.7, 127.2, 127.0, 122.1, 121.1, 114.4 ppm. LC/MS: m/z = 395 and 397 [M + H$^+$], 789 and 791 [2M + H$^+$]; t_R = 14.07 min; > 99.9% pure (UV).

Methyl 3-([1,1'-biphenyl]-4-ylcarboxamido)-5-(4-methoxyphenyl)thiophene-2-carboxylate (**48a**)
yellow solid, yield: 82%. ^{1}H NMR (500 MHz, $CDCl_3$) δ = 11.29 (s, 1 H, NH), 8.49 (s, 1 H), 8.15–8.09 (m, 2 H), 7.78–7.74 (m, 2 H), 7.70–7.63 (m, 4 H), 7.54–7.47 (m, 2 H), 7.46–7.39 (m, 1 H), 7.00–6.92 (m, 2 H), 3.96 (s, 3 H, OCH_3), 3.87 (s, 3 H, OCH_3) ppm. ^{13}C NMR (125 MHz, $CDCl_3$) δ = 165.3, 164.0, 160.6, 150.4, 145.8, 145.1, 139.9, 132.3, 129.0, 128.1, 128.0, 127.6, 127.5, 127.2, 125.9, 117.0, 114.5, 108.0, 55.4 (OCH_3), 52.0 (OCH_3) ppm. LC/MS: m/z = 444 [M + H$^+$], 485 [M + H$^+$ + CH_3CN], 887 [2M + H$^+$]; t_R = 17.96 min; 97.3% pure (UV).

6.2.3 General Procedure for the synthesis of benzamidobenzoate or benzamidothiophenecarboxylate derivatives 39–47, 50 (ester cleavage).

The methyl or ethyl esters of the title compounds (**39a**–**47a, 50a**) were hydrolyzed with 5 M NaOH in THF/MeOH (2:1) at room temperature (18 h). The mixture was acidified by the addition of 1 M HCl, filtered and the precipitate was washed with 1 M HCl to provide the title compounds (**39**, **50**). If the compound was not pure at this stage of procedure it was washed with CH_2Cl_2 (**41**–**43**) or CH_2Cl_2 and MeOH (**40**, **44**–**47**).

3-([1,1'-Biphenyl]-4-ylcarboxamido)benzoic acid (**39**)
white solid, yield: 42%. Mp: 288–289 °C. ^{1}H NMR (500 MHz, DMSO-d_6) δ = 10.49 (s, 1 H, NH), 8.47 (s, 1 H), 8.15–8.05 (m, 3 H), 7.84 (d, J = 8.3 Hz, 2 H), 7.76 (d, J = 7.3 Hz, 2 H), 7.72–7.65 (m, 1 H), 7.56–7.47 (m, 3 H), 7.47–7.36 (m, 1 H) ppm. ^{13}C NMR (125 MHz, DMSO-d_6) δ = 167.2, 165.3, 143.3, 139.5, 139.1, 133.4, 131.3, 129.1, 128.9, 128.4, 128.2, 126.9, 126.6, 124.5, 121.2, 116.9 ppm. LC/MS: m/z = 318 [M + H$^+$], 359 [M + H$^+$ + CH_3CN]; t_R = 11.17 min; 99.0% pure (UV).

3-([1,1'-Biphenyl]-4-ylcarboxamido)-4-bromobenzoic acid (**40**)
white solid, yield: 89%. Mp: 281–282 °C. ^{1}H NMR (500 MHz, DMSO-d_6) δ = 10.24 (s, 1 H, NH), 8.15–8.12 (m, 2 H), 8.12–8.09 (m, 1 H), 7.90–7.85 (m, 3 H), 7.80–7.74 (m, 3 H), 7.55–7.49 (m, 2 H), 7.46–7.40 (m, 1 H) ppm. ^{13}C NMR (125 MHz, DMSO-d_6) δ = 166.3, 165.1, 143.5, 139.1, 136.9, 133.2, 132.5, 130.8, 129.1, 129.0, 128.4, 128.2, 128.2, 127.0, 126.7, 125.5 ppm. LC/MS: m/z = 396 and 398 [M + H$^+$], 437 and 439 [M + H$^+$ + CH_3CN]; t_R = 12.60 min; 97.3% pure (UV).

3-([1,1'-Biphenyl]-4-ylcarboxamido)-5-bromobenzoic acid (**41**)
beige solid, yield: 94%. Mp: 285–286 °C. ^{1}H NMR (500 MHz, DMSO-d_6) δ = 10.60 (s, 1 H, NH), 8.46–8.37 (m, 2 H), 8.12–8.06 (m, 2 H), 7.89–7.84 (m, 2 H), 7.81–7.73 (m, 3 H), 7.54–7.48 (m, 2 H), 7.48–7.39 (m, 1 H) ppm. ^{13}C NMR (125 MHz, DMSO-d_6) δ = 165.9, 165.5, 143.5, 141.0, 139.0, 133.2, 132.9, 129.1, 128.5, 128.2, 126.9, 126.7, 126.5, 126.2, 121.4, 119.9 ppm. LC/MS: m/z = 396 and 398 [M + H$^+$], 437 and 439 [M + H$^+$ + CH_3CN]; t_R = 13.01 min; 99.4% pure (UV).

4-([1,1'-Biphenyl]-4-ylcarboxamido)benzoic acid (**42**) [12]
beige solid, yield: 92%. Mp: 337 °C (decomposition). ^{1}H NMR (500 MHz, DMSO-d_6) δ = 10.58 (s, 1 H, NH), 8.08 (d, *J* = 8.3 Hz, 2 H), 7.99–7.91 (m, 4 H), 7.85 (d, *J* = 8.3 Hz, 2 H), 7.80–7.74 (m, 2 H), 7.54–7.48 (m, 2 H), 7.46–7.40 (m, 1 H) ppm. ^{13}C NMR (125 MHz, DMSO-d_6) δ = 167.0, 165.6, 143.4, 143.3, 139.1, 133.4, 130.3, 129.1, 128.5, 128.2, 127.0, 126.6, 125.5, 119.5 ppm. LC/MS: m/z = 318 [M + H^+], 359 [M + H^+ + CH_3CN]; t_R = 11.29 min; 99.4% pure (UV).

3-([1,1'-Biphenyl]-4-ylcarboxamido)thiophene-2-carboxylic acid (**43**) [13]
yellow solid, yield: 87%. Mp: 242–243 °C. ^{1}H NMR (500 MHz, DMSO-d_6) δ = 11.27 (s, 1 H, NH), 8.13 (d, *J* = 5.5 Hz, 1 H), 8.01 (d, *J* = 8.5 Hz, 2 H), 7.95–7.87 (m, 3 H), 7.80–7.73 (m, 2 H), 7.54–7.48 (m, 2 H), 7.47–7.39 (m, 1 H) ppm. ^{13}C NMR (125 MHz, DMSO-d_6) δ = 165.5, 163.0, 144.0, 143.8, 138.8, 132.6, 132.1, 129.1, 128.4, 127.8, 127.3, 127.0, 121.8, 112.0 ppm. LC/MS: m/z = 324 [M + H^+], 365 [M + H^+ + CH_3CN], 647 [2M + H^+]; t_R = 12.80 min; 99.8% pure (UV).

4-([1,1'-Biphenyl]-4-ylcarboxamido)thiophene-3-carboxylic acid (**44**) [13]
yellow solid, yield: 90%. Mp: 265–265 °C. ^{1}H NMR (500 MHz, DMSO-d_6) δ = 11.23 (s, 1 H, NH), 8.39 (d, *J* = 3.5 Hz, 1 H), 8.10 (d, *J* = 3.5 Hz, 1 H), 8.01–7.97 (m, 2 H), 7.93–7.87 (m, 2 H), 7.79–7.73 (m, 2 H), 7.55–7.48 (m, 2 H), 7.46–7.41 (m, 1 H) ppm. ^{13}C NMR (125 MHz, DMSO-d_6) δ = 165.7, 163.2, 143.7, 138.9, 136.0, 133.9, 132.4, 129.1, 128.3, 127.4, 127.3, 126.9, 122.7, 110.6 ppm. LC/MS: m/z = 324 [M + H^+], 647 [2M + H^+]; t_R = 12.82 min; 99.5% pure (UV).

2-([1,1'-Biphenyl]-4-ylcarboxamido)thiophene-3-carboxylic acid (**45**)
brown solid, yield: 92%. Mp: 242–244 °C. ^{1}H NMR (500 MHz, DMSO-d_6) δ = 12.12 (s, 1 H, NH), 8.03–8.00 (m, 2 H), 7.95–7.91 (m, 2 H), 7.79–7.75 (m, 2 H), 7.54–7.50 (m, 2 H), 7.48–7.41 (m, 1 H), 7.24 (d, *J* = 5.7 Hz, 1 H), 7.08 (d, *J* = 5.7 Hz, 1 H) ppm. ^{13}C NMR (125 MHz, DMSO-d_6) δ = 166.8, 162.5, 147.9, 144.3, 138.7, 130.6, 129.1, 128.4, 127.8, 127.4, 127.0, 124.3, 116.9, 114.1 ppm. LC/MS: m/z = 324 [M + H^+], 365 [M + H^+ + CH_3CN], 647 [2M + H^+]; t_R = 13.53 min; 96.2% pure (UV).

3-([1,1'-Biphenyl]-4-ylcarboxamido)-5-phenylthiophene-2-carboxylic acid (**46**)
beige solid, yield: 81%. Mp: 224–225 °C. ^{1}H NMR (500 MHz, DMSO-d_6) δ = 11.31 (s, 1 H, NH), 8.46 (s, 1 H), 8.05–8.02 (m, 2 H), 7.93–7.90 (m, 2 H), 7.78–7.75 (m, 4 H), 7.53–7.49 (m, 4 H), 7.47–7.42 (m, 2 H) ppm. ^{13}C NMR (125 MHz, DMSO-d_6) δ = 165.3, 163.0, 148.0, 144.2, 144.0, 138.8, 132.5, 132.0, 129.4, 129.1, 128.4, 127.8, 127.3, 127.0, 125.8, 117.8, 111.1, 92.8 ppm. LC/MS: m/z = 400 [M + H^+], 441 [M + H^+ + CH_3CN], 799 [2M + H^+]; t_R = 15.73 min; 98.2% pure (UV).

3-([1,1'-Biphenyl]-4-ylcarboxamido)-5-(4-chlorophenyl)thiophene-2-carboxylic acid (**47**)
grey-green solid, yield: 81%. Mp: 225–226 °C. ^{1}H NMR (500 MHz, DMSO-d_6) δ = 11.26 (s, 1 H, NH), 8.46 (s, 1 H), 8.03–8.01 (m, 2 H), 7.92–7.89 (m, 2 H), 7.79–7.75 (m, 4 H), 7.55–7.50 (m, 4 H), 7.46–7.41 (m, 1 H) ppm. ^{13}C NMR (125 MHz, DMSO-d_6) δ = 165.2, 163.0, 146.5, 144.2, 144.1, 138.8, 134.0, 131.9, 131.3, 129.4, 129.1, 128.4, 127.8, 127.6, 127.3, 127.0, 118.3, 111.4 ppm. LC/MS: m/z = 434 and 436 [M + H^+], 867 and 869 [2M + H^+]; t_R = 16.31 min; > 99.9% pure (UV).

2-([1,1'-Biphenyl]-4-ylsulfonamido)-5-bromobenzoic acid (**50**) [14].
beige solid, yield: 96%. Mp: 218–219 °C. ^{1}H NMR (500 MHz, DMSO-d_6) δ = 11.12 (br. s., 1 H, NH), 7.98 (d, *J* = 2.5 Hz, 1 H), 7.92–7.85 (m, 4 H), 7.75 (dd, *J* = 8.8, 2.5 Hz, 1 H), 7.72–7.67 (m, 2 H), 7.54–7.47 (m, 3 H), 7.47–7.40 (m, 1 H) ppm. ^{13}C NMR (125 MHz, DMSO-d_6) δ = 168.4, 145.0, 138.9, 138.0, 137.2, 137.0, 133.6, 129.1, 128.8, 127.7, 127.6, 127.1, 120.7, 119.1, 115.1 ppm. LC/MS: m/z = 430 and 432 [M + H^+] (negative mode); t_R = 13.70 min; > 99.9% pure (UV).

6.2.4. Compounds prepared by different procedures (35b, 35a, 35, 36a, 48, 49, 50a).

2-Amino-6-hydroxybenzoic acid (**35b**). To a solution of 2-amino-6-methoxybenzoic acid (1 equiv) in anhydrous CH_2Cl_2 at −78 °C (dry ice/acetone bath), boron tribromide (1 M in CH_2Cl_2, 3 equiv) was added dropwise. The reaction mixture was stirred for 18 h at room temperature under a nitrogen atmosphere. After addition of EtOH and MeOH the solvents were evaporated to provide a brown solid which was used for the next reaction step without further purification; brown solid, yield: 75%.

2-([1,1'-Biphenyl]-4-yl)-5-hydroxy-4H-benzo[d][1,3]oxazin-4-one (**35a**) was prepared according to 6.2.2.3. The solvent was evaporated and the remaining solid was suspended in MeOH. After filtration the precipitate was washed with MeOH to provide a mixture of the title compound (80%) and 2-([1,1'-biphenyl]-4-yl)-4-oxo-4H-benzo[d][1,3]oxazin-5-yl [1,1'-biphenyl]-4-carboxylate (20%). This beige solid was used for the next reaction step without further purification; beige solid, yield: 50%.

2-([1,1'-Biphenyl]-4-ylcarboxamido)-6-hydroxybenzoic acid (**35**). 2-([1,1'-biphenyl]-4-yl)-5-hydroxy-4H-benzo[d][1,3]oxazin-4-one (**35a**) was dissolved in THF and hydrolyzed by an aqueous solution containing 1 M LiOH at room temperature (18 h). The mixture was acidified by the addition of 1 M HCl, filtered and the precipitate was successively washed with 1 M HCl and MeOH to provide the title compound. Sufficient purity was achieved without further purification; brown solid, yield: 61%. Mp: 209–210 °C. ^{1}H NMR (500 MHz, DMSO-d_6) δ = 11.99 (s, 1 H, NH), 8.04–8.02 (m, 2 H), 7.99 (dd, J = 8.2, 1.1 Hz, 1 H), 7.87–7.85 (m, 2 H), 7.77–7.75 (m, 2 H), 7.52–7.49 (m, 2 H), 7.44–7.39 (m, 2 H), 6.69 (dd, J = 8.2, 1.1 Hz, 1 H) ppm. ^{13}C NMR (125 MHz, DMSO-d_6) δ = 171.8, 164.4, 161.3, 143.5, 140.6, 139.0, 133.7, 133.7, 129.2, 128.3, 127.9, 127.1, 127.0, 112.3, 111.5, 105.9 ppm. LC/MS: m/z = 334 [M + H$^+$], 667 [2M + H$^+$]; t_R = 11.00 min; 96.2% pure (UV).

2-Amino-5-bromobenzamide (**36a**). Methyl 2-amino-5-bromobenzoate (1 equiv) was added to a solution of NH_3 in MeOH (7 M, 10 equiv) under a N_2 atmosphere. The reaction mixture was stirred for 2 weeks at room temperature. After evaporation of the solvent the remaining solid was purified by CC (*n*-hexane/EtOAc 1:1) to provide the pure compound; white solid, yield: 11%. ^{1}H NMR (500 MHz, DMSO-d_6) δ = 7.84 (br. s., 1 H), 7.70 (d, J = 2.3 Hz, 1 H), 7.25 (dd, J = 8.8, 2.3 Hz, 1 H), 7.22–7.09 (m, 1 H), 6.70 (s, 2 H, NH_2), 6.66 (d, J = 8.8 Hz, 1 H) ppm. ^{13}C NMR (125 MHz, DMSO-d_6) δ = 169.9, 149.4, 134.3, 130.8, 118.5, 115.2, 104.7 ppm. LC/MS: m/z = 215 and 217 [M + H$^+$], 198 and 200 [M$^+$ – NH_2]; t_R = 6.65 min; 97.0% pure (UV).

3-([1,1'-Biphenyl]-4-ylcarboxamido)-5-(4-methoxyphenyl)thiophene-2-carboxylic acid (**48**). Methyl 3-([1,1'-biphenyl]-4-ylcarboxamido)-5-(4-methoxyphenyl)thiophene-2-carboxylate (**48a**) was dissolved in THF/MeOH (2:1). An aqueous solution containing 1 M NaOH and 5 M LiOH was added and the mixture was stirred at 80 °C for 8 h. After acidification by the addition of 1 M HCl the resulting suspension was filtered and the precipitate was washed with 1 M HCl to provide the title compound. Sufficient purity was achieved without further purification; yellow solid, yield: 37%. Mp: 210–212 °C. ^{1}H NMR (500 MHz, DMSO-d_6) δ = 11.29 (s, 1 H, NH), 8.34 (s, 1 H), 8.04–8.01 (m, 2 H), 7.93–7.90 (m, 2 H), 7.78–7.75 (m, 2 H), 7.72–7.67 (m, 2 H), 7.54–7.50 (m, 2 H), 7.46–7.41 (m, 1 H), 7.08–7.02 (m, 2 H), 3.81 (s, 3 H, OCH_3) ppm. ^{13}C NMR (125 MHz, DMSO-d_6) δ = 165.5, 163.1, 160.4, 148.5, 144.5, 144.1, 138.8, 132.1, 129.2, 128.5, 127.9, 127.4, 127.4, 127.0, 125.1, 116.6, 114.9, 109.7, 55.4 (OCH_3) ppm. LC/MS: m/z = 430 [M + H$^+$], 859 [2M + H$^+$]; t_R = 15.43 min; 95.4% pure (UV).

2-([1,1'-Biphenyl]-4-ylcarboxamido)-5-phenylthiophene-3-carboxylic acid (**49**). Ethyl 2-([1,1'-biphenyl]-4-ylcarboxamido)-5-phenylthiophene-3-carboxylate (**49a**) was dissolved in THF/MeOH (2:1) and hydrolyzed at room temperature with an aqueous solution containing 5 M NaOH and 5 M

KOH (18 h). The mixture was acidified by the addition of 1 M HCl, filtered and the precipitate was washed with 1 M HCl to provide the title compounds. Sufficient purity was achieved without further purification; yellow solid, yield: 62%. Mp: 249–250 °C. ^{1}H NMR (500 MHz, DMSO-d_6) δ = 12.18 (s, 1 H, NH), 8.05–8.01 (m, 2 H,) 7.97–7.91 (m, 2 H), 7.80–7.75 (m, 2 H), 7.71–7.66 (m, 2 H), 7.60 (s, 1 H), 7.55–7.51 (m, 2 H), 7.47–7.41 (m, 3 H), 7.35–7.29 (m, 1 H) ppm. ^{13}C NMR (125 MHz, DMSO-d_6) δ = 166.7, 162.5, 147.0, 144.4, 138.7, 133.2, 132.6, 130.4, 129.2, 129.1, 128.5, 127.9, 127.6, 127.4, 127.0, 125.1, 120.2, 115.3 ppm. LC/MS: m/z = 400 [M + H^+], 441 [M + H^+ + CH_3CN], 799 [2M + H^+]; t_R = 14.64 min; 98.2% pure (UV).

Methyl 2-([1,1'-biphenyl]-4-ylsulfonamido)-5-bromobenzoate (**50a**). Methyl 2-amino-5-bromobenzoate (1 equiv) and a catalytic amount of DMAP were added to a suspension of [1,1'-biphenyl]-4-sulfonyl chloride (1.5 equiv) in pyridine under a N_2 atmosphere. The reaction mixture was stirred for 6 days at room temperature and 2 M HCl was added. The mixture was extracted with EtOAc, the combined organic layers washed with saturated $NaHCO_3$ and dried over $MgSO_4$. For purification the solvent was evaporated and the remaining solid was suspended in MeOH. After filtration the precipitate was washed with MeOH to provide the pure compound; slightly yellow solid, yield: 78%. ^{1}H NMR (500 MHz, $CDCl_3$) δ = 10.59 (s, 1 H, NH), 8.06 (d, *J* = 2.5 Hz, 1 H), 7.92–7.89 (m, 2 H), 7.68–7.65 (m, 3 H), 7.59–7.55 (m, 3 H), 7.49–7.44 (m, 2 H), 7.43–7.38 (m, 1 H), 3.89 (s, 3 H, OCH_3) ppm. ^{13}C NMR (125 MHz, $CDCl_3$) δ = 167.1, 146.1, 139.5, 139.0, 137.6, 137.3, 133.8, 129.0, 128.6, 127.7, 127.7, 127.2, 120.8, 117.4, 115.7, 52.8 (OCH_3) ppm. LC/MS: m/z = 446 and 448 [M + H^+], 487 and 489 [M + H^+ + CH_3CN]; t_R = 15.61 min; 95.4% pure (UV).

6.3 Biology

RNAP transcription inhibition assay. RNAP transcription inhibition assay was performed as described previously [9, 11].

PqsD inhibition assay. PqsD inhibition assay was performed as described previously [8].

7. ACKNOWLEDGMENT

We thank Jeannine Jung and Carina Scheid for determination of RNAP and PqsD inhibition values.

8. REFERENCES

[1] A.J. McAdam, D.C. Hooper, A. DeMaria, B.M. Limbago, T.F. O'Brien, B. McCaughey, Antibiotic resistance: how serious is the problem, and what can be done?, Clin. Chem. 58 (2012) 1182–1186.

[2] L.B. Rice, Unmet medical needs in antibacterial therapy, Biochem. Pharmacol. 71 (2006) 991−995.

[3] A.E. Clatworthy, E. Pierson, D.T. Hung, Targeting virulence: a new paradigm for antimicrobial therapy, Nat. Chem. Biol. 3 (2007) 541−548.

[4] T.B. Rasmussen, M. Givskov, Quorum-sensing inhibitors as anti-pathogenic drugs, Int. J. Med. Microbiol. 296 (2006) 149−161.

[5] M. Hentzer, M. Givskov, Pharmacological inhibition of quorum sensing for the treatment of chronic bacterial infections, J. Clin. Invest. 112 (2003) 1300−1307.

[6] D. Pistorius, A. Ullrich, S. Lucas, R.W. Hartmann, U. Kazmaier, R. Müller, Biosynthesis of 2-alkyl-4(1H)-quinolones in *Pseudomonas aeruginosa*: potential for therapeutic interference with pathogenicity, ChemBioChem 12 (2011) 850−853.

[7] S. Hinsberger, K. Hüsecken, M. Groh, M. Negri, J. Haupenthal, R.W. Hartmann, Discovery of Novel Bacterial RNA Polymerase Inhibitors: Pharmacophore based Virtual Screening and Hit Optimization, J. Med. Chem. 56 (2013) 8332–8338.

[8] E. Weidel, J.C. de Jong, C. Brengel, M.P. Storz, A. Braunshausen, M. Negri, A. Plaza, A. Steinbach, R. Müller, R.W. Hartmann, Structure optimization of 2-benzamidobenzoic acids as PqsD inhibitors for *Pseudomonas aeruginosa* infections and elucidation of binding mode by SPR, STD NMR, and molecular docking, J. Med. Chem. 56 (2013), 6146–6155.

[9] J.H. Sahner, M. Groh, M. Negri, J. Haupenthal, R.W. Hartmann, Novel small molecule inhibitors targeting the "switch region" of bacterial RNAP: structure-based optimization of a virtual screening hit, Eur. J. Med. Chem. 65 (2013) 223−231.

[10] M.P. Storz, C.K. Maurer, C. Zimmer, N. Wagner, C. Brengel, J.C. de Jong, S. Lucas, M. Müsken, S. Häussler, A. Steinbach, R.W. Hartmann, Validation of PqsD as an anti-biofilm target in *Pseudomonas aeruginosa* by development of small-molecule inhibitors, J. Am. Chem. Soc. 134 (2012) 16143−16146.

[11] J. Haupenthal, K. Hüsecken, M. Negri, C.K. Maurer, R.W. Hartmann, Influence of DNA template choice on transcription and inhibition of *Escherichia coli* RNA polymerase, Antimicrob. Agents Ch. 56 (2012) 4536−4539.

[12] K. Kato, J. Terauchi, M. Mori, N. Suzuki, Y. Shimomura, S. Takekawa, Y. Ishihara, Preparation of N-tetrahydronaphthalenyl carboxamides as melanin concentrating hormone antagonists, PCT Int. Appl. (2001), WO 2001021577 A2 20010329.

[13] T.D. Ocain, C.M. Bastos, Z. Shi, R. Patch, B. Feng, Preparation of isoquinolonecarboxylates and related compounds as immunosuppressive agents, PCT Int. Appl. (1999), WO 9938846 A1 19990805.

[14] T.H. Jozefiak, C.M. Bastos, A.T. Papoulis, S.R. Holmes-Farley, Preparation of biaryl phosphate transport inhibitors, PCT Int. Appl. (2003), WO 2003057225 A2 20030717.

4. Final Discussion

4.1 Hit identification and RNAP in *vitro* activity

The overall aim of the present study was the design of novel anti-infectives that are able to overcome bacterial tolerance to clinically used antibiotics and do not provoke the fast emergence of new resistances. As RNAP is an attractive and validated but underexploited drug target the first part of this work focuses on the development of new RNAP inhibitors active against rifampicin resistant bacteria. For this purpose, a pharmacophore model was created by flexible alignment of different selected RNAP inhibitors described in literature. The chosen inhibitors have similar structural features in common although partly binding to different sites of the enzyme. Even a compound (**VII/I***) which had been published as an inhibitor of transcription/ translation (TT) without knowledge of the exact target [Larsen *et al.* 2006] was included into the model, as we were able to demonstrate that this TT inhibitor is also acting via RNAP inhibition. This practice of including molecules binding to different sites into one pharmacophore model is rather unusual as it has the disadvantage that the mode of action of the resulting hit compounds is unknown. On the other hand, since this kind of pharmacophore model is not restricted to a single binding domain, the approach supports the discovery of an increased number of RNAP inhibitors independent of their binding mode, and should result in a larger hit rate. Thus, a higher probability to identify novel RNAP inhibitors is achievable, although being much more purposive than a random screening approach. Additionally, using this model allows to identify compounds binding to more than one binding site of RNAP, rendering the emergence of resistance against the compound less probable.

---

* For the sake of clarity, all compounds in chapter 4 are characterized by their Arabic compound number (or Roman compound number, in case of the compounds used for the flexbile alignment) in combination with a Roman numeral (**I**–**III**) to identify the paper in which they have been published (e.g., **VII/I** is compound **VII** from paper I, **7/I** is compound **7** from paper I).

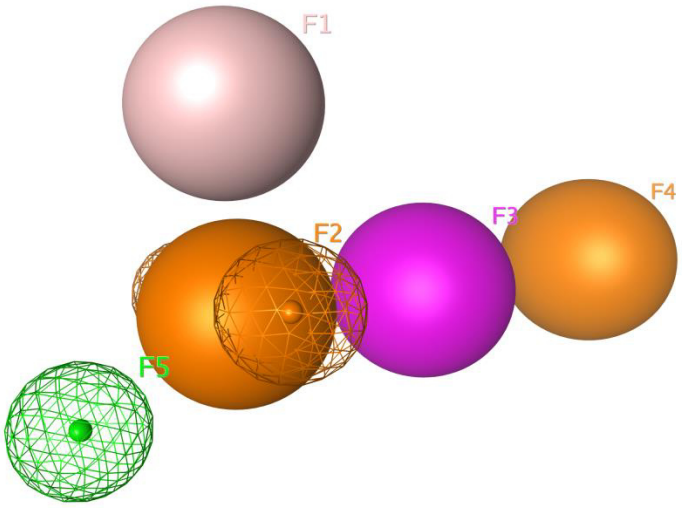

Figure 5. Pharmacophore model containing four core features (F1: O2/anion, F2: aromatic, F3: HBD/HBA/aromatic, F4: aromatic), one accessory feature (F5: hydrophobic), and two aromatic projections (dashed orange, one in front of and one hidden behind F2)

With this pharmacophore consisting of four core features (F1–F4; Fig. 5), two aromatic projections (dashed orange in front and hidden behind F2; Fig. 5) and one accessory feature (F5; Fig. 5) we screened our in-house database comprising approximately 2000 compounds. Sixty-four hit compounds were identified of which eleven, originating from five different structural classes could be experimentally confirmed to be active in the *in vitro* transcription assay. Three of these compounds belonging to the class of benzamidobenzoic acids were chosen for chemical optimization, since they were the most promising congeners regarding their potency and chemical modifiability. With the objective to explore the structure-activity relationship (SAR) and to increase the RNAP *in vitro* activity several derivatives were synthesized varying in substituents and substitution pattern around the anthranilic acid core (Fig. 6).

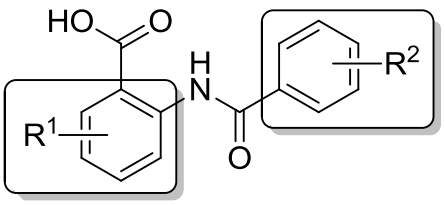

Figure 6. General structure of synthesized benzamidobenzoic acids

A first important finding revealed that the unsubstituted 2-benzamidobenzoic acid core alone (**4/I**; Table 1) is not able to inhibit RNAP. Either a phenoxy or benzyl substituent in 3′-position or a phenyl substituent in 4′-position was obligatory for acceptable activity. This structural information had not been comprised by the pharmacophore model. Although it has been demonstrated to be a suitable tool to identify novel inhibitors, the model was not able to reliably differentiate between active and inactive compounds, since **4/I** would also have been recognized as active. Therefore, the original pharmacophore was extended at its eastern side by two additional features, of which at least one feature has to be present in a screened compound to designate it as a hit compound. The use of the resulting model should improve efficacy and reduce the occurrence of false positives in future screenings of larger databases. Thus, this extended pharmacophore is representing a promising tool for prospective attempts to discover novel classes of RNAP inhibitors.

Further SAR exploration of the newfound class of benzamidobenzoic acid RNAP inhibitors revealed that lipophilic electron withdrawing substituents in 4- and 5-position of the anthranilic acid core are advantageous for the inhibitory activity (e.g., **6/I** and **8/I** compared to **1/I**). In contrast, a hydrophilic electron donating group in one of these positions reduced the compound's potency (e.g., **24/I** compared to **1/I**). These findings were consistent with our expectations since the pharmacophore model (Fig. 5) possesses a lipophilic accessory feature in this position. In addition it can be concluded that the aromatic moiety of the anthranilic acid should be electron-poor for an ideal interaction with its receptor and is probably involved in some kind of aromatic interaction with an electron-rich opponent. Interestingly, the lipophilic electron withdrawing substituents were not tolerated in 3- and 6-position (e.g., **5/I** and **9/I** compared to **1/I**), presumably due to an "out of the plane"-torsion by some parts of the anthranilic acid, caused by a steric clash. A hydroxy group in 6-position (**35/III**), however, led to an increased activity and can be explained either by an additional hydrogen bond interaction with the enzyme or by a favorable adjustment of the carboxylic acid by the OH group. The most potent *in vitro* RNAP inhibitor was **34/I** representing a combination of several beneficial features by carrying a chlorine substituent at the anthranilic acid core in 4-position and 3′-OPh, 4′-Ph substituents at the benzamide part.

Table 1. Inhibitory activities of selected compounds against *E. coli* RNAP

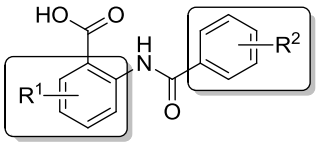

Cpd	R^1	R^2	RNAP inhibition[a]	Cpd	R^1	R^2	RNAP inhibition[a]
1/I	H	4′-Ph	31%	**8/I**	5-Cl	4′-Ph	46 µM
2/I	H	3′-OPh	23%	**9/I**	6-Cl	4′-Ph	n.i.
3/I	H	3′-OPh, 4′-Ph	20 µM	**24/I**	5-OH	4′-Ph	17%
4/I	H	H	n.i.	**34/I**	4-Cl	3′-OPh, 4′-Ph	9 µM
5/I	3-Cl	4′-Ph	n.i.	**35/III**	6-OH	4′-Ph	74 µM
6/I	4-Cl	4′-Ph	37 µM				

[a] IC_{50} value (SD <20%) or percentage inhibition at 200 µM (SD <40%) for *E. coli* RNAP; Data represent the mean values of at least three experiments.
n.i.: no inhibition

Further structural modifications altering the core of the benzamidobenzoic acids were performed and provided an advanced insight into this class of compounds. The replacement of the carboxylic acid (**36/III**–**38/III**; Table 2) was accompanied by severe solubility problems highlighting the importance of this group. Even if it is not needed for the inhibitors' binding to the enzyme, it is essential for a reasonable aqueous solubility. Shifting the carboxylic acid from *ortho* to *meta* or *para* position (**39/III** and **42/III** compared to **2/III**; **40/III** and **41/III** compared to **22/III**) resulted in just one case (**39/III** compared to **2/III**) in a slightly increased activity. Nevertheless, these modifications were a valuable tool to demonstrate that the carboxylic acid might even have a more meaningful role than only being responsible for the solubility. Bioisosteric replacement of the anthranilic acid phenyl ring by differently substituted thiophenes (**43/III**–**49/III**) merely caused moderate changes in activity, but afforded three new compounds possessing IC_{50} values as low as ~10 µM (**46/III**–**48/III**). In addition, by dint of **50/III** it was demonstrated that the amide function of the benzamide substructure is exchangeable for sulfonamide without a loss of *in vitro* potency. Altogether, altering the benzamidobenzoic acid core did not generate compounds more potent than **34/I** but a valuable gain of additional SAR knowledge. Moreover, the fact that several modifications without a loss of activity were obtained exhibits the variability and potential for further changes of this class of

benzamidobenzoic acids and encourages that the design of more potent derivatives is possible.

Table 2. Inhibitory activities of selected compounds against *E. coli* RNAP

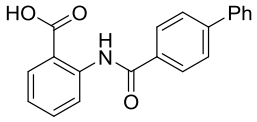

2/III

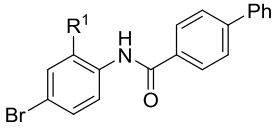

22/III, 36/III–38/III

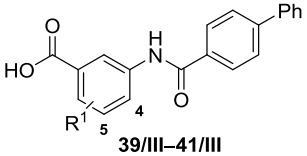

39/III–41/III

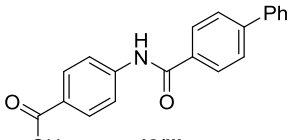

42/III

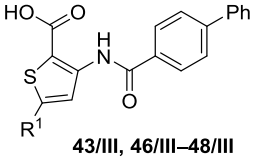

43/III, 46/III–48/III

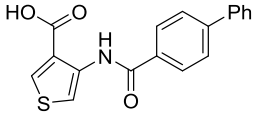

44/III

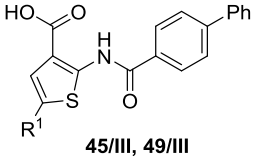

45/III, 49/III

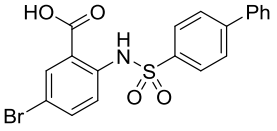

50/III

Cpd	R^1	RNAP inhibition[a]	Cpd	R^1	RNAP inhibition[a]
2/III	–	31% @ 200 µM	**43/III**	H	28% @ 200 µM
22/III	COOH	31 µM	**44/III**	–	33% @ 200 µM
36/III	$CONH_2$	n.i.[b]	**45/III**	H	161 µM
37/III	CN	n.i.[b]	**46/III**	Ph	10 µM
38/III	COOMe	n.i.[b]	**47/III**	*p*-Cl-Ph	13 µM
39/III	H	31% @ 100 µM	**48/III**	*p*-OMe-Ph	9 µM
40/III	4-Br	25% @ 200 µM	**49/III**	Ph	33% @ 50 µM
41/III	5-Br	110 µM	**50/III**	–	35 µM
42/III	–	15% @ 100 µM			

[a] IC_{50} value (SD <20%) or percentage inhibition (SD <40%) for *E. coli* RNAP; Data represent the mean values of at least three experiments.
[b] low solubility: no inhibition in saturated solution

4.2 Mechanistic investigations on RNAP inhibition and revelation of the binding site

In order to understand the mechanism behind the RNAP inhibition by benzamidobenzoic acids, several binding experiments and functional assays were performed. As, amongst others, inhibitors of the σ:core protein-protein interaction (PPI) were employed to build the pharmacophore model used to identify the hits, PPI inhibition could also be the possible mechanism of action of our compounds. Therefore, an enzyme-linked immunosorbent assay (ELISA)-based RNAP assembly test (Fig. 7) was established to ascertain whether the benzamidobenzoic acids are indeed able to prevent the interaction between the RNAP core enzyme and σ^{70}. Here, all tested compounds of the new series that were potent in the *in vitro* transcription assay exhibited comparable activity to the positive control. However, comparing the IC_{50} values obtained in the ELISA with the ones from the functional assay, it is also noticeable, that the compounds are slightly less active in the ELISA, except for reference PPI inhibitor **V/I**, thereby meaning that other accessory mechanisms of inhibition cannot be fully excluded.

Since inhibitors of the σ:core interaction would be expected to have a more intense effect on a σ^{70}-dependent transcription reaction than on a transcription independent of σ^{70}, this kind of experimental comparison was also performed for the benzamidobenzoic acids. As a matter of fact they inhibited the holo enzyme more strongly than the core enzyme, thereby providing a further proof of being σ:core interaction inhibitors.

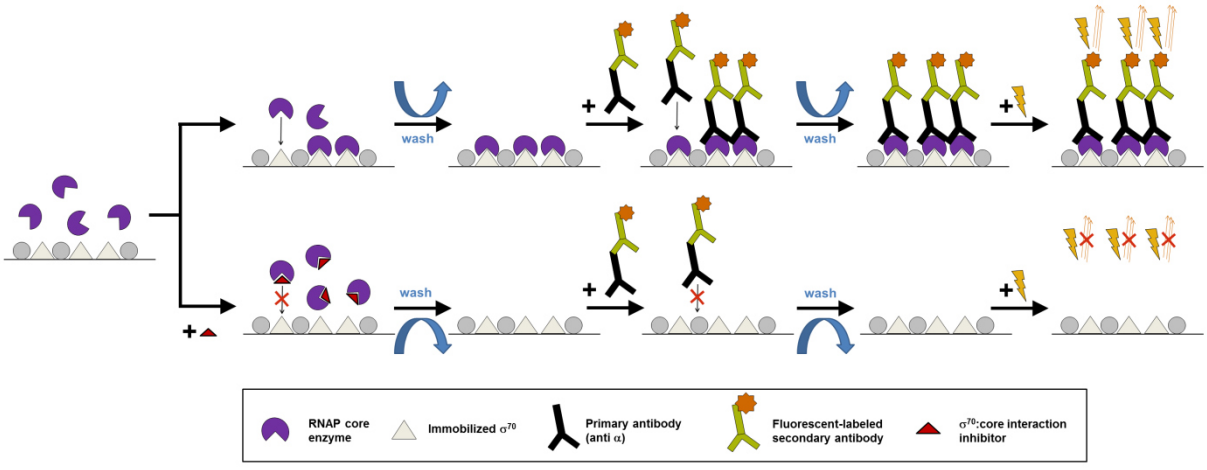

Figure 7. Schematic procedure of the ELISA based RNAP assembly assay

Beside the knowledge about the mechanism of action, having more detailed information about the binding site would be desirable to enable structure-based inhibitor design. An inhibition of the σ:core interaction can be caused by the compound binding either to the σ factor or to the β′ subunit or is induced by an allosteric mechanism. Although displaying a reduced activity in the σ^{70}-independent assay, where only core enzyme is present, the benzamidobenzoic acids are not entirely inactive indicating the presence of a binding site for the compounds at the core enzyme.

To further specify the binding site of the inhibitors, surface plasmon resonance (SPR) was employed. SPR is a biophysical technology to measure the binding affinity between an injected analyte and an immobilized biomolecule in real-time [Cooper 2002]. It is particularly suitable for demonstrating the binding of a molecule to a defined part of the enzyme, since the different subunits or parts of them can be separately immobilized to the SPR chip and labeling of compounds or proteins is not required. Immobilization of a truncated RNAP β′ subunit containing the so-called β′coiled-coil and lid-rudder-system (β′CC-LRS), which had been identified as σ^{70}:core interaction hot spot [Arthur *et al.* 1998, Hüsecken *et al.* 2013], ensures that the event of binding is only observed if a compound directly binds to this key region of the enzyme. Additionally, in the competition experiments with σ^{70} the likelihood of an allosteric mechanism is reduced to a minimum due to the small size of the protein. The positive results of the benzamidobenzoic acids in the SPR assays, comprising the dose-dependent binding to β′CC-LRS, the linear correlation between dissociation rate constant, and the *in vitro* transcription inhibitory activity, as well as the effective inhibition of σ^{70}:β′CC-LRS interaction in the competition experiment, revealed this class of compounds as true inhibitors of σ:core PPI.

Subsequent molecular modeling guided by the results of SPR-based mutant studies provided a detailed insight into the suggested binding pose of the benzamidobenzoic acids (Fig. 8). Here, the carboxyl function seems to be firmly complexed by the guanidine moieties of the arginines R271, R275 and R278, stressing its considerable role for the compounds' activity. Furthermore, the outer phenyl ring of the compounds' extended benzamide part appears to interact with threonine T317.

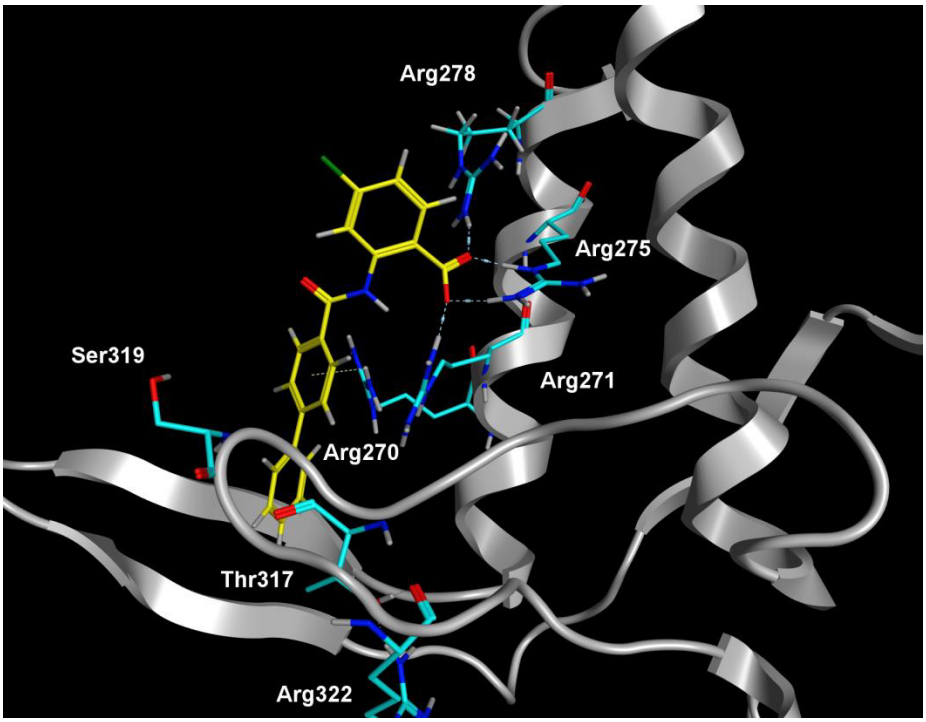

Figure 8. Suggested binding pose of **6**/**I** (in yellow) to the β' CC-LRS of *T. thermophilus* (PDB 3EQL). Amino acids important for the SPR mutant studies are shown in turquois and with *E. coli* numbering.

It has to be mentioned that, although computational docking experiments are an appropriate tool to calculate and illustrate reasonable binding poses of molecules to a certain protein, of course they are not infallible and the calculated poses have to be experimentally proven (e.g., by X-ray structure or NMR experiments). Furthermore, the truncated β′ used in the SPR experiments is a well-suited, but artificial model and the explanatory power of the results should not be overestimated. Nevertheless, all the results are in good accordance with the *in vitro* RNAP inhibition SAR studies presented above, where it has already been demonstrated that the carboxylic acid group has a larger impact than only being responsible for the compounds' solubility and that the outer phenyl ring is a crucial feature for potent inhibitors.

Binding to the σ:core interface turns the benzamidobenzoic acids into a highly attractive option to avoid and to overcome bacterial resistance. On the one hand, the σ:core interface is a highly conserved region [Burgess *et al.* 2001] and mutations occur rarely, since many different σ factors must be able to bind to this site. On the other hand no cross-resistance to clinically used rifamycins, which are binding to a distinct binding site, has to be expected.

4.3 Antibacterial activity

A good *in vitro* activity against a validated antibacterial target is not sufficient to designate a compound as antibiotic. As the newly developed inhibitors are intended to act against living bacteria, they must also have the ability to unfold their activity *in cellulo*. This could for example be hampered by an unsatisfactory permeation into the bacterial cell or rapid inactivation of the compound by the bacterium. Therefore, the antibacterial profile of the class of benzamidobenzoic acids was investigated. In a first approach the minimum inhibitory concentration (MIC) values of the inhibitors were determined in *E. coli* TolC. This organism defective in the AcrAB–TolC multidrug efflux system, was chosen to reduce effects associated with drug efflux, as these effects would have impeded first structure-antibacterial activity relationship studies. Subsequently, the most interesting inhibitors were further tested for antibacterial activity against wild-type Gram-negative and Gram-positive bacteria. Beside a few exceptions (e.g., **33/I** and **34/I**), which are probably due to pharmacokinetic reasons, the benzamidobenzoic acids are strongly active against the TolC deficient *E. coli*. Importantly, this also applies for rifampicin-resistant strains [Fruth, unpublished results]. However, the inhibitors do not show any effect against the tested wild-type Gram-negative bacteria. This leads to the assumption that the compounds in principle are active against Gram-negatives, but are quickly expelled by efflux pumps. To make the compounds active against this type of bacteria elaborate chemical modifications would probably be necessary to get them out of the efflux pumps' substrate spectrum. With respect to the Gram-positive bacteria, however, the benzamidobenzoic acids are highly potent, even against a set of clinically relevant methicillin-resistant *Staphylococcus aureus* (MRSA) strains they were shown to be effective [Fruth, unpublished results].

Table 3. Inhibitory *E. coli* RNAP *in vitro* activities and Minimum Inhibitory Concentrations (MIC) for selected compounds

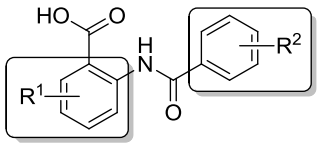

Cpd	R^1	R^2	IC_{50} (RNAP) [µM][a]	MIC [µg/mL][b]				
				E. coli TolC	*E. coli* K12	*PAO1*[c]	*B. subtilis*	*S. aureus*
rifampicin			0.03	10	7	13	5	0.02
myxopyronin B			0.35	1	>25	>25	0.9	0.5
6/I	4-Cl	4′-Ph	37	3	>50	>50	2	24
7/I	4-Cl	3′-OPh	44	3	>50	>50	3	14
12/I	5-F	3′-OPh	98	5	>100	>100	4	48
15/I	4-Br	3′-OPh	34	3	>25	>25	3	8
28/I	5-CF_3	4′-Ph	28	2	>50	>50	4	5
32/I	5-Ph	3′-OPh	13	2	>25	>25	3	6
33/I	4-F	3′-OPh, 4′-Ph	13	>25	>25	>25	>25	17
34/I	4-Cl	3′-OPh, 4′-Ph	9	>25	-	-	-	-

[a] IC_{50} value (SD <20%) for *E. coli* RNAP; Data represent the mean values of at least three experiments.
[b] Minimum inhibitory concentration; Data represent the mean values of at least two independent experiments (three for MIC <10 µg/mL).
[c] *P. aeruginosa*

Comparison of SAR derived from the MIC values for *E. coli* TolC and from *in vitro* RNAP inhibition IC_{50} values exhibited a rough correlation. This indicates that indeed the inhibition of RNAP induces bacterial cell death. Nevertheless, it is conspicuous that the benzamidobenzoic acids possess very low MIC values comparable to the reference compounds (rifampicin, myxopyronin), although they display distinctly less pronounced RNAP inhibitory activities *in vitro* (Table 3). Investigation of the impact of benzamidobenzoic acids on macromolecule biosynthesis in *E. coli* TolC revealed, beside the expected inhibition of RNA formation comparable to rifampicin, a strong decrease in lipid biosynthesis. In literature, benzamidobenzoic acids have been described as inhibitors of FabH [Nie *et al.* 2005], an enzyme involved in fatty acid synthesis. This could explain the observed reduction of lipid production. Thus, it can be supposed that the good antibacterial activity is the result of a dual target mechanism comprising RNAP and FabH inhibition. This is of special interest

regarding our goal to develop new anti-infectives which are less prone to provoke bacterial resistances, as mutations occurring in two different enzymes in parallel will definitely be less likely than the occurrence of a mutation in one single enzyme. Indeed, it has also been reflected in experiments in which a significantly reduced resistance frequency for benzamidobenzoic acids compared to reference rifampicin has been demonstrated. These results highlight the great potential of this promising class of compounds and motivate to further develop them for use as anti-infective drugs.

4.4 Benzamidobenzoic acids as selective PqsD inhibitors

PqsD is an appropriate and attractive target for an anti-virulence strategy to fight infections caused by *P. aeruginosa*. As hit compound **3/I**, which had been discovered in the VS for RNAP inhibitors, was described in 2011 to inhibit PqsD *in vitro* [Pistorius *et al.* 2011], it has been assumed that the synthesized derivatives of the benzamidobenzoic acid class could also be inhibitors of PqsD. Additionally, at least some of them have been shown to be inhibitors of FabH, which closely resembles PqsD, and they possess a structural similarity to PqsD inhibitors published in 2013 also containing a benzamidobenzoic acid core [Weidel *et al.* 2013]. Testing of the derivatives in an *in vitro* PqsD assay identified several new potent PqsD inhibitors, some of them even more active than **3/I**. However, bacterial cell death caused by potent RNAP inhibition is not intended for an anti-virulence concept by PqsD inhibition, since it could provoke selective pressure. Therefore it is of particular interest to disclose not only the SAR of benzamidobenzoic acids for PqsD inhibition, but also the relationship between structure and selectivity for PqsD over RNAP.

In general, many similarities between the structural elements beneficial for PqsD and RNAP inhibition, respectively, can be discovered. For example, a substituent in 3′- or 4′-position of the benzamide moiety is a minimum requirement for the inhibition of both enzymes (**4/III** compared to **3/I**, **2/III**, and **3/III**) and a compound with a substituent in both positions is even more potent (**3/I** compared to **2/III** and **3/III**). Furthermore, the introduction of lipophilic electron withdrawing substituents or phenyl rings in 4- and 5-position of the anthranilic acid moiety is also considerably advantageous for PqsD inhibition (e.g., **11/III**–**15/III**, **22/III**, **23/III** and **25/III**–**27/III**

compared to **2/III** and **3/III**). The drawback of this kind of substituents is that they do not afford the required selectivity over RNAP. However, structural modifications that predominantly or selectively increase PqsD activity can also be determined. Especially the introduction of a 3-Cl substituent to the anthranilic acid core strongly increases PqsD inhibition while in parallel leading to a total loss of RNAP inhibitory activity (**5/III**). A further interesting compound is the one containing a hydroxy substituent in 5-position also exhibiting highly selective PqsD inhibition (**31/III**). If instead the hydroxy substituent is introduced in 6-position, RNAP as well as PqsD activity are increased, but to a varying extent, resulting in a compound which is about 50 times more active on PqsD than on RNAP (**35/III**). In addition, several bioisosteric replacements like the exchange of the anthranilic acid phenyl ring for a thiophene (e.g., **43/III**) or of the amide for a sulfonamide function (**50/III**) can afford potent and selective PqsD inhibitors. Selectivity can also be gained by the introduction of aliphatically substituted sulfonamides in 3′-position of the benzamide moiety (e.g., SO_2NEt_2, $SO_2N(n\text{-}Pr)_2$) like in the series of published benzamidobenzoic acid PqsD inhibitors [Weidel *et al.* 2013] (e.g., **51/III**, **56/III**–**63/III**, **69/III** and **80/III**). Interestingly, **86/III**, containing an aromatic 3-SO_2NEtBn substituent, represents a similarly potent RNAP inhibitor as **2/III** and **3/III**. Therefore, it can be concluded that in general in this position aromatics should be avoided to yield a selective PqsD inhibitor, as aromatics seem to be an essential feature for RNAP inhibition.

The presented structure-activity and structure-selectivity studies reveal that compounds from the same structural class can be used for two totally different approaches to treat bacterial infections, one effectively killing bacteria, the other intended to reduce bacterial virulence and to hamper biofilm formation. By simple bioisosteric replacements or the introduction of small substituents the biological profile can be shifted in favor of the different targets, respectively, accentuating the enormous versatility and potential of benzamidobenzoic acids to act as anti-infectives in the fight against bacterial resistances.

Table 4. Inhibitory activities of selected compounds against PqsD and RNAP

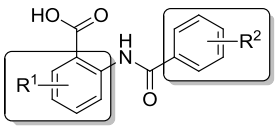

1–35

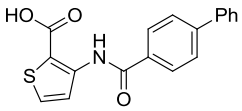

43

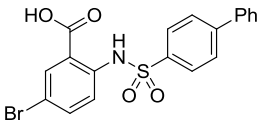

50

Cpd	R^1	R^2	RNAP inhibition[a]	PqsD inhibition[b]
3/I	H	3′-OPh, 4′-Ph	20 µM	6.6 µM
2/III	H	4′-Ph	31%	55%
3/III	H	3′-OPh	23%	37%
4/III	H	H	n.i.	n.i.
5/III	3-Cl	4′-Ph	n.i.	6.2 µM
12/III	4-Br	3′-OPh	34 µM	5.1 µM
14/III	4-CF_3	4′-Ph	27 µM	4.9 µM
15/III	4-Ph	3′-OPh	14 µM	6.6 µM
22/III	5-Br	4′-Ph	31 µM	3.2 µM
23/III	5-Br	3′-OPh	34 µM	4.4 µM
26/III	5-CF_3	4′-Ph	28 µM	3.4 µM
27/III	5-Ph	3′-OPh	13 µM	7.7 µM
31/III	5-OH	4′-Ph	17%	4.2 µM
35/III	6-OH	4′-Ph	74 µM	1.3 µM
43/III	-	-	28%	5.2 µM
50/III	-	-	35 µM	1.3 µM
51/III	H	3′-SO_2NEt_2	n.i.	19.8 µM
60/III	5-CF_3	3′-SO_2NEt_2	n.i. @ 50 µM	12.4 µM
62/III	5-Br	3′-SO_2NEt_2	n.i. @ 50 µM	9.9 µM
69/III	5-Ph	3′-SO_2NEt_2	n.i. @ 100 µM	3.0 µM
80/III	H	3′-$SO_2N(n\text{-}Pr)_2$	n.i.	5.4 µM
86/III	H	3′-SO_2NEtBn	29%	16.5 µM

[a] IC_{50} value (SD <20%) or percentage inhibition at 200 µM (SD <40%) for *E. coli* RNAP; Data represent the mean values of at least three experiments.
[b] IC_{50} value (SD <23%) or percentage inhibition at 50 µM (SD <40%); Data represent the mean values of at least two experiments.
n.i.: no inhibition

4.5 Outlook

Despite their promising results in the *in vitro* enzyme inhibition assays and their excellent activity against several bacteria, the benzamidobenzoic acids still possess several drawbacks that should be abolished in future development before the compounds are appropriate to be used as anti-infective drugs. Especially the comparatively high lipophilicity (logP > 3; determined by SiriusT3, Sirius Analytical Instruments Ltd., East Sussex, UK) and the resulting rather poor aqueous solubility should be improved in a subsequent optimization program. Several possibilities for structural modifications which should enhance solubility are conceivable, e.g., the replacement of phenyl rings by different (nitrogen containing) heterocycles. As in general the eastern part of the compounds has not been fully explored until now, different hydrophilic substituents and substitution patterns can also be tested. Furthermore, the introduction of a substituent at the biphenyl moiety of the compounds creating an *ortho*-effect, thereby reducing the planarity of the compound, could improve solubility.

A more complex drawback is posed by the fact that the benzamidobenzoic acids do not seem to reach their target in Gram-negative bacteria so far. Possibly chemical modifications could enhance permeability or get the compounds off the substrate spectrum of the efflux pumps, which are presumably responsible for the inactivity against the wild-type Gram-negative bacteria. Another possibility to increase compound concentration in the Gram-negative cell could be a coupling of the benzamidobenzoic acids to carrier systems like siderophores and thereby provoking an active uptake of the anti-infective [Fardeau *et al.* 2011, Ji *et al.* 2012, Starr *et al.* 2014].

Since it is crucial to know about the exact modes of action of the benzamidobenzoic acids for further improvements, the probable binding pose to RNAP, proposed in this work, should be experimentally proven by X-ray structure or NMR experiments in a next step. Concerning the binding site on PqsD there are first hints that the compounds act as channel blockers [Weidel, unpublished results] in analogy to the series of published benzamidobenzoic acid inhibitors [Weidel *et al.* 2013], thus preventing anthraniloyl-CoA from accessing the PqsD active site. Nevertheless, this should also be further evaluated by X-ray or NMR. These continuative experiments

will enable a rational structural improvement of the compounds with the aim to turn them into clinically usable anti-infective drugs.

5. References

André, E.; Bastide, L.; Michaux-Charachon, S.; Gouby, A.; Villain-Guillot, P.; Latouche, J.; Bouchet, A.; Gualtiéri, M.; Leonetti, J.P. Novel synthetic molecules targeting the bacterial RNA polymerase assembly. *J. Antimicrob. Chemother.* **2006**, *57*, 245–251.

Arhin, F.; Bélanger, O.; Ciblat, S.; Dehbi, M.; Delorme, D.; Dietrich, E.; Dixit, D.; Lafontaine, Y.; Lehoux, D.; Liu, J.; McKay, G.A.; Moeck, G.; Reddy, R.; Rose, Y.; Srikumar, R.; Tanaka, K.S.; Williams, D.M.; Gros, P.; Pelletier, J.; Parr, T.R. Jr.; Far, A.R. A new class of small molecule RNA polymerase inhibitors with activity against rifampicin-resistant *Staphylococcus aureus*. *Bioorg. Med. Chem.* **2006**, *14*, 5812–5832.

Arthur, T.M.; Burgess, R.R. Localization of a σ^{70} binding site on the N terminus of the *Escherichia coli* RNA polymerase β′ subunit. *J. Biol. Chem.* **1998**, *273*, 31381–31387.

Artsimovitch, I.; Chu, C.; Lynch, A.S.; Landick, R. A new class of bacterial RNA polymerase inhibitor affects nucleotide addition. *Science* **2003**, *302*, 650–654.

Asboe, D.; Gant, V.; Aucken, H.M.; Moore, D.A.; Umasankar, S.; Bingham, J.S.; Kaufmann, M.E.; Pitt, T.L. Persistence of *Pseudomonas aeruginosa* strains in respiratory infection in AIDS patients. *AIDS* **1998**, *12*, 1771−1775.

Baldry, P. The Battle Against Bacteria: A fresh look, 2nd ed. *Cambridge University Press*, Cambridge, **1976**.

Bera, A.K.; Atanasova, V.; Robinson, H.; Eisenstein, E.; Coleman, J.P.; Pesci, E.C.; Parsons, J.F. Structure of PqsD, a *Pseudomonas* quinolone signal biosynthetic enzyme, in complex with anthranilate. *Biochemistry* **2009**, *48*, 8644–8655.

Bergendahl, V.; Heyduk, T.; Burgess, R.R. Luminescence resonance energy transfer-based high-throughput screening assay for inhibitors of essential protein-protein interactions in bacterial RNA polymerase. *Appl. Environ. Microb.* **2004**, *69*, 1492–1498.

Bjarnsholt, T.; Jensen P.Ø.; Burmølle, M.; Hentzer, M.; Haagensen, J.A.; Hougen, H.P.; Calum, H.; Madsen, K.G.; Moser, C.; Molin, S.; Høiby, N.; Givskov, M. *Pseudomonas aeruginosa* tolerance to tobramycin, hydrogen peroxide and polymorphonuclear leukocytes is quorum-sensing dependent. *Microbiology* **2005**, *151*, 373–383.

Bjarnsholt, T.; Tolker-Nielsen, T.; Høiby, N.; Givskov, M. Interference of *Pseudomonas aeruginosa* signalling and biofilm formation for infection control. *Expert Rev. Mol. Med.* **2010**, *12*, e11.

Bodey, G.P.; Bolivar, R.; Fainstein, V.; Jadeja, L. Infections caused by *Pseudomonas aeruginosa. Rev. Infect. Dis.* **1983**, *5*, 279–313.

Braine T. Race against time to develop new antibiotics. *B. World Health Organ.* **2011**, *89*, 88–89.

Burgess, R.R.; Travers, A.A.; Dunn, J.J.; Bautz, E.K. Factor stimulating transcription by RNA polymerase. *Nature* **1969**, *221*, 43–46.

Burgess, R.R.; Anthony, L. How sigma docks to RNA polymerase and what sigma does. *Curr. Opin. Microbiol.* **2001**, *4*, 126–131.

Butaye, P.; Michael, G.B.; Schwarz, S.; Barrett, T.J.; Brisabois, A.; White, D.G. The clonal spread of multidrug-resistant non-typhi Salmonella serotypes. *Microbes Infect.* **2006**, *8*, 1891–1897.

Buurman, E.T.; Foulk, M.A.; Gao, N.; Laganas, V.A.; McKinney, D.C.; Moustakas, D.T.; Rose, J.A.; Shapiro, A.B.; Fleming, P.R. Novel rapidly diversifiable antimicrobial RNA polymerase switch region inhibitors with confirmed mode of action in *Haemophilus influenzae. J. Bacteriol.* **2012**, *194*, 5504–5512.

Cao, H.; Krishnan, G.; Goumnerov, B.; Tsongalis, J.; Tompkins, R.; Rahme, L.G. A quorum sensing-associated virulence gene of *Pseudomonas aeruginosa* encodes a LysR-like transcription regulator with a unique self-regulatory mechanism. *Proc. Natl. Acad. Sci. U.S.A.* **2001**, *98*, 14613–14618.

Centers for Disease Control and Prevention (CDC). Threat Report 2013 "Antibiotic resistance threats in the United States." **2013**. *http://www.cdc.gov/drugresistance/ threat-report-2013/pdf/ar-threats-2013-508.pdf*

Chopra I. Bacterial RNA polymerase: a promising target for the discovery of new antimicrobial agents. *Curr. Opin. Investig. Drugs* **2007**, *8*, 600–607.

Chopra, I. The 2012 Garrod Lecture: Discovery of antibacterial drugs in the 21st century. *J. Antimicrob. Chemother.* **2013**, *68*, 496–505.

Christensen, L.D.; van Gennip, M.; Jakobsen, T.H.; Alhede, M.; Hougen, H.P.; Høiby, N.; Bjarnsholt, T.; Givskov, M. Synergistic antibacterial efficacy of early combination treatment with tobramycin and quorum-sensing inhibitors against *Pseudomonas aeruginosa* in an intraperitoneal foreign-body infection mouse model. *J. Antimicrob. Chemother.* **2012**, *67*, 1198–1206.

Ciciliato, I.; Corti, E.; Sarubbi, E., Stefanelli, S.; Gastaldo, L.; Montanini, N.; Kurz, M.; Losi, D.; Marinelli, F.; Selva, E. Antibiotics GE23077, novel inhibitors of bacterial RNA polymerase. I. Taxonomy, isolation and characterization. *J. Antibiot.* **2004,** *57*, 210–217.

Clatworthy, A.E.; Pierson, E.; Hung, D.T. Targeting virulence: a new paradigm for antimicrobial therapy. *Nat. Chem. Biol.* **2007**, *3*, 541–548.

Coleman, J.P.; Hudson, L.L.; McKnight, S.L.; Farrow, J.M. 3rd; Calfee, M.W.; Lindsey, C.A.; Pesci, E.C. *Pseudomonas aeruginosa* PqsA is an anthranilate-coenzyme A ligase. *J. Bacteriol.* **2008**, *190*, 1247–1255.

Cooper, M.A. Optical biosensors in drug discovery. *Nat. Rev. Drug Discov.* **2002**, *1*, 515–528.

Cramer, P. Multisubunit RNA polymerases. *Curr. Opin. Struct. Biol.* **2002**, *12*, 89–97.

de Kievit, T.R.; Iglewski, B.H. Bacterial quorum sensing in pathogenic relationships. *Infect. Immun*. **2000**, *68*, 4839–4849.

de Kievit, T.R. Quorum sensing in *Pseudomonas aeruginosa* biofilms. *Environ. Microbiol.* **2009**, *11*, 279–288.

Déziel, E.; Lépine, F.; Milot, S.; He, J.; Mindrinos, M.N.; Tompkins, R.G.; Rahme, L.G. Analysis of *Pseudomonas aeruginosa* 4-hydroxy-2-alkylquinolines (HAQs) reveals a role for 4-hydroxy-2-heptylquinoline in cell-to-cell communication. Proc. *Natl. Acad. Sci. U.S.A.* **2004**, *101*, 1339–1344.

Déziel, E.; Gopalan, S.; Tampakaki, A.P.; Lépine, F.; Padfield, K.E.; Saucier, M.; Xiao, G.; Rahme, L.G. The contribution of MvfR to *Pseudomonas aeruginosa* pathogenesis and quorum sensing circuitry regulation: multiple quorum sensing-regulated genes are modulated without affecting *lasRI*, *rhlRI* or the production of *N*-acyl-L-homoserine lactones. *Mol. Microbiol.* **2005**, *55*, 998–1014.

Diaz Högberg, L.; Heddini, A.; Cars, O. The global need for effective antibiotics: challenges and recent advances. *Trends Pharmacol. Sci.* **2010**, *31*, 509–515.

Diggle, S.P.; Winzer, K.; Chhabra, S.R.; Worrall, K.E.; Cámara, M.; Williams, P. The *Pseudomonas aeruginosa* quinolone signal molecule overcomes the cell density-dependency of the quorum sensing hierarchy, regulates *rhl*-dependent genes at the onset of stationary phase and can be produced in the absence of LasR. *Mol. Microbiol.* **2003**, *50*, 29–43.

Diggle, S.P.; Lumjiaktase, P.; Dipilato, F.; Winzer, K.; Kunakorn, M.; Barrett, D.A.; Chhabra, S.R.; Cámara, M.; Williams, P. Functional genetic analysis reveals a 2-alkyl-4-quinolone signaling system in the human pathogen *Burkholderia pseudomallei* and related bacteria. *Chem. Biol.* **2006**,*13*, 701–710.

Diggle, S.P.; Matthijs, S.; Wright, V.J.; Fletcher, M.P.; Chhabra, S.R.; Lamont, I.L.; Kong, X.; Hider, R.C.; Cornelis, P.; Cámara, M.; Williams, P. The *Pseudomonas aeruginosa* 4-quinolone signal molecules HHQ and PQS play multifunctional roles in quorum sensing and iron entrapment. *Chem. Biol*. **2007**, *14*, 87–96.

Driffield, K.; Miller, K.; Bostock, J.M.; O'Neill, A.J.; Chopra, I. Increased mutability of *Pseudomonas aeruginosa* in biofilms. *J. Antimicrob. Chemother.* **2008**, *61*, 1053–1056.

Dulcey, C.E.; Dekimpe, V.; Fauvelle, D.A.; Milot, S.; Groleau, M.C.; Doucet, N.; Rahme, L.G.; Lépine, F.; Déziel, E. The end of an old hypothesis: the *pseudomonas* signaling molecules 4-hydroxy-2-alkylquinolines derive from fatty acids, not 3-ketofatty acids. *Chem. Biol.* **2013**, *20*, 1481–1491.

Ebright, R.H. RNA polymerase: structural similarities between bacterial RNA polymerase and eukaryotic RNA polymerase II. *J. Mol. Biol.* **2000**, *304*, 687−698.

Engebrecht, J.; Nealson, K.; Silverman, M. Bacterial bioluminescence: isolation and genetic analysis of functions from *Vibrio fischeri*. *Cell* **1983**, *32*, 773−781.

Engebrecht, J.; Silverman, M. Identification of genes and gene products necessary for bacterial bioluminescence. *Proc. Natl. Acad. Sci. U.S.A.* **1984**, *81*, 4154−4158.

Ezekiel, D.H.; Hutchins, J.E. Mutations affecting RNAP associated with rifampicin resistance in *Escherichia coli*. *Nature* **1968**, *220*, 276–277.

Fardeau, S.; Mullié, C.; Dassonville-Klimpt, A.; Audic, N.; Sasaki, A.; Sonnet, P. ”Bacterial iron uptake: a promising solution against multidrug resistant bacteria” (695−705). Science against microbial pathogens: communicating current research and technological advances, Vol. 2, *Formatex Research Center (A. Méndez-Vilas (Ed.))*, Badajoz, **2011**.

Fleming, A. Nobel Lecture “Penicillin”. **1945**. *http://nobelprize.org/nobel_prizes/medicine/laureates/1945/fleming-lecture.html*

Floss, H.G.; Yu, T.W. Rifamycin-mode of action, resistance, and biosynthesis. *Chem. Rev.* **2005**, *105*, 621–632.

Frearson, J.A.; Wyatt, P.G.; Gilbert, I.H.; Fairlamb, A.H. Target assessment for antiparasitic drug discovery. *Trends Parasitol.* **2007**, *23*, 589−595.

Fuqua, W.C.; Winans, S.C.; Greenberg, E.P. Quorum sensing in bacteria: the LuxR-LuxI family of cell density-responsive transcriptional regulators. *J. Bacteriol*. **1994**, *176*, 269−275.

Gallagher, L.A.; McKnight, S.L.; Kuznetsova, M.S.; Pesci, E.C.; Manoil, C. Functions Required for Extracellular Quinolone Signaling by *Pseudomonas aeruginosa*. *J. Bacteriol.* **2002**, *184*, 6472–6480.

Gambello, M.J.; Iglewski, B.H. Cloning and characterization of the *Pseudomonas aeruginosa lasR* gene, a transcriptional activator of elastase expression. *J. Bacteriol*. **1991**, *173*, 3000–3009.

González, J.E.; Keshavan, N.D. Messing with bacterial quorum sensing. *Microbiol. Mol. Biol. Rev.* **2006**, *70*, 859−875.

Greenwood, D.; Whitley, R. "Modes of action." Antibiotics and chemotherapy, 7th ed. *Churchill Livingstone*, New York, **1997**.

Haebich, D.; von Nussbaum, F. Lost in transcription−inhibition of RNA polymerase. *Angew. Chem. Int. Ed. Engl.* **2009**, *48*, 3397−3400.

Hakki, M.; Limaye, A. P.; Kim, H. W.; Kirby, K. A.; Corey, L.; Boeckh, M. Invasive *Pseudomonas aeruginosa* infections: high rate of recurrence and mortality after hematopoietic cell transplantation. *Bone Marrow Transplant.* **2007**, *39*, 687−693.

Hardesty, J. S.; Juang, P. Fidaxomicin: a macrocyclic antibiotic for the treatment of *Clostridium difficile* infection. *Pharmacotherapy* **2011**, *31*, 877−886.

Heads of Medicines Agencies. HMA definitions of the terms “Antibiotic” and “Antimicrobial”. **2012**. *http://www.hma.eu/fileadmin/dateien/Veterinary_medicines/00-HMA_Vet/02-HMA_Task_Force/03_HMA_vet_TF_AMR/2012_11_HMA_agreed_AB_ AM_definitions.pdf*

Hentzer, M.; Riedel, K.; Rasmussen, T.B.; Heydorn, A.; Andersen, J.B.; Parsek, M.R.; Rice, S.A.; Eberl, L.; Molin, S.; Høiby, N.; Kjelleberg, S.; Givskov, M. Inhibition of quorum sensing in *Pseudomonas aeruginosa* biofilm bacteria by a halogenated furanone compound. *Microbiology* **2002**, *148*, 87−102.

Hentzer, M.; Givskov, M. Pharmacological inhibition of quorum sensing for the treatment of chronic bacterial infections. *J. Clin. Invest.* **2003**, *112*, 1300−1307.

Hentzer, M.; Wu, H.; Andersen, J.B.; Riedel, K.; Rasmussen, T.B.; Bagge, N.; Kumar, N.; Schembri, M.A.; Song, Z.; Kristoffersen, P.; Manefield, M.; Costerton, J.W.; Molin, S.; Eberl, L.; Steinberg, P.; Kjelleberg, S.; Høiby, N.; Givskov, M. Attenuation of *Pseudomonas aeruginosa* virulence by quorum sensing inhibitors. *EMBO J.* **2003**, *22*, 3803–3815.

Ho, M.X.; Hudson, B.P.; Das, K.; Arnold, E.; Ebright, R.H. Structures of RNA polymerase−antibiotic complexes. *Curr. Opin. Struct. Biol.* **2009**, *19*, 715−723.

Høiby, N.; Bjarnsholt, T.; Givskov, M.; Molin, S.; Ciofu, O. Antibiotic resistance of bacterial biofilms. *Int. J. Antimicrob. Agents* **2010**, *35*, 322−332.

Hüsecken, K.; Negri, M.; Fruth, M.; Boettcher, S.; Hartmann, R.W.; Haupenthal, J. Peptide-based investigation of the *Escherichia coli* RNA polymerase σ^{70}:core interface as target site. *ACS Chem. Biol.* **2013**, *8*, 758−766.

Hutter, M.C.; Brengel, C.; Negri, M.; Henn, C.; Zimmer, C.; Hartmann R.W.; Empting, M.; Steinbach, A. Mechanistic details for anthraniloyl transfer in PqsD: the initial step in HHQ biosynthesis. *J. Mol. Model*. **2014**, *20*, 2255.

Irschik, H.; Gerth, K.; Höfle, G.; Kohl, W.; Reichenbach, H. The myxopyronins, new inhibitors of bacterial RNA synthesis from *Myxococcus fulvus* (Myxobacterales). *J. Antibiot.* **1983**, *36*, 1651–1658.

Irschik, H.; Jansen, R.; Höfle, G.; Gerth, K.; Reichenbach, H. The corallopyronins, new inhibitors of bacterial RNA synthesis from *Myxobacteria*. *J. Antibiot.* **1985**, *38*, 145–152.

Irschik, H.; Jansen, R.; Gerth, K.; Höfle, G.; Reichenbach, H. The sorangicins, novel and powerful inhibitors of eubacterial RNA polymerase isolated from *myxobacteria*. *J. Antibiot.* **1987**, *40*, 7–13.

Jakobsen, T.H.; Bragason, S.K.; Phipps, R.K.; Christensen, L.D.; van Gennip, M.; Alhede, M.; Skindersoe, M.; Larsen, T.O.; Høiby, N.; Bjarnsholt, T.; Givskov, M. Food as a source for QS inhibitors: iberin from horseradish revealed as a quorum sensing inhibitor of *Pseudomonas aeruginosa*. *Appl. Environ. Microbiol.* **2012**, *78*, 2410−2421.

Ji, C.; Miller, P.A.; Miller, M.J. Iron transport-mediated drug delivery: practical syntheses and in vitro antibacterial studies of tris-catecholate siderophore-aminopenicillin conjugates reveals selectively potent antipseudomonal activity. *J. Am. Chem. Soc.* **2012**, *134*, 9898−9901.

Khan, N.H.; Ahsan, M.; Taylor, W.D.; Kogure, K. Culturability and survival of marine, freshwater and clinical *Pseudomonas aeruginosa*. *Microbes Environ.* **2010**, *25*, 266–274.

Koch, C.; Høiby, N.; Pathogenesis of cystic fibrosis. *Lancet* **1993**, *341*, 1065–1069.

Koehn, F.E.; Carter, G.T. The evolving role of natural products in drug discovery. *Nat. Rev. Drug Discov.* **2005**, *4*, 206–220.

Kuznedelov, K.; Semenova, E.; Knappe, T.A.; Mukhamedyarov, D.; Srivastava, A.; Chatterjee, S.; Ebright, R.H.; Marahiel, M.A.; Severinov, K. The antibacterial threaded-lasso peptide capistruin inhibits bacterial RNA polymerase. *J. Mol. Biol.* **2011**, *412*, 842–848.

Larsen, S.D.; Hester, M.R.; Craig Ruble, J.; Kamilar, G.M.; Romero, D.L.; Wakefield, B.; Melchior, E.P.; Sweeney, M.T.; Marotti, K.R. Discovery and initial development of a novel class of antibacterials: inhibitors of *Staphylococcus aureus* transcription/translation. *Bioorg. Med. Chem. Lett.* **2006**, *16*, 6173–6177.

Lépine, F.; Milot, S.; Déziel, E.; He, J.; Rahme, L.G. Electrospray/mass spectrometric identification and analysis of 4-hydroxy-2-alkylquinolines (HAQs) produced by *Pseudomonas aeruginosa*. *J. Am. Soc. Mass Spectrom.* **2004**, *15*, 862–869.

Machan, Z.A.; Taylor, G.W.; Pitt, T.L.; Cole, P.J.; Wilson, R. 2-Heptyl-4-hydroxyquinoline N-oxide, an antistaphylococcal agent produced by *Pseudomonas aeruginosa*. *J. Antimicrob. Chemother.* **1992**, *30*, 615–623.

Mann, E.E.; Wozniak, D.J. *Pseudomonas* biofilm matrix composition and niche biology. *FEMS Microbiol. Rev.* **2012**, *36*, 893–916.

Margalith, P.; Beretta, G. Rifomycin XI: taxonomic study on *Streptomyces mediterranei* nov. sp. *Mycopathologia* **1960,** *13*, 321–330.

Mariani, R; Maffioli, S.I. Bacterial RNA polymerase inhibitors: an organized overview of their structure, derivatives, biological activity and current clinical development status. *Curr. Med. Chem.* **2009**, *16*, 430–454.

Mariner, K.R.; Trowbridge, R.; Agarwal, A.K.; Miller, K.; O'Neill, A.J.; Fishwick, C.W.G.; Chopra, I. Furanyl-rhodanines are unattractive drug candidates for development as inhibitors of bacterial RNA polymerase. *Antimicrob. Agents Chemother.* **2010**, *54*, 4506–4509.

McClure, W.R.; Cech, C.L. On the mechanism of rifampicin inhibition of RNA synthesis. *J. Biol. Chem.* **1978**, *253*, 8949–8956.

McKnight, S.L.; Iglewski, B.H.; Pesci, E.C. The *Pseudomonas* quinolone signal regulates *rhl* quorum sensing in *Pseudomonas aeruginosa*. *J. Bacteriol.* **2000**, *182*, 2702–2708.

McLean, K.J.; Carroll, P.; Lewis, D.G.; Dunford, A.J.; Seward, H.E.; Neeli, R.; Cheesman, M.R.; Marsollier, L.; Douglas, P.; Smith, W.E.; Rosenkrands, I.; Cole, S.T.; Leys, D.; Parish, T.; Munro A.W. Characterization of active site structure in CYP121. A cytochrome P450 essential for viability of Mycobacterium tuberculosis H37Rv. *J. Biol. Chem.* **2008**, *283*, 33406-33416.

McPhillie, M.J.; Trowbridge, R.; Mariner, K.R.; O'Neill, A.J.; Johnson, A.P.; Chopra, I.; Fishwick, C.W.G. Structure-based ligand design of novel bacterial RNA polymerase inhibitors. *ACS Med. Chem. Lett.* **2011**, *2*, 729–734.

Miller, M.B.; Bassler, B.L. Quorum sensing in bacteria. *Annu. Rev. Microbiol*. **2001**, *55*, 165−199.

Molin, S.; Tolker-Nielsen, T. Gene transfer occurs with enhanced efficiency in biofilms and induces enhanced stabilisation of the biofilm structure. *Curr. Opin. Biotechnol.* **2003**, 14, 255−261.

Mukhopadhyay, J.; Sineva, E.; Knight, J.; Levy, R.M.; Ebright, R.H. Antibacterial peptide microcin J25 inhibits transcription by binding within and obstructing the RNA polymerase secondary channel. *Mol. Cell* **2004**, *14*, 739−751.

Mukhopadhyay, J.; Das, K.; Ismail, S.; Koppstein, D.; Jang, M.; Hudson, B.; Sarafianos, S.; Tuske, S.; Patel, J.; Jansen, R.; Irschik, H.; Arnold, E:; Ebright, R.H. The RNA polymerase "switch region" is a target for inhibitors. *Cell* **2008**, *135*, 295−307.

Murakami, K.S. X-ray crystal structure of *Escherichia coli* RNA polymerase σ^{70} holoenzyme. *J. Biol. Chem.* **2013**, *288*, 9126−9134.

Nachega, J.B.; Chaisson, R.E. Tuberculosis drug resistance: a global threat. *Clin. Infect. Dis.* **2003**, *36*, 24−30.

Nealson, K.H.; Platt, T.; Hastings, J.W. Cellular control of the synthesis and activity of the bacterial luminescent system. *J. Bacteriol.* **1970**, *104*, 313–322.

Nie, Z.; Perretta, C.; Lu, J.; Su, Y.; Margosiak, S.; Gajiwala, K. S.; Cortez, J.; Nikulin, V.; Yager, K. M.; Appelt, K.; Chu, S. Structure-based design, synthesis, and study of potent inhibitors of β-ketoacyl-acyl carrier protein synthase III as potential antimicrobial agents. *J. Med. Chem.* **2005**, *48*, 1596−1609.

Ochsner, U.A.; Koch, A.K.; Fiechter, A.; Reiser, J. Isolation and characterization of a regulatory gene affecting rhamnolipid biosurfactant synthesis in *Pseudomonas aeruginosa*. *J. Bacteriol*. **1994**, *176*, 2044–2054.

Okamoto, K.; Gotoh, N.; Nishino, T. *Pseudomonas aeruginosa* reveals high intrinsic resistance to penem antibiotics: penem resistance mechanisms and their interplay. *Antimicrob. Agents Chemother.* **2001**, *45*, 1964–1971.

O'Neill, A,; Oliva, B.; Storey, C.; Hoyle, A.; Fishwick, C.; Chopra, I. RNA polymerase inhibitors with activity against rifampin-resistant mutants of *Staphylococcus aureus*. *Antimicrob. Agents Chemother.* **2000**, *44*, 3163−3166.

O'Shea, R.; Moser, H.E. Physicochemical properties of antibacterial compounds: implications for drug discovery. *J. Med. Chem.* **2008**, *51*, 2871−2878.

Palumbi, S.R. The evolution explosion: how humans cause rapid evolutionary change, 1st ed. *Norton*, New York, **2001**.

Parenti, F.; Pagani, H.; Beretta, G. Lipiarmycin, a new antibiotic from *Actinoplanes.* I. Description of the producer strain and fermentation studies. *J. Antibiot.* **1975,** *28*, 247−252.

Payne D.J.; Gwynn, M.N.; Holmes D.J.; Pompliano D.L. Drugs for bad bugs: confronting the challenges of antibacterial discovery. *Nat. Rev. Drug Discov.* **2007**, *6*, 29–40.

Pearson, J.P.; Gray, K.M.; Passador, L.; Tucker, K.D.; Eberhard, A.; Iglewski, B.H.; Greenberg, E.P. Structure of the autoinducer required for expression of *Pseudomonas aeruginosa* virulence genes. *Proc. Natl. Acad. Sci. U.S.A.* **1994**, *91*, 197–201.

Pearson, J.P.; Passador, L.; Iglewski, B.H.; Greenberg, E.P. A second *N*-acylhomoserine lactone signal produced by *Pseudomonas aeruginosa*. *Proc. Natl. Acad. Sci. U.S.A.* **1995**, *92*, 1490–1494.

Pesci, E.C.; Milbank, J.B.; Pearson, J.P.; McKnight, S.; Kende, A.S.; Greenberg, E.P.; Iglewski, B.H. Quinolone signaling in the cell-to-cell communication system of *Pseudomonas aeruginosa*. *Proc. Natl. Acad. Sci. U.S.A.* **1999**, *96*, 11229–11234.

Pistorius, D.; Ullrich, A.; Lucas, S.; Hartmann, R.W.; Kazmaier, U.; Müller, R. Biosynthesis of 2-alkyl-4(1*H*)-quinolones in *Pseudomonas aeruginosa*: potential for therapeutic interference with pathogenicity. *Chembiochem* **2011**, *12*, 850–853.

Prince, A.S. Biofilms, antimicrobial resistance, and airway infection. *N. Engl. J. Med*. **2002**, *347*, 1110–1111.

Ramaswamy, S.; Musser, J.M. Molecular genetic basis of antimicrobial agent resistance in *Mycobacterium tuberculosis*: 1998 update. *Tuber. Lung Dis.* **1998**, *79*, 3–29.

Rasmussen, T.B.; Givskov, M. Quorum-sensing inhibitors as anti-pathogenic drugs. *Int. J. Med. Microbiol.* **2006**, *296*, 149–161.

Rice, L.B. Unmet medical needs in antibacterial therapy. *Biochem. Pharmacol.* **2006**, *71*, 991–995.

Rowe, S.M.; Miller, S.; Sorscher, E.J. Cystic Fibrosis. *N. Engl. J. Med.* **2005**, *352*, 1992–2001.

(A) Sahner, J.H.; Groh, M.; Negri, M.; Haupenthal, J.; Hartmann, R.W. Novel small molecule inhibitors targeting the “switch region” of bacterial RNAP: structure-based optimization of a virtual screening hit. *Eur. J. Med. Chem.* **2013**, *65*, 223–231.

(B) Sahner, J.H.; Brengel, C.; Storz, M.P.; Groh, M.; Plaza, A.; Müller, R.; Hartmann, R.W. Combining in silico and biophysical methods for the development of *Pseudomonas aeruginosa* quorum sensing inhibitors: an alternative approach for structure-based drug design. *J. Med. Chem.* **2013**, *56*, 8656–8664.

Salomon, R.A.; Farias, R.N. Microcin 25, a novel antimicrobial peptide produced by *Escherichia coli*. *J. Bacteriol.* **1992,** *174*, 7428–7435.

Schertzer, J.W.; Brown, S.A.; Whiteley, M. Oxygen levels rapidly modulate *Pseudomonas aeruginosa* social behaviours via substrate limitation of PqsH. *Mol. Microbiol.* **2010**, 77, 1527–1538.

Silver, L.L. Challenges of antibacterial discovery. *Clin. Microbiol. Rev.* **2011**, *24*, 71–109.

Singh, P.K.; Schaefer, A.L.; Parsek, M.R.; Moninger, T.O.; Welsh, M.J.; Greenberg, E.P. Quorum-sensing signals indicate that cystic fibrosis lungs are infected with bacterial biofilms. *Natur*e **2000**, *407*, 762−764.

Spellberg, B. Dr. William H. Stewart: Mistaken or Maligned? *Clin. Infect. Dis.* **2008**, *47*, 294.

Srivastava, A.; Talaue, M.; Liu, S.; Degen, D.; Ebright, R.Y.; Sineva, E.; Chakraborty, A.; Druzhinin, S.Y.; Chatterjee, S.; Mukhopadhyay, J.; Ebright, Y.W.; Zozula, A.; Shen, J.; Sengupta, S.; Niedfeldt, R.R.; Xin, C.; Kaneko, T.; Irschik, H.; Jansen, R.; Donadio, S.; Connell, N.; Ebright, R.H. New target for inhibition of bacterial RNA polymerase: "switch region". *Curr. Opin. Microbiol.* **2011**, *14*, 532–543.

Starr, J.; Brown, M.F.; Aschenbrenner, L.; Caspers, N.; Che, Y.; Gerstenberger, B.S.; Huband, M.; Knafels, J.D.; Lemmon, M.M.; Li, C.; McCurdy, S.P.; McElroy, E.; Rauckhorst, M.R.; Tomaras, A.P.; Young, J.A.; Zaniewski, R.P.; Shanmugasundaram, V.; Han, S. Siderophore receptor-mediated uptake of lactivicin analogues in gram-negative bacteria. *J. Med. Chem.* **2014**, *57*, 3845–3855.

Storz, M.P.; Maurer, C.K.; Zimmer, C.; Wagner, N.; Brengel, C.; de Jong, J.C.; Lucas, S.; Müsken, M.; Häussler, S.; Steinbach, A.; Hartmann, R.W. Validation of PqsD as an anti-biofilm target in *Pseudomonas aeruginosa* by development of small-molecule inhibitors. *J. Am. Chem. Soc.* **2012**, *134*, 16143−16146.

Storz, M.P.; Allegretta, G.; Kirsch, B.; Empting, M.; Hartmann, R.W. From *in vitro* to *in cellulo*: structure–activity relationship of (2-nitrophenyl)methanol derivatives as inhibitors of PqsD in *Pseudomonas aeruginosa. Org. Biomol. Chem*. **2014**, *12*, 6094-6104.

Swift, S.; Downie, J.A.; Whitehead, N.A.; Barnard, A.M.; Salmond, G.P.; Williams, P. Quorum sensing as a population-density-dependent determinant of bacterial physiology. *Adv. Microb. Physiol*. **2001**, *45*, 199−270.

Tuske, S.; Sarafianos, S.G.; Wang, X.; Hudson, B.; Sineva, E.; Mukhopadhyay, J.; Birktoft, J.J.; Leroy, O.; Ismail, S.; Clark, A.D.; Dharia, C.; Napoli, A.; Laptenko, O.; Lee, J.; Borukhov, S.; Ebright, R.H.; Arnold, E. Inhibition of bacterial RNA polymerase by streptolydigin: stabilization of a straight-bridge-helix active-center conformation. *Cell* **2005**, *122*, 541–552.

van Delden, C.; Iglewski, B.H. Cell-to-cell signaling and *Pseudomonas aeruginosa* infections. *Emerging Infect. Dis.* **1998**, *4*, 551–560.

Vassylyev, D.G.; Sekine, S.; Laptenko, O.; Lee, J.; Vassylyeva, M.N.; Borukhov, S.; Yokoyama, S. Crystal structure of a bacterial RNA polymerase holoenzyme at 2.6 Å resolution. *Nature* **2002**, *417*, 712−709.

Villain-Guillot, P.; Bastide, L.; Gualtieri, M.; Leonetti, J.-P. Progress in targeting bacterial transcription. *Drug Discov. Today* **2007**, *12*, 200−208.

Waksman, S.A. What is an antibiotic or an antibiotic substance? *Mycologia* **1947**, *39*, 565–569.

Waksman, S.A. Nobel Lecture “Streptomycin: background, isolation, properties, and utilization”. **1952**. *http://www.nobelprize.org/nobel_prizes/medicine/laureates/1952/waksman-lecture.html*

Wehrli, W.; Neusch, J.; Knusel, F.; Staehelin, M. Action of rifamycin on RNA polymerase from sensitive and resistant bacteria. *Biochem. Biophys. Res. Commun.* **1968**, *32*, 284–288.

Weidel, E.; de Jong, J.C.; Brengel, C.; Storz, M.P.; Braunshausen, A.; Negri, M.; Plaza, A.; Steinbach, A.; Müller, R.; Hartmann, R.W. Structure optimization of 2-benzamidobenzoic acids as PqsD inhibitors for *Pseudomonas aeruginosa* infections and elucidation of binding mode by SPR, STD NMR, and molecular docking. *J. Med. Chem.* **2013**, *56*, 6146−6155.

World Health Organization (WHO). Fact Sheet N° 268 “Use of antimicrobials outside human medicine and resultant antimicrobial resistance in humans”. **2002**. *http://whqlibdoc.who.int/fact_sheet/2002/FS_268.pdf*

World Health Organization (WHO). World health report 2007 “A safer future: global public health security in the 21st century”. **2007**. *www.who.int/whr/2007/whr07_en.pdf*

World Health Organization (WHO). Fact Sheet N°194 “Antimicrobial resistance”. **2014**. *http://www.who.int/mediacentre/factsheets/fs194/en/*

Xiao, G.; Déziel, E.; He, J.; Lépine, F.; Lesic, B.; Castonguay, M.H.; Milot, S.; Tampakaki, A.P.; Stachel, S.E.; Rahme, L.G. MvfR, a key *Pseudomonas aeruginosa* pathogenicity LTTR-class regulatory protein, has dual ligands. *Mol. Microbiol.* **2006**, *62*, 1689−1699.

Xu, M.; Zhou, Y.N.; Goldstein, B.P.; Jin, D.J. Cross-resistance of *Escherichia coli* RNA polymerases conferring rifampin resistance to different antibiotics. *J. Bacteriol.* **2005**, *187*, 2783–2792.

Yakushiji, F.; Miyamoto, Y.; Kunoh, Y.; Okamoto, R.; Nakaminami, H.; Yamazaki, Y.; Noguchi, N.; Hayashi, Y. Novel hybrid-type antimicrobial agents targeting the switch region of bacterial RNA polymerase. *ACS Med. Chem. Lett.* **2013**, *4*, 220–224.

6. Supporting Information

This section contains the supporting information of the publications presented in section 3. It provides further experimental results and detailed experimental methods as well as additional figures.

6.1 Supporting Information for Publication I

Full supporting information is available online:
http://pubs.acs.org/doi/suppl/10.1021/jm400485e/suppl_file/jm400485e_si_001.pdf

6.1.1 General directions

Chemical names follow IUPAC nomenclature. Starting materials were purchased from Sigma-Aldrich, Acros, Maybridge, Combi Blocks, Fluka, ABCR, Alfa Aesar, Apollo and were used without purification.

Column chromatography (CC) was performed on silica gel (63–200 µm), preparative thin layer chromatography (TLC) on 1 mm SIL G-100 UV_{254} glass plates (Macherey-Nagel), and reaction progress was monitored by TLC on Alugram SIL G UV_{254} (Macherey-Nagel).

^{1}H NMR and ^{13}C NMR spectra were recorded on a Bruker AM500 spectrometer (500 MHz and 125 MHz) at 300 K in $CDCl_3$ or CD_3SOCD_3. Chemicals shifts are reported in δ values (ppm), the hydrogenated residues of deuterated solvent were used as internal standard ($CDCl_3$: δ = 7.27 ppm in ^{1}H NMR and δ = 77.0 ppm in ^{13}C NMR, DMSO-d_6: δ = 2.50 ppm in ^{1}H NMR and δ = 39.5 ppm in ^{13}C NMR). Signals are described as s, d, t, dd, ddd, dt and m for singlet, doublet, triplet, doublet of doublet, doublet of doublet of doublet, doublet of triplet and multiplet, respectively. Coupling constants (*J*) are given in Hertz (Hz).

The reported yields are the isolated yields of purified material and are not optimized.

Purity of compounds **1** to **34** was determined using LC/MS as follows:
The SpectraSystems®-LC-system consisted of a pump, an autosampler, and a UV detector. Mass spectrometry was performed on a MSQ® electro spray mass spectrometer (Thermo Fisher, Dreieich, Germany). The system was operated by the standard software Xcalibur®. A RP C18 NUCLEODUR® 100-5 (125 x 3 mm) column (Macherey-Nagel GmbH, Duehren, Germany) was used as stationary phase. All solvents were HPLC grade.
Solvent system:
In a gradient run the percentage of acetonitrile (containing 0,1 % triflouro-acetic acid) in 0,1 % triflouro-acetic acid was increased from an initial concentration of 0 % at 0 min to 100 % at 15 min and kept at 100 % for 5 min.

The injection volume was 10 µL and flow rate was set to 800 µL/min. MS analysis was carried out at a spray voltage of 3800 V, a capillary temperature of 350 °C and a source CID of 10 V. Spectra were acquired in positive mode from 100 to 1000 m/z and at 254 nm for the UV trace.

Melting points were determined on a Stuart Scientific melting point apparatus SMP3 and are uncorrected.

6.1.2 Experimental and spectroscopic data of all compounds

4-(N,N-dipropylsulfamoyl)benzoic acid (VIIb). To a solution of 4-(chlorosulfonyl)benzoic acid (1 equiv) in anhydrous CH_2Cl_2 at 0° C dipropylamine (3 equiv) was added slowly by means of a syringe. The reaction mixture was stirred at room temperature for 18 h followed by extraction with 1N HCl. The organic layer was washed with H_2O and dried over $MgSO_4$. Evaporation of the solvent provided the title compound; yield: 99 %. ^{1}H NMR (500 MHz, CD_3COCD_3) δ = 8.24–8.19 (m, 2 H), 7.99–7.94 (m, 2 H), 3.17–3.12 (m, 4 H), 1.61–1.51 (m, 4 H), 0.86 (t, *J* = 7.4 Hz, 6 H) ppm.
^{13}C NMR (125 MHz, CD_3COCD_3) δ = 166.6, 145.3, 134.9, 131.3, 128.1, 50.9, 22.8, 11.4 ppm.
LC/MS: m/z = 286 [M + H$^+$]; t_R = 11.58 min; 94.8 % pure (UV).

4-(4-oxo-4H-naphtho[2,3-d][1,3]oxazin-2-yl)-N,N-dipropylbenzenesulfonamide (VIIa). 4-(N,N-dipropylsulfamoyl)benzoic acid (**VIIb**, 1.5 equiv) was converted to the corresponding benzoyl chloride via reaction with thionyl chloride (3.75 equiv) in CH_2Cl_2 in the presence of catalytic amounts of dimethylformamide (4 h reflux). After evaporation of the solvent the resulting benzoyl chloride and 3-amino-2-naphthoic acid (1 equiv) were suspended in toluene and the mixture was refluxed for 18 h. The product was purified by CC (*n*-hexane/EtOAc 8:2); yield: 28 %. ^{1}H NMR (500 MHz, $CDCl_3$) δ = 8.89 (s, 1 H), 8.49–8.44 (m, 2 H), 8.19 (s, 1 H), 8.09–8.00 (m, 2 H), 7.99–7.94 (m, 2 H), 7.74–7.69 (m, 1 H), 7.66–7.60 (m, 1 H), 3.19–3.12 (m, 4 H), 1.61–1.55 (m, 4 H), 0.90 (t, *J* = 7.4 Hz, 6 H, CH_3) ppm.
^{13}C NMR (125 MHz, $CDCl_3$) δ = 159.4, 153.8, 143.6, 140.8, 137.6, 133.9, 132.4, 131.4, 129.9, 129.7, 128.7, 128.3, 127.5, 127.3, 125.8, 115.4, 49.9, 21.9, 11.2 ppm.
LC/MS: m/z = 437 [M + H$^+$], 478 [M$^+$ + CH_3CN]; t_R = 17.57 min; 98.0 % pure (UV).

3-(4-(N,N-dipropylsulfamoyl)benzamido)-2-naphthoic acid[1] (VII). 4-(4-oxo-4H-naphtho[2,3-d][1,3]oxazin-2-yl)-N,N-dipropylbenzenesulfonamide (**VIIa**) was dissolved in a mixture of THF/MeOH (2:1) and hydrolyzed by an aqueous solution containing 1 mol/L LiOH at room temperature (18 h). The mixture was acidified by the addition of 1 M HCl, filtered and the precipitate was successively washed with 1 M HCl. The product was purified by preparative TLC (CH_2Cl_2/MeOH 9:1); yield: 24 %. ^{1}H NMR (500 MHz, CD_3SOCD_3) δ = 12.63 (br. s., 1 H, NH), 9.09 (s, 1 H), 8.76 (s, 1 H), 8.21–8.14 (m, 2 H), 8.06 (d, *J* = 8.2 Hz, 1 H), 8.04–7.99 (m, 2 H), 7.94 (d, *J* = 8.2 Hz, 1 H), 7.68–7.59 (m, 1 H), 7.56–7.47 (m, 1 H), 3.07 (t, *J* = 7.6 Hz, 4 H), 1.55–1.43 (m, 4 H), 0.82 (t, *J* = 7.4 Hz, 6 H, CH_3) ppm.
^{13}C NMR (125 MHz, CD_3SOCD_3) δ = 169.9, 163.5, 142.4, 138.2, 136.1, 135.4, 133.2, 129.2, 129.1, 128.6, 128.1, 127.5, 127.3, 125.8, 118.7, 117.0, 49.7, 21.7, 11.0 ppm.
LC/MS: m/z = 455 [M + H$^+$]; t_R = 15.80 min; 99.0 % pure (UV).

methyl 2-([1,1'-biphenyl]-4-ylcarboxamido)benzoate (1a) was prepared according to method BIII. For purification the solvent was evaporated and the remaining solid was suspended in MeOH. After filtration the precipitate was washed with MeOH to provide the pure compound; yield: 58 %. ^{1}H NMR (500 MHz, $CDCl_3$) δ = 12.11 (br. s, 1 H, NH), 8.98 (dd, *J* = 8.5, 0.9 Hz, 1 H), 8.16–8.13 (m, 2 H), 8.11 (dd, *J* = 8.2, 1.6 Hz, 1 H), 7.78–7.75 (m, 2 H), 7.68–7.61 (m, 3 H), 7.51–7.47 (m, 2 H), 7.45–7.39 (m, 1 H), 7.18–7.12 (m, 1 H), 3.99 (s, 3 H, OCH_3) ppm.

^{13}C NMR (125 MHz, $CDCl_3$) δ = 169.1, 165.4, 144.7, 141.9, 140.0, 134.9, 133.6, 131.0, 128.9, 128.0, 127.9, 127.5, 127.2, 122.6, 120.5, 115.1, 52.5 (OCH_3) ppm.
LC/MS: m/z = 332 [M + H^+], 373 [M + H^+ CH_3CN], 663 [2M + H^+]; t_R = 14.92 min; 100.0 % pure (UV).

2-([1,1'-biphenyl]-4-ylcarboxamido)benzoic acid[2] (1) was prepared according to method C. Sufficient purity was achieved without further purification; yield: 74 %. Mp: 190 °C (decomposition). ^{1}H NMR (500 MHz, DMSO-d_6) δ = 12.26 (br. s, 1 H, NH), 8.74 (dd, *J* = 8.5, 0.9 Hz, 1 H), 8.07 (dd, *J* = 7.9, 1.5 Hz, 1 H), 8.06–8.02 (m, 2 H), 7.90–7.86 (m, 2 H), 7.77–7.74 (m, 2 H), 7.70–7.63 (m, 1 H), 7.53–7.49 (m, 2 H), 7.46–7.40 (m, 1 H), 7.27–7.17 (m, 1 H) ppm.
^{13}C NMR (125 MHz, DMSO-d_6) δ = 163.8, 163.7, 143.0, 143.0, 140.9, 140.7, 138.9, 133.9, 133.8, 131.5, 131.4, 130.9, 128.9, 128.0, 127.8, 126.8, 121.8, 121.7, 118.5, 118.4 ppm.
LC/MS: m/z = 318 [M + H^+], 635 [2M + H^+]; t_R = 12.38 min; 99.4 % pure (UV).

methyl 2-(3-phenoxybenzamido)benzoate (2a) was prepared according to method BI. For purification the solvent was evaporated and the remaining solid was suspended in MeOH. After filtration the precipitate was washed with MeOH to provide the pure compound; yield: 45 %. ^{1}H NMR (500 MHz, $CDCl_3$) δ = 12.02 (br. s, 1 H, NH), 8.91 (dd, *J* = 8.5, 1.3 Hz, 1 H), 8.09 (dd, *J* = 8.0, 1.7 Hz, 1 H), 7.77–7.74 (m, 1 H), 7.71–7.69 (m, 1 H), 7.61 (ddd, *J* = 8.6, 7.2, 1.9 Hz, 1 H), 7.49 (dd, *J* = 7.9, 7.9 Hz, 1 H), 7.42–7.36 (m, 2 H), 7.21 (ddd, *J* = 8.2, 2.5, 0.9 Hz, 1 H), 7.18–7.11 (m, 2 H), 7.11–7.07 (m, 2 H), 3.96 (s, 3 H, OCH_3) ppm.
^{13}C NMR (125 MHz, $CDCl_3$) δ = 169.0, 165.1, 158.1, 156.5, 141.7, 136.9, 134.8, 130.9, 130.2, 129.9, 123.8, 122.7, 122.0, 121.5, 120.5, 119.5, 117.6, 115.2, 52.5 (OCH_3) ppm.
LC/MS: m/z = 348 [M + H^+], 389 [M + H^+ CH_3CN], 695 [2M + H^+]; t_R = 15.88 min; 96.9 % pure (UV).

2-(3-phenoxybenzamido)benzoic acid[3] (2) was prepared according to method C. Sufficient purity was achieved without further purification; yield: 85 %. Mp: 204–206 °C. ^{1}H NMR (500 MHz, DMSO-d_6) δ = 14.64 (br. s, 1H, NH), 8.70 (dd, *J* = 8.2 Hz, 0.9 Hz, 1H), 8.18 (dd, *J* = 7.9 Hz, 1.6 Hz, 1H), 7.84–7.82 (m, 1H), 7.63 (t, *J* = 1.9 Hz, 1H), 7.49 (t, *J* = 7.9 Hz, 1H), 7.43–7.39 (m, 3H), 7.19–7.15 (m, 2H), 7.07–7.03 (m, 3H) ppm.
^{13}C NMR (125 MHz, DMSO-d_6) δ = 171.7, 163.4, 157.2, 156.2, 140.8, 137.2, 131.6, 131.2, 130.4, 130.2, 123.9, 123.1, 122.0, 121.7, 121.5, 118.6, 119.0, 117.2 ppm.
LC/MS: m/z = 334 [M + H^+]; t_R = 13.73 min; 96.9 % pure (UV).

2-(2-phenoxy-[1,1'-biphenyl]-4-ylcarboxamido)benzoic acid[3] (3) was prepared using the procedure described by *Nie et al.*[3] ^{1}H NMR (500 MHz, Acetone-d_6) δ = 12.32 (br. s, 1 H, NH), 7.89 (dd, *J* = 8.5, 1.9 Hz, 1 H), 8.18 (dd, *J* = 7.9, 1.6 Hz, 1 H), 7.89 (dd, *J* = 8.2, 1.9 Hz, 1 H), 7.71 (d, *J* = 7.9 Hz, 1 H), 7.65–7.63 (m, 4 H), 7.44–7.41 (m, 2 H), 7.37–7.34 (m, 3 H), 7.23–7.20 (m, 1 H), 7.11–7.08 (m, 1 H), 7.03–7.00 (m, 2 H) ppm.
^{13}C NMR (125 MHz, $CDCl_3$) δ = 171.0, 164.9, 158.3, 155.0, 143.2, 138.1, 127.9, 136.7, 135.6, 132.8, 132.5, 131.0, 130.1, 129.2, 128.8, 124.3, 123.7, 123.3, 120.9, 120.8, 120.1, 119.2 ppm.
LC/MS: m/z = 410 [M + H^+]; t_R = 14.40 min; 95.2 % pure (UV).

methyl 2-benzamidobenzoate (4a) was prepared according to method BIII. For purification the solvent was evaporated and the remaining solid was resolved in a small amount of CH_2Cl_2. After addition of MeOH the CH_2Cl_2 was evaporated. Crystals formed overnight in the remaining MeOH provided the pure compound; yield: 69 %. ^{1}H NMR (500 MHz, $CDCl_3$) δ = 12.05 (br. s, 1 H, NH), 8.95 (dd, *J* = 8.5, 1.3 Hz, 1 H), 8.10 (dd, *J* = 7.9, 1.6 Hz, 1 H), 8.08–8.04 (m, 2 H), 7.64–7.60 (m, 1 H), 7.60–7.50 (m, 3 H), 7.17–7.09 (m, 1 H), 3.98 (s, 3 H, OCH_3) ppm.
^{13}C NMR (125 MHz, $CDCl_3$) δ = 169.1, 165.7, 141.9, 134.9, 134.8, 131.9, 130.9, 128.8, 127.4, 122.6, 120.5, 115.2, 52.5 (OCH_3) ppm.
LC/MS: m/z = 256 [M + H^+], 511 [2M + H^+]; t_R = 12.32 min; 100.0 % pure (UV).

2-benzamidobenzoic acid[4] (4) was prepared according to method C. Sufficient purity was achieved without further purification; yield: 94 %. Mp: 179–181 °C. ^{1}H NMR (500 MHz, DMSO-d_6) δ = 12.18 (br. s, 1 H, NH), 8.72 (dd, *J* = 8.2, 0.9 Hz, 1 H), 8.06 (dd, *J* = 7.9, 1.6 Hz, 1 H), 7.98–7.94 (m, 2 H), 7.69–7.63 (m, 2 H), 7.62–7.57 (m, 2 H), 7.23–7.19 (m, 1 H) ppm.
^{13}C NMR (125 MHz, DMSO-d_6) δ = 170.0, 164.7, 141.1, 134.5, 134.3, 132.2, 131.3, 129.0, 127.0, 122.9, 119.9, 116.5 ppm.
LC/MS: m/z = 242 [M + H$^+$], 483 [2M + H$^+$]; t_R = 9.88 min; 100.0 % pure (UV).

methyl 2-amino-3-chlorobenzoate (5b) was prepared according to method A. The product was purified by CC (*n*-hexane/EtOAc 1:1); yield: 60 %. ^{1}H NMR (500 MHz, $CDCl_3$) δ = 7.82 (dd, *J* = 7.9, 1.6 Hz, 1 H), 7.41 (dd, *J* = 7.9, 1.6 Hz, 1 H), 6.59 (dd, *J* = 7.9, 7.9 Hz, 1 H), 6.28 (br. s, 2 H, NH_2), 3.89 (s, 3 H, OCH_3) ppm.
^{13}C NMR (125 MHz, $CDCl_3$) δ = 168.1, 146.6, 133.78, 129.9, 120.2, 115.7, 111.8, 51.8 (OCH_3) ppm.
LC/MS: m/z = 186 [M + H$^+$], 227 [M + H$^+$ CH_3CN]; t_R = 11.68 min; 98.4 % pure (UV).

methyl 2-([1,1'-biphenyl]-4-ylcarboxamido)-3-chlorobenzoate (5a) was prepared according to method BIII. For purification the solvent was evaporated and the remaining solid was resolved in a small amount of CH_2Cl_2. After addition of MeOH the CH_2Cl_2 was evaporated. Crystals formed overnight in the remaining MeOH provided the pure compound; yield: 40 %. ^{1}H NMR (500 MHz, $CDCl_3$) δ = 9.51 (br. s, 1 H, NH), 8.12–8.06 (m, 2 H), 7.90 (dd, *J* = 7.9, 1.6 Hz, 1 H), 7.77–7.72 (m, 2 H), 7.68 (dd, *J* = 7.9, 1.6 Hz, 1 H), 7.67–7.63 (m, 2 H), 7.52–7.46 (m, 2 H), 7.44–7.39 (m, 1 H), 7.27 (dd, *J* = 7.9, 7.9 Hz, 1 H), 3.90 (s, 3 H, OCH_3) ppm.
^{13}C NMR (125 MHz, $CDCl_3$) δ = 167.1, 165.0, 145.1, 140.0, 135.7, 134.3, 132.5, 131.2, 129.1, 128.9, 128.2, 128.1, 127.5, 127.3, 126.0, 126.0, 52.7 (OCH_3) ppm.
LC/MS: m/z = 365 and 367 [M + H$^+$], 731 and 733 [2M + H$^+$]; t_R = 13.00 min; 93.8 % pure (UV).

2-([1,1'-biphenyl]-4-ylcarboxamido)-3-chlorobenzoic acid (5) was prepared according to method C. The product was purified by preparative TLC (*n*-hexane/EtOAc 1:1); yield: 93 %. Mp: 203–205 °C. ^{1}H NMR (500 MHz, DMSO-d_6) δ = 10.33 (br. s, 1 H, NH), 8.11–8.07 (m, 2 H), 7.86–7.75 (m, 6 H), 7.54–7.49 (m, 2 H), 7.47–7.40 (m, 2 H) ppm.
^{13}C NMR (125 MHz, DMSO-d_6) δ = 166.8, 165.1, 143.3, 139.2, 134.7, 132.8, 132.7, 131.9, 129.9, 129.0, 128.5, 128.2, 127.6, 127.0, 126.7 ppm.
LC/MS: m/z = 352 [2 + H$^+$], 703 [2M + H$^+$]; t_R = 11.55 min; 99.2 % pure (UV).

methyl 2-([1,1'-biphenyl]-4-ylcarboxamido)-4-chlorobenzoate (6a) was prepared according to method BI. For purification the solvent was evaporated and the remaining solid was suspended in MeOH. After filtration the precipitate was washed with MeOH to provide the pure compound; yield: 59 %. ^{1}H NMR (500 MHz, $CDCl_3$) δ = 12.13 (br. s, 1 H, NH), 9.08 (d, *J* = 2.1 Hz, 1 H), 8.14–8.09 (m, 2 H), 8.01 (d, *J* = 8.8 Hz, 1 H), 7.78–7.74 (m, 2 H), 7.69–7.61 (m, 2 H), 7.53–7.45 (m, 2 H), 7.44–7.38 (m, 1 H), 7.10 (dd, *J* = 8.8, 2.1 Hz, 1 H), 3.98 (s, 3 H, OCH_3) ppm.
^{13}C NMR (125 MHz, $CDCl_3$) δ = 168.5, 165.4, 144.9, 142.7, 141.2, 139.9, 133.0, 132.0, 128.9, 128.1, 127.9, 127.5, 127.2, 122.8, 120.3, 113.3, 52.6 (OCH_3) ppm.
LC/MS: m/z = 367 [M + H$^+$], 733 [2M + H$^+$]; t_R = 16.36 min; 98.2 % pure (UV).

2-([1,1'-biphenyl]-4-ylcarboxamido)-4-chlorobenzoic acid (6) was prepared according to method C. Sufficient purity was achieved without further purification; yield: 55 %. Mp: 323–324 °C. ^{1}H NMR (500 MHz, DMSO-d_6) δ = 15.29 (br. s, 1 H, NH), 8.81 (d, *J* = 2.2 Hz, 1 H), 8.15–8.08 (m, 3 H), 7.84–7.78 (m, 2 H), 7.74–7.68 (m, 2 H), 7.52–7.45 (m, 2 H), 7.44–7.38 (m, 1 H), 7.09 (dd, *J* = 8.2, 2.2 Hz, 1 H) ppm.
^{13}C NMR (125 MHz, DMSO-d_6) δ = 169.6, 164.2, 143.3, 142.0, 139.0, 134.8, 133.6, 133.1, 129.0, 128.2, 127.9, 126.9, 126.9, 122.8, 121.5, 117.9 ppm.
LC/MS: m/z = 351 and 353 [M + H$^+$]; t_R = 14.11 min; 99.1 % pure (UV).

methyl 4-chloro-2-(3-phenoxybenzamido)benzoate (7a) was prepared according to method BI. For purification the solvent was evaporated and the remaining solid was suspended in MeOH. After filtration the precipitate was washed with MeOH to provide the pure compound; yield: 71 %. ^{1}H NMR (500 MHz, $CDCl_3$) δ = 12.07 (br. s, 1 H, NH), 9.02 (d, *J* = 2.2 Hz, 1 H), 8.00 (d, *J* = 8.8 Hz, 1 H), 7.75–7.71 (m, 1 H), 7.70–7.65 (m, 1 H), 7.49 (dd, *J* = 8.2, 8.2 Hz, 1 H), 7.41–7.37 (m, 2 H), 7.22 (ddd, *J* = 8.2, 2.2, 0.9 Hz, 1 H), 7.19–7.15 (m, 1 H), 7.14–7.07 (m, 3 H), 3.96 (s, 3 H, OCH_3) ppm.
^{13}C NMR (125 MHz, $CDCl_3$) δ = 168.4, 165.1, 158.2, 156.4, 142.5, 141.2, 136.3, 133.0, 130.2, 130.0, 124.0, 123.0, 122.2, 121.4, 120.4, 119.5, 117.5, 113.4, 52.6 (OCH_3) ppm.
LC/MS: m/z = 382 [M + H^+]; t_R = 15.99 min; 95.5 % pure (UV).

4-chloro-2-(3-phenoxybenzamido)benzoic acid (7) was prepared according to method C. Sufficient purity was achieved without further purification; yield: 61 %. Mp: 205–206 °C. ^{1}H NMR (500 MHz, DMSO-d_6) δ = 12.26 (br. s, 1 H, NH), 8.75 (d, *J* = 1.9 Hz, 1 H), 8.03 (d, *J* = 8.5 Hz, 1 H), 7.72–7.66 (m, 1 H), 7.61 (dd, *J* = 7.9, 7.9 Hz, 1 H), 7.52 (s, 1 H), 7.47–7.41 (m, 2 H), 7.33–7.25 (m, 2 H), 7.23–7.17 (m, 1 H), 7.16–7.02 (m, 2 H) ppm.
^{13}C NMR (125 MHz, DMSO-d_6) δ = 169.3, 164.2, 157.4, 155.9, 141.9, 138.7, 136.0, 132.9, 130.9, 130.3, 124.1, 123.0, 122.3, 121.6, 119.2, 119.1, 116.9, 115.4 ppm.
LC/MS: m/z = 368 [M + H^+], 409 [M + H^+ CH_3CN]; t_R = 13.98 min; 100.0 % pure (UV).

methyl 2-([1,1'-biphenyl]-4-ylcarboxamido)-5-chlorobenzoate (8a) was prepared according to method BII. For purification the solvent was evaporated and the remaining solid was suspended in MeOH. After filtration the precipitate was washed with MeOH to provide the pure compound; yield: 86 %. ^{1}H NMR (500 MHz, $CDCl_3$) δ = 12.02 (br. s, 1 H, NH), 8.97 (d, *J* = 9.1 Hz, 1 H), 8.13–8.10 (m, 2 H), 8.07 (d, *J* = 2.5 Hz, 1 H), 7.78–7.75 (m, 2 H), 7.67–7.64 (m, 2 H), 7.57 (dd, *J* = 9.1, 2.5 Hz, 1 H), 7.52–7.47 (m, 2 H), 7.45–7.37 (m, 1 H), 4.00 (s, 3 H, OCH_3) ppm.
^{13}C NMR (125 MHz, $CDCl_3$) δ = 168.1, 165.3, 144.9, 140.5, 139.9, 134.7, 133.2, 130.5, 128.9, 128.1, 127.9, 127.6, 127.5, 127.2, 121.9, 116.3, 52.8 (OCH_3) ppm.
LC/MS: m/z = 366 [M + H^+], 731 [2M + H^+]; t_R = 16.76 min; 97.0 % pure (UV).

2-([1,1'-biphenyl]-4-ylcarboxamido)-5-chlorobenzoic acid (8) was prepared according to method C. For purification the remaining solid was washed with MeOH and CH_2Cl_2 to provide the pure compound; yield: 96 %. Mp: 274–276 °C. ^{1}H NMR (500 MHz, DMSO-d_6) δ = 12.14 (br. s, 1 H, NH), 8.74 (d, *J* = 9.1 Hz, 1 H), 8.05–8.02 (m, 2 H), 8.00 (d, *J* = 2.5 Hz, 1 H), 7.91–7.86 (m, 2 H), 7.79–7.75 (m, 2 H), 7.73 (dd, *J* = 9.1, 2.5 Hz, 1 H), 7.54–7.48 (m, 2 H), 7.47–7.41 (m, 1 H) ppm.
^{13}C NMR (125 MHz, DMSO-d_6) δ = 168.8, 164.4, 143.8, 139.9, 138.8, 133.9, 132.9, 130.4, 129.1, 128.3, 127.8, 127.2, 127.0, 126.5, 121.8, 118.6 ppm.
LC/MS: m/z = 352 and 354 [M + H^+]; t_R = 14.32 min; 99.3 % pure (UV).

methyl 2-([1,1'-biphenyl]-4-ylcarboxamido)-6-chlorobenzoate (9a) was prepared according to method BII. The product was purified by CC (*n*-hexane/EtOAc 8:2); yield: 76 %. ^{1}H NMR (500 MHz, $CDCl_3$) δ = 10.27 (br. s, 1 H, NH), 8.56 (dd, *J* = 8.2, 0.9 Hz, 1 H), 8.04–8.01 (m, 2 H), 7.77–7.74 (m, 2 H), 7.67–7.64 (m, 2 H), 7.52–7.41 (m, 4 H), 7.24 (dd, *J* = 8.2, 0.9 Hz, 1 H), 4.03 (s, 3 H, OCH_3) ppm.
^{13}C NMR (125 MHz, $CDCl_3$) δ = 167.9, 165.0, 145.1, 139.8, 139.7, 133.6, 132.9, 132.6, 129.0, 128.2, 127.8, 127.6, 127.2, 125.9, 120.2, 119.9, 52.8 (OCH_3) ppm.
LC/MS: m/z = 366 [M + H^+], 731 [2M + H^+]; t_R = 13.90 min; 98.2 % pure (UV).

2-([1,1'-biphenyl]-4-ylcarboxamido)-6-chlorobenzoic acid (9) was prepared according to method C. For purification the remaining solid was washed with CH_2Cl_2 to provide the pure compound; yield: 79 %. Mp: 218–219 °C. ^{1}H NMR (500 MHz, DMSO-d_6) δ = 10.36 (br. s, 1 H, NH), 8.04–8.01 (m, 2 H), 7.86–7.83 (m, 2 H), 7.78–7.75 (m, 2 H), 7.61–7.58 (m, 1 H), 7.53–7.49 (m, 3 H), 7.46–7.40 (m, 2 H) ppm.

^{13}C NMR (125 MHz, DMSO-d_6) δ = 166.2, 165.2, 143.4, 139.0, 136.9, 132.7, 130.8, 130.5, 129.6, 129.1, 128.3, 128.2, 126.9, 126.8, 126.7, 125.1 ppm.
LC/MS: m/z = 352 [M + H$^+$], 705, 707 [2M + H$^+$]; t_R = 12.25 min; 100.0 % pure (UV).

methyl 2-([1,1'-biphenyl]-4-ylcarboxamido)-4-fluorobenzoate (10a) was prepared according to method BI. For purification the solvent was evaporated and the remaining solid was suspended in MeOH. After filtration the precipitate was washed with MeOH to provide the pure compound; yield: 42 %. ^{1}H NMR (500 MHz, $CDCl_3$) δ = 12.25 (br. s, 1 H, NH), 8.80 (dd, *J* = 11.8, 2.4 Hz, 1 H), 8.21–8.03 (m, 3 H), 7.82–7.72 (m, 2 H), 7.72–7.61 (m, 2 H), 7.57–7.48 (m, 2 H), 7.48–7.39 (m, 1 H), 6.96–6.79 (m, 1 H), 3.99 (s, 3 H, OCH_3) ppm.
^{13}C NMR (125 MHz, $CDCl_3$) δ = 168.5, 166.1 (d, *J* = 253.9 Hz), 165.6, 145.0, 144.1 (d, J_{CF} = 12.8 Hz), 139.9, 133.3 (d, J_{CF} = 11.0 Hz), 133.1, 128.9, 128.1, 127.9, 127.5, 127.2, 111.3 (d, J_{CF} = 2.7 Hz), 109.9 (d, J_{CF} = 22.9 Hz), 107.6 (d, J_{CF} = 28.4 Hz), 52.5 ppm (OCH_3).
LC/MS: m/z = 350 [M + H$^+$], 391 [M + H$^+$ CH_3CN], 699 [2M + H$^+$]; t_R = 15.69 min; 96.4 % pure (UV).

2-([1,1'-biphenyl]-4-ylcarboxamido)-4-fluorobenzoic acid (10) was prepared according to method C. For purification the compound was recrystallized from MeOH; yield: 24 %. Mp: 258–260 °C. ^{1}H NMR (500 MHz, DMSO-d_6) δ = 12.47 (br. s, 1 H, NH), 8.59 (dd, *J* = 12.3, 2.5 Hz, 1 H), 8.14 (dd, *J* = 9.0, 6.8 Hz, 1 H), 8.07–8.00 (m, 2 H), 7.93–7.87 (m, 2 H), 7.81–7.72 (m, 2 H), 7.57–7.49 (m, 2 H), 7.49–7.41 (m, 1 H), 7.10–7.01 (m, 1 H) ppm.
^{13}C NMR (125 MHz, DMSO-d_6) δ = 169.4, 165.1 (d, J_{CF} = 248.0 Hz), 164.6, 143.9, 143.3 (d, J_{CF} = 12.8 Hz), 138.8, 134.0 (d, J_{CF} = 11.0 Hz), 132.7, 129.1, 128.3, 127.7, 127.2, 127.0, 112.8 (d, J_{CF} = 2.7 Hz), 109.9 (d, J_{CF} = 22.0 Hz), 106.3 (d, J_{CF} = 28.4 Hz) ppm.
LC/MS: m/z = 336 [M + H$^+$], 377 [M + H$^+$ CH_3CN], 671 [2M + H$^+$]; t_R = 13.94 min; 100.0 % pure (UV).

methyl 2-([1,1'-biphenyl]-4-ylcarboxamido)-5-fluorobenzoate (11a) was prepared according to method BI. For purification the solvent was evaporated and the remaining solid was suspended in MeOH. After filtration the precipitate was washed with MeOH to provide the pure compound; yield: 64 %. ^{1}H NMR (500 MHz, $CDCl_3$) δ = 11.94 (br. s, 1 H, NH), 8.99 (dd, *J* = 9.1, 4.7 Hz, 1 H), 8.16–8.05 (m, 2 H), 7.81–7.71 (m, 3 H), 7.70–7.60 (m, 2 H), 7.54–7.45 (m, 2 H), 7.45–7.38 (m, 1 H), 7.38–7.30 (m, 1 H), 4.00 (s, 3 H, OCH_3) ppm.
^{13}C NMR (125 MHz, $CDCl_3$) δ = 168.1, 165.3, 157.4 (d, J_{CF} = 244.0 Hz), 144.8, 140.0, 138.3 (d, J_{CF} = 2.7 Hz), 133.3, 128.9, 128.1, 127.9, 127.5, 127.2, 122.3 (d, J_{CF} = 6.4 Hz), 121.9 (d, J_{CF} = 22.0 Hz), 117.0, (d, J_{CF} = 23.8 Hz), 116.4 (d, J_{CF} = 7.3 Hz), 52.8 ppm (OCH_3).
LC/MS: m/z = 350 [M + H$^+$], 391 [M + H$^+$ CH_3CN], 699 [2M + H$^+$]; t_R = 15.11 min; 96.7 % pure (UV).

2-([1,1'-biphenyl]-4-ylcarboxamido)-5-fluorobenzoic acid (11) was prepared according to method C. Sufficient purity was achieved without further purification; yield: 61 %. Mp: 259–263 °C. ^{1}H NMR (500 MHz, DMSO-d_6) δ = 14.97 (br. s, 1 H, NH), 8.75 (dd, *J* = 9.1, 5.4 Hz, 1 H), 8.15–8.07 (m, 2 H), 7.85 (dd, *J* = 9.9, 3.3 Hz, 1 H), 7.83–7.79 (m, 2 H), 7.75–7.70 (m, 2 H), 7.53–7.45 (m, 2 H), 7.44–7.37 (m, 1 H), 7.28–7.19 (m, 1 H) ppm.
^{13}C NMR (125 MHz, DMSO-d_6) δ = 168.9 (d, J_{CF} = 1.8 Hz), 163.7, 156.9 (d, J_{CF} = 239.2 Hz), 143.1, 139.1, 137.4 (d, J_{CF} = 1.8 Hz), 134.0, 129.1, 128.1, 127.8, 126.9, 126.6 (d, J_{CF} = 7.3 Hz), 120.1 (d, J_{CF} = 7.3 Hz), 117.3 (d, J_{CF} = 22.9 Hz), 117.2 (d, J_{CF} = 22.9 Hz), 117.0 ppm.
LC/MS: m/z = 334 [M - H$^+$]; t_R = 12.89 min; 96.8 % pure (UV).

methyl 5-fluoro-2-(3-phenoxybenzamido)benzoate (12a) was prepared according to method BI. For purification the solvent was evaporated and the remaining solid was suspended in MeOH. After filtration the precipitate was washed with MeOH to provide the pure compound; yield: 20 %. ^{1}H NMR (500 MHz, $CDCl_3$) δ = 11.86 (br. s, 1 H, NH), 8.92 (dd, *J* = 9.4, 5.0 Hz, 1 H), 7.77–7.71 (m, 2 H), 7.71–7.65 (m, 1 H), 7.49 (dd, *J* = 7.9, 7.9 Hz, 1 H), 7.42–7.35 (m, 2 H), 7.32 (ddd, *J* = 9.4, 7.5, 3.0 Hz,

1 H), 7.21 (ddd, *J* = 8.1, 2.4, 0.8 Hz, 1 H), 7.19–7.12 (m, 1 H), 7.12–7.07 (m, 2 H), 3.97 (s, 3 H, OCH_3) ppm.
^{13}C NMR (125 MHz, $CDCl_3$) δ = 167.9 (d, J_{CF} = 2.7 Hz), 164.9, 158.1, 157.6 (d, J_{CF} = 242.9 Hz), 138.1 (d, J_{CF} = 1.8 Hz), 136.5, 130.2, 129.9, 123.9, 122.2 (d, *J* = 7.3 Hz), 122.0, 121.8 (d, *J* = 22.0 Hz), 121.4, 120.8, 119.4, 117.5, 117.0 (d, J_{CF} = 23.8 Hz), 116.4 (d, J_{CF} = 7.3 Hz), 52.8 (OCH_3) ppm.
LC/MS: m/z = 366 [M + H^+]; t_R = 14.93 min; 93.7 % pure (UV).

5-fluoro-2-(3-phenoxybenzamido)benzoic acid (12) was prepared according to method C. Sufficient purity was achieved without further purification; yield: 87 %. Mp: 186–187 °C. ^1H NMR (500 MHz, DMSO-d_6) δ = 12.02 (br. s, 1 H, NH), 8.62 (dd, *J* = 9.4, 5.2 Hz, 1 H), 7.74 (dd, *J* = 9.4, 3.2 Hz, 1 H), 7.72–7.68 (m, 1 H), 7.59 (dd, *J* = 7.9, 7.9 Hz, 1 H), 7.56–7.50 (m, 2 H), 7.49–7.39 (m, 2 H), 7.27 (ddd, *J* = 7.9, 2.6, 0.9 Hz, 1 H), 7.23–7.16 (m, 1 H), 7.14–7.04 (m, 2 H) ppm.
^{13}C NMR (125 MHz, DMSO-d_6) δ = 168.7 (d, J_{CF} = 1.8 Hz), 163.8, 157.3, 157.0 (d, J_{CF} = 242.0 Hz), 156.0, 137.2 (d, J_{CF} = 1.8 Hz), 136.3, 130.8, 130.2, 124.1, 122.3 (d, J_{CF} = 7.3 Hz), 122.0, 121.6, 120.9 (d, J_{CF} = 22.0 Hz), 119.4 (d, J_{CF} = 7.3 Hz),119.1, 117.0 (d, J_{CF} = 22.0 Hz), 116.9 ppm.
LC/MS: m/z = 351 [M + H^+], 392 [M + H^+ CH_3CN]; t_R = 12.87 min; 96.2 % pure (UV).

methyl 2-([1,1'-biphenyl]-4-ylcarboxamido)-6-fluorobenzoate (13a) was prepared according to method BII. For purification the solvent was evaporated and the remaining solid was suspended in MeOH. After filtration the precipitate was washed with MeOH to provide the pure compound; yield: 90 %. ^1H NMR (500 MHz, $CDCl_3$) δ = 11.68 (br. s, 1 H, NH), 8.70 (d, *J* = 8.8 Hz, 1 H), 8.12–8.07 (m, 2 H), 7.78–7.73 (m, 2 H), 7.68–7.64 (m, 2 H), 7.57–7.52 (m, 1 H), 7.51–7.47 (m, 2 H), 7.45–7.39 (m, 1 H), 6.89 (ddd, *J* = 11.0, 8.8, 0.9 Hz, 1 H), 4.03 (s, 3 H, OCH_3) ppm.
^{13}C NMR (125 MHz, $CDCl_3$) δ = 167.9 (d, J_{CF} = 3.7 Hz), 165.3, 162.4 (d, J_{CF} = 258.4 Hz), 144.9, 142.1 (d, J_{CF} = 2.7 Hz), 139.9, 134.8 (d, J_{CF} = 11.0 Hz), 133.2, 128.9, 128.1, 127.9, 127.5, 127.2, 116.5 (d, J_{CF} = 3.7 Hz), 111.1 (d, J_{CF} = 23.8 Hz), 106.2 (d, J_{CF} = 12.8 Hz), 52.9 (OCH_3) ppm.
LC/MS: m/z = 350 [M + H^+], 699 [2M + H^+]; t_R = 15.22 min; 97.5 % pure (UV).

2-([1,1'-biphenyl]-4-ylcarboxamido)-6-fluorobenzoic acid (13) was prepared according to method C. Sufficient purity was achieved without further purification; yield: 87 %. Mp: 232–233 °C. ^1H NMR (500 MHz, DMSO-d_6) δ = 11.23 (br. s, 1 H, NH), 8.05–8.00 (m, 3 H), 7.90–7.84 (m, 2 H), 7.79–7.73 (m, 2 H), 7.61 (td, *J* = 8.3, 6.1 Hz, 1 H), 7.53–7.49 (m, 2 H), 7.46–7.41 (m, 1 H), 7.11 (ddd, *J* = 10.6, 8.4, 0.9 Hz, 1 H) ppm.
^{13}C NMR (125 MHz, DMSO-d_6) δ = 166.5 (d, J_{CF} = 1.8 Hz), 164.7, 160.8 (d, J_{CF} = 254.0 Hz), 143.6, 139.7 (d, J_{CF} = 4.6 Hz), 138.9, 133.2 (d, J_{CF} = 11.0 Hz), 132.9, 129.1, 128.3, 128.0, 126.9, 118.3 (d, J_{CF} = 3.7 Hz), 112.0 (d, J_{CF} = 14.7 Hz), 111.8 (d, J_{CF} = 22.9 Hz) ppm.
LC/MS: m/z = 336 [M + H^+], 671 [2M + H^+]; t_R = 12.85 min; 100.0 % pure (UV).

methyl 2-([1,1'-biphenyl]-4-ylcarboxamido)-4-bromobenzoate (14a) was prepared according to method BII. For purification the solvent was evaporated and the remaining solid was suspended in MeOH. After filtration the precipitate was washed with MeOH to provide the pure compound; yield: 69 %. ^1H NMR (500 MHz, $CDCl_3$) δ = 12.12 (br. s, 1 H, NH), 9.25 (d, *J* = 1.9 Hz, 1 H), 8.14–8.09 (m, 2 H), 7.94 (d, *J* = 8.5 Hz, 1 H), 7.79–7.74 (m, 2 H), 7.68–7.63 (m, 2 H), 7.52–7.47 (m, 2 H), 7.45–7.39 (m, 1 H), 7.27 (dd, *J* = 8.5, 1.9 Hz, 1 H), 3.99 (s, 3 H, OCH_3) ppm.
^{13}C NMR (125 MHz, $CDCl_3$) δ = 168.7, 165.4, 145.0, 142.7, 139.9, 133.0, 132.0, 129.9, 128.9, 128.1, 127.9, 127.5, 127.2, 125.8, 123.3, 113.7, 52.7 (OCH_3) ppm.
LC/MS: m/z = 409 and 411 [M + H^+]; t_R = 17.07 min; 100.0 % pure (UV).

2-([1,1'-biphenyl]-4-ylcarboxamido)-4-bromobenzoic acid (14) was prepared according to method C. For purification the remaining solid was washed with MeOH and CH_2Cl_2 to provide the pure compound; yield: 81 %. Mp: 246–250 °C. ^1H NMR (500 MHz, DMSO-d_6) δ = 12.30 (br. s, 1 H, NH),

8.99 (d, *J* = 1.9 Hz, 1 H), 8.05–8.00 (m, 2 H), 7.97 (d, *J* = 8.5 Hz, 1 H), 7.93–7.87 (m, 2 H), 7.80–7.73 (m, 2 H), 7.55–7.48 (m, 2 H), 7.47–7.41 (m, 1 H), 7.41 (dd, *J* = 8.5, 1.9 Hz, 1 H) ppm.
^{13}C NMR (125 MHz, DMSO-d_6) δ = 169.5, 164.6, 143.9, 142.1, 138.8, 133.0, 132.7, 129.1, 128.3, 127.8, 127.8, 127.2, 127.0, 125.8, 122.1, 115.5 ppm.
LC/MS: m/z = 793 [2M + H^+]; t_R = 14.71 min; 96.4 % pure (UV).

methyl 4-bromo-2-(3-phenoxybenzamido)benzoate (15a) was prepared according to method BII. For purification the solvent was evaporated and the remaining solid was suspended in MeOH. After filtration the precipitate was washed with MeOH to provide the pure compound; yield: 61 %. ^{1}H NMR (500 MHz, $CDCl_3$) δ = 12.04 (br. s, 1 H, NH), 9.18 (d, *J* = 2.2 Hz, 1 H), 7.92 (d, *J* = 8.5 Hz, 1 H), 7.73 (dd, *J* = 1.6, 0.9 Hz, 1 H), 7.69–7.65 (m, 1 H), 7.49 (dd, *J* = 7.9, 7.9 Hz, 1 H), 7.42–7.35 (m, 2 H), 7.26 (dd, *J* = 8.5, 2.2 Hz, 1 H), 7.22 (ddd, *J* = 8.2, 2.5, 0.9 Hz, 1 H), 7.19–7.14 (m, 1 H), 7.12–7.07 (m, 2 H), 3.96 (s, 3 H, OCH_3) ppm.
^{13}C NMR (125 MHz, $CDCl_3$) δ = 168.5, 165.0, 158.2, 156.3, 142.5, 136.3, 132.0, 130.2, 130.0, 129.9, 126.0, 124.0, 123.3, 122.2, 121.4, 119.5, 117.4, 113.8, 52.7 (OCH_3) ppm.
LC/MS: m/z = no ionization; t_R = 16.93 min; 99.8 % pure (UV).

4-bromo-2-(3-phenoxybenzamido)benzoic acid (15) was prepared according to method C. For purification the remaining solid was washed with MeOH and CH_2Cl_2 to provide the pure compound; yield: 74 %. Mp: 194–195 °C. ^{1}H NMR (500 MHz, DMSO-d_6) δ = 12.22 (br. s, 1 H, NH), 8.90 (d, *J* = 2.2 Hz, 1 H), 7.95 (d, *J* = 8.5 Hz, 1 H), 7.70–7.68 (m, 1 H), 7.61 (dd, *J* = 7.9, 7.9 Hz, 1 H), 7.53–7.51 (m, 1 H), 7.46–7.40 (m, 3 H), 7.29 (ddd, *J* = 8.2, 2.5, 0.9 Hz, 1 H), 7.21 (tt, *J* = 7.4, 1.1 Hz, 1 H), 7.11–7.08 (m, 2 H) ppm.
^{13}C NMR (125 MHz, DMSO-d_6) δ = 169.4, 164.1, 157.4, 155.9, 141.8, 136.0, 132.9, 130.9, 130.3, 127.7, 125.9, 124.1, 122.3, 122.2, 121.6, 119.1, 116.8, 115.8 ppm.
LC/MS: m/z = 823 and 825 and 827 [2M + H^+]; t_R = 14.65 min; 100.0 % pure (UV).

methyl 2-([1,1'-biphenyl]-4-ylcarboxamido)-5-bromobenzoate (16a) was prepared according to method BI. For purification the solvent was evaporated and the remaining solid was suspended in MeOH. After filtration the precipitate was washed with MeOH to provide the pure compound; yield: 26 %. ^{1}H NMR (500 MHz, $CDCl_3$) δ = 12.01 (br. s, 1 H, NH), 8.91 (d, *J* = 9.1 Hz, 1 H), 8.22 (d, *J* = 2.5 Hz, 1 H), 8.15–8.08 (m, 2 H), 7.79–7.74 (m, 2 H), 7.71 (dd, *J* = 9.1, 2.5 Hz, 1 H), 7.68–7.62 (m, 2 H), 7.54–7.46 (m, 2 H), 7.45–7.38 (m, 1 H), 4.00 (s, 3 H, OCH_3) ppm.
^{13}C NMR (125 MHz, $CDCl_3$) δ = 168.0, 165.4, 144.9, 141.0, 139.9, 137.5, 133.5, 133.1, 128.9, 128.1, 127.9, 127.5, 127.2, 122.1, 116.6, 115.0, 52.8 (OCH_3) ppm.
LC/MS: m/z = 409 and 411 [M + H^+], 820 and 822 [2M + H^+]; t_R = 16.41 min; 98.4 % pure (UV).

2-([1,1'-biphenyl]-4-ylcarboxamido)-5-bromobenzoic acid[5] (16) was prepared according to method C. Sufficient purity was achieved without further purification; yield: 31 %. Mp: 289–293 °C. ^{1}H NMR (500 MHz, DMSO-d_6) δ = 15.22 (br. s, 1 H, NH), 8.68 (d, *J* = 8.8 Hz, 1 H), 8.23 (d, *J* = 2.5 Hz, 1 H), 8.15–8.06 (m, 2 H), 7.87–7.82 (m, 2 H), 7.79–7.70 (m, 2 H), 7.54 (dd, *J* = 8.8, 2.5 Hz, 1 H), 7.53–7.47 (m, 2 H), 7.45–7.39 (m, 1 H) ppm.
^{13}C NMR (125 MHz, DMSO-d_6) δ = 168.3, 163.9, 143.2, 140.2, 139.0, 133.8, 133.8, 132.9, 129.0, 128.2, 127.9, 126.9, 120.6, 117.4, 115.8, 113.5 ppm.
LC/MS: m/z = 395 [2M - H^+]; t_R = 13.90 min; 98.3 % pure (UV).

methyl 5-bromo-2-(3-phenoxybenzamido)benzoate (17a) was prepared according to method BI. For purification the solvent was evaporated and the remaining solid was suspended in MeOH. After filtration the precipitate was washed with MeOH to provide the pure compound; yield: 78 %. ^{1}H NMR (500 MHz, $CDCl_3$) δ = 11.94 (br. s, 1 H, NH), 8.83 (d, *J* = 9.1 Hz, 1 H), 8.19 (d, *J* = 2.5 Hz, 1 H), 7.74–7.71 (m, 1 H), 7.70–7.66 (m, 2 H), 7.48 (dd, *J* = 7.9 7.9 Hz, 1 H), 7.42–7.36 (m, 2 H), 7.21 (ddd, *J* = 7.9, 2.5, 0.9 Hz, 1 H), 7.19–7.14 (m, 1 H), 7.11–7.07 (m, 2 H), 3.96 (s, 3 H, OCH_3) ppm.

^{13}C NMR (125 MHz, $CDCl_3$) δ = 167.8, 165.0, 158.1, 156.4, 140.7, 137.5, 136.4, 133.4, 130.2, 129.9, 123.9, 122.1, 122.1, 121.4, 119.5, 117.5, 116.7, 115.1, 52.8 (OCH_3) ppm.
LC/MS: m/z = no ionization; t_R = 16.15 min; 95.1 % pure (UV).

5-bromo-2-(3-phenoxybenzamido)benzoic acid[5] (17) was prepared according to method C. For purification the remaining solid was washed with hot MeOH to provide the pure compound; yield: 52 %. Mp: 240–242 °C. ^{1}H NMR (500 MHz, DMSO-d_6) δ = 12.05 (br. s, 1 H, NH), 8.59 (d, *J* = 9.1 Hz, 1 H), 8.10 (d, *J* = 2.5 Hz, 1 H), 7.83 (dd, *J* = 9.1, 2.5 Hz, 1 H), 7.72–7.67 (m, 1 H), 7.63–7.57 (m, 1 H), 7.53–7.50 (m, 1 H), 7.47–7.40 (m, 2 H), 7.30–7.26 (m, 1 H), 7.24–7.17 (m, 1 H), 7.14–7.06 (m, 2 H) ppm.
^{13}C NMR (125 MHz, DMSO-d_6) δ = 168.6, 163.9, 157.3, 156.0, 140.0, 136.7, 136.2, 133.2, 130.8, 130.2, 130.1, 124.1, 122.2, 122.1, 121.6, 119.0, 116.9, 114.5 ppm.
LC/MS: m/z = 409 and 411 [M - H^+]; t_R = 13.90 min; 95.2 % pure (UV).

3-benzylbenzoic acid (18d). A mixture of methyl 3-(bromomethyl)benzoate (1 equiv), phenylboronic acid (1.5 equiv), $CsCO_3$ (3 equiv) and tetrakis(triphenylphosphine)-palladium (0.01 equiv) in a degased DME/water (1:1) solution was refluxed under a nitrogen atmosphere for 18 h. The reaction mixture was cooled to room temperature. The mixture was extracted with EtOAc. The combined organic layers were washed with 1 M HCl and dried over $MgSO_4$. The product was purified by CC (CH_2Cl_2); yield: 81 %. ^{1}H NMR (500 MHz, Acetone-d_6) δ = 7.93–7.92 (m, 1H), 7.89–7.87 (m, 1H), 7.52–7.50 (m, 1H), 7.44–7.41 (m, 1H), 7.31–7.26 (m, 4H), 7.22–7.17 (m, 1H), 4.07 (s, 2H, CH_2) ppm.
^{13}C NMR (125 MHz, Acetone-d_6) δ = 167.7, 143.0, 141.9, 134.3, 131.7, 130.9, 129.8, 129.5, 129.5, 128.3, 127.1, 42.1 (CH_2) ppm.
LC/MS: m/z = no ionization; t_R = 11.15 min; 98.4 % pure (UV).

methyl 2-(3-benzylbenzamido)-5-bromobenzoate (18a) was prepared according to method BII. For purification the solvent was evaporated and the remaining solid was suspended in MeOH. After filtration the precipitate was washed with MeOH to provide the pure compound; yield: 23 %. ^{1}H NMR (500 MHz, $CDCl_3$) δ = 11.94 (s, 1H), 8.87 (d, *J* = 9.0 Hz, 1H), 8.21 (d, *J* = 2.4 Hz, 1H), 7.93–7.89 (m, 1H), 7.89–7.82 (m, 1H), 7.69 (dd, *J* = 2.4, 9.0 Hz, 1H), 7.46–7.43 (m, 1H), 7.42–7.37 (m, 1H), 7.35–7.29 (m, 2H), 7.26–7.20 (m, 3H), 4.09 (s, 2H, CH_2), 3.98 (s, 3H, CH_3) ppm.
^{13}C NMR (125 MHz, $CDCl_3$) δ = 167.8, 165.8, 142.1, 140.9, 140.4, 137.5, 134.7, 133.4, 132.7, 129.0, 129.0, 128.6, 128.2, 126.3, 124.9, 122.1, 116.7, 114.9, 52.8 (CH_3), 41.8 (CH_2) ppm.
LC/MS: m/z = 424 and 426 [M + H^+]; t_R = 16.82 min; 99.5 % pure (UV).

2-(3-benzylbenzamido)-5-bromobenzoic acid (18) was prepared according to method C. Sufficient purity was achieved without further purification; yield: 98 %. Mp: 225–227 °C. ^{1}H NMR (500 MHz, DMSO-d_6) δ = 12.06 (s, 1H), 8.62 (d, *J* = 9.1 Hz, 1H), 8.10 (d, *J* = 2.2 Hz, 1H), 7.85–7.80 (m, 2H), 7.77–7.72 (m, 1H), 7.52–7.47 (m, 2H), 7.32–7.24 (m, 4H), 7.22–7.16 (m, 1H), 4.04 (s, 2H, CH_2) ppm.
^{13}C NMR (125 MHz, DMSO-d_6) δ = 168.8, 164.9, 142.4, 140.8, 140.3, 136.8, 134.5, 133.3, 132.8, 129.2, 128.8, 128.7, 127.6, 126.3, 124.7, 122.1, 118.9, 114.4, 41.0 (CH_2) ppm.
LC/MS: m/z = 410 and 412 [M + H^+]; t_R = 14.62 min; 100.0 % pure (UV).

methyl 2-([1,1'-biphenyl]-4-ylcarboxamido)-4,5-dimethoxybenzoate (19a) was prepared according to method BI. For purification the solvent was evaporated and the remaining solid was suspended in MeOH. After filtration the precipitate was washed with MeOH to provide the pure compound; yield: 40 %. ^{1}H NMR (500 MHz, $CDCl_3$) δ = 12.21 (br. s, 1 H, NH), 8.75 (s, 1 H), 8.15–8.12 (m, 2 H), 7.78–7.75 (m, 2 H), 7.68–7.65 (m, 2 H), 7.52 (s, 1 H), 7.51–7.47 (m, 2 H), 7.44–7.39 (m, 1 H), 4.05 (s, 3 H, OCH_3), 3.97 (s, 3 H, OCH_3), 3.93 (s, 3 H, OCH_3) ppm.
^{13}C NMR (125 MHz, $CDCl_3$) δ = 168.8, 165.4, 154.1, 144.6, 144.0, 140.0, 138.1, 133.5, 128.9, 128.0, 127.8, 127.5, 127.2, 112.1, 106.8, 103.4, 56.2 (OCH_3), 56.1 (OCH_3), 52.3 (OCH_3) ppm.
LC/MS: m/z = 392 [M + H^+]; t_R = 14.81 min; 98.4 % pure (UV).

2-([1,1'-biphenyl]-4-ylcarboxamido)-4,5-dimethoxybenzoic acid (19) was prepared according to method C. Sufficient purity was achieved without further purification; yield: 29 %. Mp: 185 °C (decomposition). ^{1}H NMR (500 MHz, DMSO-d_6) δ = 14.78 (br. s, 1 H, NH), 8.54 (s, 1 H), 8.14–8.08 (m, 2 H), 7.78–7.73 (m, 2 H), 7.72–7.61 (m, 3 H), 7.56–7.33 (m, 3 H), 3.81 (s, 3 H, OCH_3), 3.74 (s, 3 H, OCH_3) ppm.
^{13}C NMR (125 MHz, DMSO-d_6) δ = 163.4, 150.5, 143.2, 142.9, 139.0, 135.7, 134.1, 129.0, 128.1, 127.8, 126.8, 126.8, 117.6, 117.4, 114.3, 102.6, 55.5 (OCH_3), 55.4 (OCH_3) ppm.
LC/MS: m/z = 378 [M + H$^+$]; t_R = 12.37 min; 95.6 % pure (UV).

methyl 4,5-dimethoxy-2-(3-phenoxybenzamido)benzoate (20a) was prepared according to method BI. For purification the solvent was evaporated and the remaining solid was suspended in MeOH. After filtration the precipitate was washed with MeOH to provide the pure compound; yield: 57 %. ^{1}H NMR (500 MHz, $CDCl_3$) δ = 12.12 (br. s, 1 H, NH), 8.67 (s, 1 H), 7.76–7.73 (m, 1 H), 7.69 (dd, J = 2.0, 2.0 Hz, 1 H), 7.51–7.47 (m, 2 H), 7.40–7.34 (m, 2 H), 7.21 (ddd, J = 8.2, 2.5, 0.9 Hz, 1 H), 7.17–7.12 (m, 1 H), 7.12–7.06 (m, 2 H), 4.01 (s, 3 H, OCH_3), 3.93 (s, 3 H, OCH_3), 3.91 (s, 3 H, OCH_3) ppm.
^{13}C NMR (125 MHz, $CDCl_3$) δ = 168.6, 165.0, 158.1, 156.5, 154.0, 144.0, 137.9, 136.8, 130.1, 129.9, 123.8, 122.0, 121.3, 119.4, 117.4, 112.1, 106.8, 103.3, 56.1 (OCH_3), 56.1 (OCH_3), 52.2 (OCH_3) ppm.
LC/MS: m/z = 408 [M + H$^+$], 815 [2M + H$^+$]; t_R = 14.56 min; 95.5 % pure (UV).

4,5-dimethoxy-2-(3-phenoxybenzamido)benzoic acid (20) was prepared according to method C. Sufficient purity was achieved without further purification; yield: 98 %. Mp: 218–219 °C. ^{1}H NMR (500 MHz, DMSO-d_6) δ = 12.29 (br. s, 1 H, NH), 8.45 (s, 1 H), 7.70–7.66 (m, 1 H), 7.59 (dd, J = 7.9, 7.9 Hz, 1 H), 7.52–7.49 (m, 1 H), 7.49–7.41 (m, 3 H), 7.27 (ddd, J = 8.2, 2.5, 0.9 Hz, 1 H), 7.21 (tt, J = 7.5, 1.0 Hz, 1 H), 7.14–7.06 (m, 2 H), 3.84 (s, 3 H, OCH_3), 3.78 (s, 3 H, OCH_3) ppm.
^{13}C NMR (125 MHz, DMSO-d_6) δ = 169.8, 163.6, 157.4, 155.9, 153.3, 143.8, 136.7, 136.5, 130.8, 130.3, 124.1, 121.9, 121.3, 119.2, 116.7, 112.8, 107.8, 103.1, 55.6 (OCH_3), 55.6 (OCH_3) ppm.
LC/MS: m/z = 394 [M + H$^+$], 435 [M + H$^+$ CH_3CN]; t_R = 12.32 min; 96.9 % pure (UV).

methyl 2-amino-4-methoxybenzoate (21b) was prepared according to method A. The product was purified by CC (*n*-hexane/EtOAc 6:4); yield: 12 %. ^{1}H NMR (500 MHz, $CDCl_3$) δ = 7.79 (d, J = 8.8 Hz, 1 H), 6.24 (dd, J = 8.8, 2.2 Hz, 1 H), 6.11 (d, J = 2.2 Hz, 1 H), 5.80 (br. s, 2 H, NH_2), 3.84 (s, 3 H, OCH_3), 3.79 (s, 3 H, OCH_3) ppm.
^{13}C NMR (125 MHz, $CDCl_3$) δ = 168.3, 164.2, 152.4, 133.0, 104.5, 104.4, 99.4, 55.1 (OCH_3), 51.2 (OCH_3) ppm.
LC/MS: m/z = 182 [M + H$^+$]; t_R = 8.73 min; 100.0 % pure (UV).

methyl 2-([1,1'-biphenyl]-4-ylcarboxamido)-4-methoxybenzoate (21a) was prepared according to method BI. For purification the solvent was evaporated and the remaining solid was suspended in MeOH. After filtration the precipitate was washed with MeOH to provide the pure compound; yield: 26 %. ^{1}H NMR (500 MHz, $CDCl_3$) δ = 12.32 (br. s, 1 H, NH), 8.66 (d, J = 2.5 Hz, 1 H), 8.17–8.13 (m, 2 H), 8.02 (d, J = 8.8 Hz, 1 H), 7.78–7.75 (m, 2 H), 7.68–7.64 (m, 2 H), 7.51–7.47 (m, 2 H), 7.44–7.39 (m, 1 H), 6.67 (dd, J = 8.8, 2.5 Hz, 1 H), 3.96 (s, 3 H, OCH_3), 3.95 (s, 3 H, OCH_3) ppm.
^{13}C NMR (125 MHz, $CDCl_3$) δ = 169.0, 165.7, 164.7, 144.7, 144.1, 140.0, 133.5, 132.5, 128.9, 128.0, 127.9, 127.5, 127.2, 110.2, 107.7, 103.9, 55.6 (OCH_3), 52.2 (OCH_3) ppm.
LC/MS: m/z = 362 [M + H$^+$], 403 [M + H$^+$ CH_3CN], 723 [2M + H$^+$]; t_R = 15.61 min; 99.6 % pure (UV).

2-([1,1'-biphenyl]-4-ylcarboxamido)-4-methoxybenzoic acid (21) was prepared according to method C. Sufficient purity was achieved without further purification; yield: 98 %. Mp: 248–249 °C. ^{1}H NMR (500 MHz, DMSO-d_6) δ = 12.51 (br. s, 1 H, NH), 8.44 (d, J = 2.5 Hz, 1 H), 8.06–7.99 (m, 3 H), 7.92–7.85 (m, 2 H), 7.78–7.73 (m, 2 H), 7.55–7.48 (m, 2 H), 7.47–7.39 (m, 1 H), 6.77 (dd, J = 8.8, 2.5 Hz, 1 H), 3.86 (s, 3 H, OCH_3) ppm.

^{13}C NMR (125 MHz, DMSO-d_6) δ = 170.1, 164.5, 163.8, 143.8, 143.3, 138.9, 133.2, 133.2, 129.1, 128.3, 127.7, 127.2, 127.0, 108.8, 108.5, 104.5, 55.6 (OCH_3) ppm.
LC/MS: m/z = 348 [M + H^+], 389 [M + H^+ CH_3CN], 695 [2M + H^+]; t_R = 13.50 min; 100.0 % pure (UV).

methyl 2-amino-5-methoxybenzoate (22b) was prepared according to method A. Sufficient purity was achieved without further purification; yield: 62 %. ^{1}H NMR (500 MHz, $CDCl_3$) δ = 7.36 (d, *J* = 3.2 Hz, 1 H), 6.96 (dd, *J* = 8.8, 3.2 Hz, 1 H), 6.64 (d, *J* = 8.8 Hz, 1 H), 5.43 (br. s, 2 H, NH_2), 3.88 (s, 3 H, OCH_3), 3.77 (s, 3 H, OCH_3) ppm.
^{13}C NMR (125 MHz, $CDCl_3$) δ = 168.3, 150.5, 145.1, 123.3, 118.2, 113.1, 110.7, 55.8 (OCH_3), 51.6 (OCH_3) ppm.
LC/MS: m/z = 182 [M + H^+], 223 [M + H^+ CH_3CN]; t_R = 5.88 min; 95.2 % pure (UV).

methyl 2-([1,1'-biphenyl]-4-ylcarboxamido)-5-methoxybenzoate (22a) was prepared according to method BII. For purification the solvent was evaporated and the remaining solid was suspended in MeOH. After filtration the precipitate was washed with MeOH to provide the pure compound; yield: 82 %. ^{1}H NMR (500 MHz, $CDCl_3$) δ = 11.85 (br. s, 1 H, NH), 8.91 (d, *J* = 9.1 Hz, 1 H), 8.13–8.11 (m, 2 H), 7.77–7.74 (m, 2 H), 7.67–7.64 (m, 2 H), 7.59 (d, *J* = 3.2 Hz, 1 H), 7.50–7.47 (m, 2 H), 7.44–7.38 (m, 1 H), 7.21 (dd, *J* = 9.1, 3.2 Hz, 1 H), 3.99 (s, 3 H, OCH_3), 3.86 (s, 3 H, OCH_3) ppm.
^{13}C NMR (125 MHz, $CDCl_3$) δ = 168.8, 165.0, 154.5, 144.5, 140.1, 135.6, 133.7, 128.9, 128.0, 127.8, 127.4, 127.2, 122.0, 121.2, 116.1, 114.7, 55.6 (OCH_3), 52.6 (OCH_3) ppm.
LC/MS: m/z = 362 [M + H^+], 403 [M + H^+ CH_3CN], 723 [2M + H^+]; t_R = 15.45 min; 98.1 % pure (UV).

2-([1,1'-biphenyl]-4-ylcarboxamido)-5-methoxybenzoic acid (22) was prepared according to method C. For purification the remaining solid was washed with MeOH and CH_2Cl_2 to provide the pure compound; yield: 92 %. Mp: 236–239 °C. ^{1}H NMR (500 MHz, DMSO-d_6) δ = 11.90 (br. s, 1 H, NH), 8.61 (d, *J* = 9.1 Hz, 1 H), 8.04–8.00 (m, 2 H), 7.89–7.86 (m, 2 H), 7.77–7.73 (m, 2 H), 7.54 (d, *J* = 2.8 Hz, 1 H), 7.53–7.48 (m, 2 H), 7.45–7.39 (m, 1 H), 7.28 (dd, *J* = 9.1, 2.8 Hz, 1 H), 3.80 (s, 3 H, OCH_3) ppm.
^{13}C NMR (125 MHz, DMSO-d_6) δ = 169.6, 163.9, 154.4, 143.5, 138.9, 134.5, 133.4, 129.1, 128.2, 127.6, 127.1, 126.9, 121.9, 120.3, 118.2, 115.0, 55.4 (OCH_3) ppm.
LC/MS: m/z = 348 [M + H^+], 695 [2M + H^+]; t_R = 13.07 min; 96.8 % pure (UV).

methyl 2-([1,1'-biphenyl]-4-ylcarboxamido)-6-methoxybenzoate (23a) was prepared according to method BIII. For purification the solvent was evaporated and the remaining solid was suspended in MeOH. After filtration the precipitate was washed with MeOH to provide the pure compound; yield: 46 %. ^{1}H NMR (500 MHz, $CDCl_3$) δ = 10.78 (br. s, 1 H, NH), 8.31 (dd, *J* = 8.5, 0.9 Hz, 1 H), 8.07–8.04 (m, 2 H), 7.76–7.73 (m, 2 H), 7.67–7.64 (m, 2 H), 7.51–7.47 (m, 3 H), 7.44–7.39 (m, 1 H), 6.76 (dd, *J* = 8.5, 0.9 Hz, 1 H), 3.99 (s, 3 H, OCH_3), 3.90 (s, 3 H, OCH_3) ppm.
^{13}C NMR (125 MHz, $CDCl_3$) δ = 169.2, 165.1, 159.4, 144.7, 140.2, 140.0, 133.4, 133.4, 128.9, 128.0, 127.8, 127.4, 127.2, 113.8, 109.4, 107.2, 56.3 (OCH_3), 52.6 (OCH_3) ppm.
LC/MS: m/z = 362 [M + H^+], 723 [2M + H^+]; t_R = 13.57 min; 96.5 % pure (UV).

2-([1,1'-biphenyl]-4-ylcarboxamido)-6-methoxybenzoic acid (23) was prepared according to method C. Sufficient purity was achieved without further purification; yield: 90 %. Mp: 158–162 °C. ^{1}H NMR (500 MHz, DMSO-d_6) δ = 10.44 (br. s, 1 H, NH), 8.02–7.99 (m, 2 H), 7.86–7.83 (m, 2 H), 7.77–7.75 (m, 2 H), 7.53–7.46 (m, 4 H), 7.45–7.41 (m, 1 H), 6.98 (dd, *J* = 7.9, 1.6 Hz, 1 H), 3.83 (s, 3 H, OCH_3) ppm.
^{13}C NMR (125 MHz, DMSO-d_6) δ = 167.7, 164.7, 157.5, 143.4, 139.0, 137.2, 133.1, 131.3, 129.1, 128.2, 128.1, 126.9, 126.8, 116.8, 116.6, 108.6, 56.1 (OCH_3) ppm.
LC/MS: m/z = 348 [M + H^+], 695 [2M + H^+]; t_R = 13.30 min; 99.2 % pure (UV).

2-([1,1'-biphenyl]-4-ylcarboxamido)-5-hydroxybenzoic acid (24) was prepared according to method E. The product was purified by CC (starting with *n*-hexane/EtOAc 1:1 to EtOAc + 3 ‰ formic

acid) followed by preparative TLC (CH_2Cl_2 + 7 drops formic acid per 10 mL solvent); yield: 34 %. Mp: 193–196 °C. ^{1}H NMR (500 MHz, DMSO-d_6) δ = 11.88 (br. s, 1 H, NH), 9.64 (br. s, 1 H, ArOH), 8.51 (d, J = 8.8 Hz, 1 H), 8.03–8.00 (m, 2 H), 7.89–7.85 (m, 2 H), 7.78–7.74 (m, 2 H), 7.53–7.49 (m, 2 H), 7.46 (d, J = 2.8 Hz, 1 H), 7.45–7.38 (m, 1 H), 7.08 (dd, J = 8.8, 2.8 Hz, 1 H) ppm.
^{13}C NMR (125 MHz, DMSO-d_6) δ = 169.8, 163.7, 152.7, 143.3, 139.0, 133.6, 133.1, 129.1, 128.2, 127.6, 127.1, 126.9, 121.9, 121.1, 118.4, 116.8 ppm.
LC/MS: m/z = 334 [M + H$^+$], 667 [2M + H$^+$]; t_R = 11.31 min; 96.6 % pure (UV).

methyl 2-amino-4-nitrobenzoate (25b) was prepared according to method A. The product was purified by CC (*n*-hexane/EtOAc 6:4); yield: 37 %. ^{1}H NMR (500 MHz, $CDCl_3$) δ = 8.01 (d, J = 8.8 Hz, 1 H), 7.51 (d, J = 2.2 Hz, 1 H), 7.41 (dd, J = 8.8, 2.2 Hz, 1 H), 6.06 (br. s, 2 H, NH_2), 3.93 (s, 3 H, OCH_3) ppm.
^{13}C NMR (125 MHz, $CDCl_3$) δ = 167.3, 151.3, 150.7, 132.8, 114.9, 111.1, 110.1, 52.2 (OCH_3) ppm.
LC/MS: m/z = no ionization; t_R = 10.08 min; 100.0 % pure (UV).

methyl 2-([1,1'-biphenyl]-4-ylcarboxamido)-4-nitrobenzoate (25a) was prepared according to method BI. For purification the solvent was evaporated and the remaining solid was suspended in MeOH. After filtration the precipitate was exhaustively washed with MeOH and CH_2Cl_2 to provide the pure compound; yield: 15 %. ^{1}H NMR (500 MHz, $CDCl_3$) δ = 12.17 (br. s, 1 H, NH), 9.89 (d, J = 2.2 Hz, 1 H), 8.28 (d, J = 8.8 Hz, 1 H), 8.21–8.10 (m, 2 H), 7.94 (dd, J = 8.8, 2.2 Hz, 1 H), 7.84–7.73 (m, 2 H), 7.72–7.61 (m, 2 H), 7.54–7.47 (m, 2 H), 7.47–7.39 (m, 1 H), 4.07 (s, 3 H, OCH_3) ppm.
^{13}C NMR (125 MHz, $CDCl_3$) δ = 167.8, 165.6, 151.4, 145.3, 142.9, 139.8, 132.5, 132.1, 129.0, 128.2, 128.0, 127.6, 127.3, 119.3, 116.6, 115.5, 53.3 (OCH_3) ppm.
LC/MS: m/z = 377 [M + H$^+$], 418 [M + H$^+$ CH_3CN]; t_R = 15.03 min; 97.6 % pure (UV).

2-([1,1'-biphenyl]-4-ylcarboxamido)-4-nitrobenzoic acid (25) was prepared according to method C. For purification the remaining solid was washed with MeOH and CH_2Cl_2 to provide the pure compound; yield: 94 %. Mp: 280–283 °C. ^{1}H NMR (500 MHz, DMSO-d_6) δ = 12.48 (br. s, 1 H, NH), 9.55 (d, J = 2.2 Hz, 1 H), 8.28 (d, J = 8.8 Hz, 1 H), 8.09–8.04 (m, 2 H), 8.01 (dd, J = 8.8, 2.2 Hz, 1 H), 7.95–7.90 (m, 2 H), 7.81–7.74 (m, 2 H), 7.56–7.49 (m, 2 H), 7.47–7.41 (m, 1 H) ppm.
^{13}C NMR (125 MHz, DMSO-d_6) δ = 168.6, 164.9, 150.2, 144.1, 141.5, 138.8, 132.8, 132.6, 129.1, 128.4, 127.9, 127.3, 127.0, 122.6, 117.2, 114.3 ppm.
LC/MS: m/z = 363 [M + H$^+$], 404 [M + H$^+$ CH_3CN], 725 [2M + H$^+$]; t_R = 13.25 min; 100.0 % pure (UV).

methyl 2-([1,1'-biphenyl]-4-ylcarboxamido)-5-cyanobenzoate (26a) was prepared according to method BII. For purification the solvent was evaporated and the remaining solid was suspended in MeOH. After filtration the precipitate was washed with MeOH to provide the pure compound; yield: 43 %. ^{1}H NMR (500 MHz, $CDCl_3$) δ = 12.29 (br. s, 1 H, NH), 9.13 (d, J = 8.8 Hz, 1 H), 8.42 (d, J = 2.0 Hz, 1 H), 8.13–8.11 (m, 2 H), 7.84 (dd, J = 8.8, 2.0 Hz, 1 H), 7.79–7.76 (m, 2 H), 7.67–7.64 (m, 2 H), 7.51–7.48 (m, 2 H), 7.45–7.40 (m, 1 H), 4.04 (s, 3 H, OCH_3) ppm.
^{13}C NMR (125 MHz, $CDCl_3$) δ = 167.6, 165.6, 145.4, 145.3, 139.7, 137.6, 135.4, 132.5, 129.0, 128.2, 128.0, 127.6, 127.2, 120.9, 118.0, 115.3, 105.9, 53.1 (OCH_3) ppm.
LC/MS: m/z = 357 [M + H$^+$], 713 [2M + H$^+$]; t_R = 15.32 min; 97.2 % pure (UV).

2-([1,1'-biphenyl]-4-ylcarboxamido)-5-cyanobenzoic acid[5] (26) was prepared according to method C. Sufficient purity was achieved without further purification; yield: 80 %. Mp: 246–247 °C. ^{1}H NMR (500 MHz, DMSO-d_6) δ = 12.46 (br. s, 1 H, NH), 8.87 (d, J = 8.8 Hz, 1 H), 8.38 (d, J = 2.0 Hz, 1 H), 8.07 (dd, J = 8.8, 2.0 Hz, 1 H), 8.04–8.01 (m, 2 H), 7.90–7.87 (m, 2 H), 7.77–7.73 (m, 2 H), 7.53–7.48 (m, 2 H), 7.46–7.41 (m, 1 H) ppm.
^{13}C NMR (125 MHz, DMSO-d_6) δ = 168.6, 164.7, 144.6, 144.1, 138.7, 137.5, 135.4, 132.5, 129.1, 128.4, 127.9, 127.2, 127.0, 120.2, 118.1, 117.2, 105.0 ppm.
LC/MS: m/z = 343 [M + H$^+$], 685 [2M + H$^+$]; t_R = 13.30 min; 97.5 % pure (UV).

methyl 2-amino-4-(trifluoromethyl)benzoate (27b) was prepared according to method A. The product was purified by CC (*n*-hexane/EtOAc 1:1); yield: 61 %. ^{1}H NMR (500 MHz, $CDCl_3$) δ = 7.96 (d, J = 8.2 Hz, 1 H), 6.93–6.89 (m, 1 H), 6.88–6.82 (m, 1 H), 5.92 (br. s, 2 H, NH_2), 3.91 (s, 3 H, OCH_3) ppm.
^{13}C NMR (125 MHz, $CDCl_3$) δ = 167.7, 150.2, 135.7 (q, J_{CF} = 32.1 Hz), 132.2, 120.3 (q, J_{CF} = 272.0 Hz), 113.4 (q, J_{CF} = 3.7 Hz), 113.0 (q, J_{CF} = 1.8 Hz), 112.3 (q, J_{CF} = 3.7 Hz), 51.9 (OCH_3) ppm.
LC/MS: m/z = 261 [M + H^+ CH_3CN]; t_R = 12.01 min; 85.2 % pure (UV).

methyl 2-([1,1'-biphenyl]-4-ylcarboxamido)-4-(trifluoromethyl)benzoate (27a) was prepared according to method BII. For purification the solvent was evaporated and the remaining solid was suspended in MeOH. After filtration the precipitate was washed with MeOH to provide the pure compound; yield: 22 %. ^{1}H NMR (500 MHz, $CDCl_3$) δ = 12.16 (br. s, 1 H, NH), 9.36 (dd, J = 1.3, 0.6 Hz, 1 H), 8.22 (d, J = 8.2 Hz, 1 H), 8.15–8.12 (m, 2 H), 7.79–7.76 (m, 2 H), 7.68–7.64 (m, 2 H), 7.51–7.47 (m, 2 H), 7.46–7.40 (m, 1 H), 7.38 (ddd, J = 8.2, 1.3, 0.6 Hz, 1 H), 4.04 (s, 3 H, OCH_3) ppm.
^{13}C NMR (125 MHz, $CDCl_3$) δ = 168.2, 165.6, 145.1, 142.3, 139.9, 136.1 (q, J_{CF} = 32.0 Hz), 132.9, 131.6, 129.0, 128.2, 127.9, 127.6, 127.2, 123.4 (q, J_{CF} = 273.1 Hz), 118.9 (q, J_{CF} = 3.7 Hz), 117.5 (q, J_{CF} = 4.2 Hz), 53.0 (OCH_3) ppm.
LC/MS: m/z = 400 [M + H^+], 441 [M + H^+ CH_3CN], 799 [2M + H^+]; t_R = 16.51 min; 100.0 % pure (UV).

2-([1,1'-biphenyl]-4-ylcarboxamido)-4-(trifluoromethyl)benzoic acid (27) was prepared according to method C. Sufficient purity was achieved without further purification; yield: 84 %. Mp: 245–246 °C.
^{1}H NMR (500 MHz, DMSO-d_6) δ = 12.35 (br. s, 1 H, NH), 9.10 (d, J = 1.6 Hz, 1 H), 8.26 (d, J = 8.2 Hz, 1 H), 8.08–8.04 (m, 2 H), 7.95–7.89 (m, 2 H), 7.81–7.75 (m, 2 H), 7.57 (dd, J = 8.2, 1.6 Hz, 1 H), 7.55–7.49 (m, 2 H), 7.47–7.41 (m, 1 H) ppm.
^{13}C NMR (125 MHz, DMSO-d_6) δ = 169.0, 164.8, 144.0, 141.4, 138.8, 133.4 (q, J_{CF} = 32.0 Hz), 132.7, 132.5, 129.1, 128.4, 127.8, 127.2, 127.0, 122.9 (q, J_{CF} = 273.1 Hz), 119.2 (q, J_{CF} = 3.7 Hz), 116.3 (q, J_{CF} = 3.7 Hz) ppm.
LC/MS: m/z = 386 [M + H^+], 427 [M + H^+ CH_3CN], 771 [2M + H^+]; t_R = 14.11 min; 100.0 % pure (UV).

methyl 2-([1,1'-biphenyl]-4-ylcarboxamido)-5-(trifluoromethyl)benzoate (28a) was prepared according to method BII. For purification the solvent was evaporated and the remaining solid was suspended in MeOH. After filtration the precipitate was washed with MeOH followed by CC (*n*-hexane/EtOAc 9:1) to provide the pure compound; yield: 42 %. ^{1}H NMR (500 MHz, $CDCl_3$) δ = 12.24 (br. s, 1 H, NH), 9.13 (d, J = 8.8 Hz, 1 H), 8.38 (d, J = 2.0 Hz, 1 H), 8.15–8.12 (m, 2 H), 7.85 (dd, J = 8.8, 2.0 Hz, 1 H), 7.79–7.76 (m, 2 H), 7.68–7.65 (m, 2 H), 7.52–7.48 (m, 2 H), 7.45–7.40 (m, 1 H), 4.04 (s, 3 H, OCH_3) ppm.
^{13}C NMR (125 MHz, $CDCl_3$) δ = 168.2, 165.6, 145.2, 144.6, 139.8, 132.9, 131.4 (q, J_{CF} = 3.6 Hz), 129.0, 128.3 (q, J_{CF} = 3.6 Hz), 128.2, 128.0, 127.6, 127.2, 124.5 (q, J_{CF} = 33.9 Hz), 120.6, 122.6 (q, J_{CF} = 271.3 Hz), 114.9, 52.9 (OCH_3) ppm.
LC/MS: m/z = 400 [M + H^+], 441 [M + H^+ CH_3CN], 799 [2M + H^+]; t_R = 16.70 min; 95.1 % pure (UV).

2-([1,1'-biphenyl]-4-ylcarboxamido)-5-(trifluoromethyl)benzoic acid (28) was prepared according to method C. For purification the remaining solid was washed with MeOH and CH_2Cl_2 to provide the pure compound; yield: 49 %. Mp: 265–266 °C. ^{1}H NMR (500 MHz, DMSO-d_6) δ = 12.41 (br. s, 1 H, NH), 8.93 (d, J = 8.8 Hz, 1 H), 8.28 (d, J = 2.0 Hz, 1 H), 8.06–8.03 (m, 2 H), 8.01 (dd, J = 8.8, 2.0 Hz, 1 H), 7.92–7.87 (m, 2 H), 7.78–7.73 (m, 2 H), 7.54–7.47 (m, 2 H), 7.46–7.40 (m, 1 H) ppm.
^{13}C NMR (125 MHz, DMSO-d_6) δ = 168.9, 164.7, 144.3, 144.0, 138.8, 132.7, 130.9 (q, J_{CF} = 3.7 Hz) 129.1, 128.4, 127.9 (q, J_{CF} = 3.7 Hz), 127.8, 127.2, 127.0, 123.8 (q, J_{CF} = 271.3 Hz), 122.8 (q, J_{CF} = 33.0 Hz) 120.4, 116.8 ppm.
LC/MS: m/z = 386 [M + H^+], 771 [2M + H^+]; t_R = 14.60 min; 99.8 % pure (UV).

methyl 2-amino-5-(trifluoromethoxy)benzoate (29b) was prepared according to method A. The product was purified by CC (*n*-hexane/EtOAc 1:1); yield: 26 %. ^{1}H NMR (500 MHz, $CDCl_3$) δ = 7.77–7.68 (m, 1 H), 7.20–7.11 (m, 1 H), 6.65 (d, J = 9.5 Hz, 1 H), 5.80 (br. s, 2 H, NH_2), 3.89 (s, 3 H, OCH_3) ppm.
^{13}C NMR (125 MHz, $CDCl_3$) δ = 167.6, 149.2, 138.8 (q, J_{CF} = 1.8 Hz), 127.9, 123.8, 120.7 (q, J_{CF} = 256.0 Hz), 117.5, 110.5, 51.8 (OCH_3) ppm.
LC/MS: m/z = 236 [M + H$^+$], 277 [M + H$^+$ CH_3CN]; t_R = 12.13 min; 96.0 % pure (UV).

methyl 2-([1,1'-biphenyl]-4-ylcarboxamido)-5-(trifluoromethoxy)benzoate (29a) was prepared according to method BIII. For purification the solvent was evaporated and the remaining solid was suspended in MeOH. After filtration the precipitate was washed with MeOH to provide the pure compound; yield: 86 %. ^{1}H NMR (500 MHz, $CDCl_3$) δ = 12.06 (br. s, 1 H, NH), 9.05 (d, J = 9.1 Hz, 1 H), 8.16–8.09 (m, 2 H), 7.96 (d, J = 2.5 Hz, 1 H), 7.81–7.74 (m, 2 H), 7.68–7.64 (m, 2 H), 7.51–7.48 (m, 3 H), 7.44–7.40 (m, 1 H), 4.02 (s, 3 H, OCH_3) ppm.
^{13}C NMR (125 MHz, $CDCl_3$) δ = 168.0, 165.5, 145.0, 143.4 (q, J_{CF} = 1.8 Hz), 140.7, 139.9, 133.1, 130.7, 129.0, 128.1, 127.9, 127.5, 127.2, 123.4, 122.0, 120.5 (q, J_{CF} = 257.5 Hz), 116.1, 52.9 (OCH_3) ppm.
LC/MS: m/z = 416 [M + H$^+$], 457 [M + H$^+$ CH_3CN], 831 [2M + H$^+$]; t_R = 16.64 min; 100.0 % pure (UV).

2-([1,1'-biphenyl]-4-ylcarboxamido)-5-(trifluoromethoxy)benzoic acid (29) was prepared according to method C. Sufficient purity was achieved without further purification; yield: 98 %. Mp: 245–246 °C. ^{1}H NMR (500 MHz, DMSO-d_6) δ = 12.17 (br. s, 1 H, NH), 8.81 (d, J = 9.1 Hz, 1 H), 8.06–8.03 (m, 2 H), 7.92 (dd, J = 3.0, 0.8 Hz, 1 H), 7.91–7.88 (m, 2 H), 7.78–7.74 (m, 2 H), 7.74–7.68 (m, 1 H), 7.53–7.49 (m, 2 H), 7.46–7.41 (m, 1 H) ppm.
^{13}C NMR (125 MHz, DMSO-d_6) δ = 168.6, 164.5, 143.9, 142.7 (q, J_{CF} = 1.8 Hz), 140.1, 138.8, 132.9, 129.1, 128.3, 127.8, 127.2, 127.0, 127.0, 123.3, 121.9, 118.6, 120.0 (q, J_{CF} = 256.0 Hz) ppm.
LC/MS: m/z = 402 [M + H$^+$], 803 [2M + H$^+$]; t_R = 14.58 min; 100.0 % pure (UV).

methyl 2-amino-5-methylbenzoate (30b) was prepared according to method A. Sufficient purity was achieved without further purification; yield: 82 %. ^{1}H NMR (500 MHz, $CDCl_3$) δ = 7.67 (d, J = 2.2 Hz, 1 H), 7.10 (dd, J = 8.2, 2.2 Hz, 1 H), 6.60 (d, J = 8.2 Hz, 1 H), 5.55 (br. s, 2 H, NH_2), 3.88 (s, 3 H, OCH_3), 2.24 (s, 3 H, CH_3) ppm.
^{13}C NMR (125 MHz, $CDCl_3$) δ = 168.6, 148.3, 135.2, 130.8, 125.4, 116.8, 110.7, 51.4 (OCH_3), 20.2 (CH_3) ppm.
LC/MS: m/z = no ionization; t_R = 8.48 min; 98.0 % pure (UV).

methyl 2-([1,1'-biphenyl]-4-ylcarboxamido)-5-methylbenzoate (30a) was prepared according to method BII. For purification the solvent was evaporated and the remaining solid was suspended in MeOH. After filtration the precipitate was washed with MeOH to provide the pure compound; yield: 85 %. ^{1}H NMR (500 MHz, $CDCl_3$) δ = 12.00 (br. s, 1 H, NH), 8.86 (d, J = 8.8 Hz, 1 H), 8.15–8.12 (m, 2 H), 7.91 (d, J = 2.2 Hz, 1 H), 7.77–7.75 (m, 2 H), 7.68–7.65 (m, 2 H), 7.51–7.47 (m, 2 H), 7.44 (dd, J = 8.8, 2.2 Hz, 1 H), 7.43–7.39 (m, 1 H), 3.98 (s, 3 H, OCH_3), 2.38 (s, 3 H, CH_3) ppm.
^{13}C NMR (125 MHz, $CDCl_3$) δ = 169.1, 165.2, 144.5, 140.1, 139.5, 135.6, 133.7, 132.1, 131.0, 128.9, 128.0, 127.9, 127.4, 127.2, 120.4, 115.0, 52.4 (OCH_3), 20.7 (CH_3) ppm.
LC/MS: m/z = 346 [M + H$^+$], 691 [2M + H$^+$]; t_R = 16.44 min; 99.1 % pure (UV).

2-([1,1'-biphenyl]-4-ylcarboxamido)-5-methylbenzoic acid (30) was prepared according to method C. Sufficient purity was achieved without further purification; yield: 95 %. Mp: 246–248 °C. ^{1}H NMR (500 MHz, DMSO-d_6) δ = 12.13 (br. s, 1 H, NH), 8.63 (d, J = 8.8 Hz, 1 H), 8.05–8.01 (m, 2 H), 7.90–7.86 (m, 3 H), 7.79–7.74 (m, 2 H), 7.53–7.47 (m, 3 H), 7.46–7.40 (m, 1 H), 2.33 (s, 3 H, CH_3) ppm.

^{13}C NMR (125 MHz, DMSO-d_6) δ = 170.1, 164.1, 143.6, 138.9, 138.8, 134.8, 133.3, 132.1, 131.3, 129.1, 128.3, 127.6, 127.1, 126.9, 119.9, 116.4, 20.2 (CH_3) ppm.
LC/MS: m/z = 332 [M + H^+], 663 [2M + H^+]; t_R = 13.78 min; 100.0 % pure (UV).

3-(3-phenoxybenzamido)-[1,1'-biphenyl]-4-carboxylic acid (31) was prepared according to method D. The product was purified by CC (*n*-hexane/EtOAc 8:2); yield: 91 %. Mp: 189–190 °C. ^{1}H NMR (500 MHz, DMSO-d_6) δ = 12.26 (br. s, 1 H, NH), 9.02 (d, *J* = 1.9 Hz, 1 H), 8.12 (d, *J* = 8.2 Hz, 1 H), 7.74–7.71 (m, 3 H), 7.62 (d, *J* = 7.9, 7.9 Hz, 1 H), 7.55–7.50 (m, 4 H), 7.47–7.42 (m, 3 H), 7.29 (ddd, *J* = 8.2, 2.5, 0.9 Hz, 1 H), 7.21 (tt, *J* = 7.4, 1.1 Hz, 1 H), 7.14–7.08 (m, 2 H) ppm.
^{13}C NMR (125 MHz, DMSO-d_6) δ = 169.9, 164.1, 157.4, 155.9, 145.7, 141.4, 138.9, 136.4, 131.9, 130.8, 130.3, 129.2, 128.6, 126.9, 124.1, 122.1, 121.5, 121.3, 119.2, 117.9, 116.8, 115.4 ppm.
LC/MS: m/z = 410 [M + H^+], 819 [2M + H^+]; t_R = 15.23 min; 99.1 % pure (UV).

4-(3-phenoxybenzamido)-[1,1'-biphenyl]-3-carboxylic acid (32) was prepared according to method D. The product was purified by preparative TLC (*n*-hexane/EtOAc 1:1 + 7 drops formic acid per 10 mL solvent) and washed with CH_2Cl_2; yield: 42 %. Mp: 207–208 °C. ^{1}H NMR (500 MHz, DMSO-d_6) δ = 12.20 (br. s, 1 H, NH), 8.75 (d, *J* = 8.8 Hz, 1 H), 8.29 (d, *J* = 2.5 Hz, 1 H), 7.98 (dd, *J* = 8.8, 2.5 Hz, 1 H), 7.78–7.72 (m, 1 H), 7.71–7.66 (m, 2 H), 7.61 (dd, *J* = 7.9, 7.9 Hz, 1 H), 7.57–7.53 (m, 1 H), 7.53–7.42 (m, 4 H), 7.41–7.34 (m, 1 H), 7.32–7.25 (m, 1 H), 7.24–7.17 (m, 1 H), 7.16–7.04 (m, 2 H) ppm.
^{13}C NMR (125 MHz, $CDCl_3$) δ = 169.9, 163.9, 157.3, 156.0, 140.1, 138.7, 136.4, 134.7, 132.3, 130.8, 130.3, 129.1, 128.9, 127.6, 126.4, 124.1, 122.1, 121.6, 120.6, 119.1, 117.3, 116.9 ppm.
LC/MS: m/z = 410 [M + H^+], 451 [M + H^+ CH_3CN], 819 [2M + H^+]; t_R = 14.61 min; 100.0 % pure (UV).

methyl 4-bromo-3-hydroxybenzoate (33f). To 3-hydroxybenzoate (1 equiv) in acetic acid was added bromine (1 equiv) dropwise. The reaction mixture was stirred at room temperature for 18 h, water was added and the mixture was extracted with EtOAc. The combined organic layers were washed with brine and dried over $MgSO_4$. The product was purified by CC (*n*-hexane/EtOAc 92.5:7.5) followed by crystallization from EtOAc/n-hexane (in fridge overnight); yield: 48 %. ^{1}H NMR (500 MHz, METHANOL-d_4) δ = 11.51 (br. s, 1 H, OH), 8.43 (d, *J* = 8.2 Hz, 1 H), 8.33 (d, *J* = 2.0 Hz, 1 H), 8.11 (dd, *J* = 8.2, 2.0 Hz, 1 H), 4.64 (s, 3 H, OCH_3) ppm.
^{13}C NMR (125 MHz, METHANOL-d_4) δ = 175.3, 163.9, 142.9, 139.7, 130.5, 126.0, 124.7, 61.9 (OCH_3) ppm.
LC/MS: m/z = no ionization; t_R = 9.28 min; 97.8 % pure (UV).

methyl 4-bromo-3-phenoxybenzoate (33e). A mixture of methyl 4-bromo-3-hydroxybenzoate (**33f**, 1 equiv), phenylboronic acid (2 equiv), copper acetate (1 equiv), triethylamine (5 equiv) and 3 Å molecular sieves in CH_2Cl_2 was stirred at room temperature for 72 h under a N_2 atmosphere. After filtration over celite the solvent was evaporated. Purification by CC (*n*-hexane/EtOAc 8:2) provided the pure compound; yield: 37 %. ^{1}H NMR (500 MHz, $CDCl_3$) δ = 7.72 (d, *J* = 8.2 Hz, 1 H), 7.68 (dd, *J* = 8.2, 1.9 Hz, 1 H), 7.59 (d, *J* = 1.9 Hz, 1 H), 7.39–7.36 (m, 2 H), 7.16 (tt, *J* = 7.4, 1.1 Hz, 1 H), 7.02–6.97 (m, 2 H), 3.87 (s, 3 H, OCH_3) ppm.
^{13}C NMR (125 MHz, Acetone-d_6) δ = 148.0, 138.6, 136.5, 116.2, 113.2, 112.1, 107.5, 106.2, 102.2, 102.0, 100.5, 33.8 (OCH_3) ppm.
LC/MS: m/z = no ionization; t_R = 13.54 min; 97.5 % pure (UV).

2-phenoxy-[1,1'-biphenyl]-4-carboxylic acid (33d) was prepared according to method D. The product was purified by CC (*n*-hexane/EtOAc 7:3); yield: 66 %. ^{1}H NMR (500 MHz, $CDCl_3$) δ = 7.94 (dd, *J* = 7.9, 1.6 Hz, 1 H), 7.72 (d, *J* = 1.6 Hz, 1 H), 7.63–7.56 (m, 3 H), 7.43–7.39 (m, 2 H), 7.38–7.35 (m, 1 H), 7.34–7.29 (m, 2 H), 7.09 (tt, *J* = 7.4, 1.1 Hz, 1 H), 7.00–6.94 (m, 2 H) ppm.
^{13}C NMR (125 MHz, $CDCl_3$) δ = 171.1, 157.1, 153.9, 139.0, 136.7, 131.4, 129.8, 129.6, 129.2, 128.3, 128.0, 125.5, 123.3, 121.2, 118.5 ppm.

LC/MS: m/z = no ionization; t_R = 12.33 min; 97.6 % pure (UV).

methyl 4-fluoro-2-(2-phenoxy-[1,1'-biphenyl]-4-ylcarboxamido)benzoate (33a) was prepared according to method BIII. The product was purified by CC (*n*-hexane/EtOAc 9:1); yield: 65 %. ^{1}H NMR (500 MHz, $CDCl_3$) δ = 12.19 (br. s, 1 H, NH), 8.72 (dd, *J* = 12.1, 2.6 Hz, 1 H), 8.09 (dd, *J* = 9.0, 6.5 Hz, 1 H), 7.84 (dd, *J* = 8.0, 1.9 Hz, 1 H), 7.70 (d, *J* = 1.9 Hz, 1 H), 7.67–7.60 (m, 3 H), 7.44–7.32 (m, 5 H), 7.11–7.08 (m, 1 H), 7.06–7.01 (m, 2 H), 6.81 (ddd, *J* = 9.0, 7.5, 2.6 Hz, 1 H), 3.94 (s, 3 H, OCH_3) ppm.
^{13}C NMR (125 MHz, $CDCl_3$) δ = 168.3, 166.4 (d, J_{CF} = 253.0 Hz), 164.9, 156.9, 154.5, 143.9 (d, J_{CF} = 13.7 Hz), 137.0, 136.8, 134.9, 133.2 (d, J_{CF} = 10.1 Hz), 131.7, 129.8, 129.2, 128.3, 127.9, 123.4, 122.0, 118.8, 118.8, 111.3 (d, J_{CF} = 2.7 Hz), 110.0 (d, J_{CF} = 22.0 Hz), 107.5 (d, J_{CF} = 28.4 Hz), 52.5 (OCH_3) ppm.
LC/MS: m/z = 442 [M + H^+], 483 [M + H^+ CH_3CN], 883 [2M + H^+]; t_R = 17.02 min; 89.0 % pure (UV).

4-fluoro-2-(2-phenoxy-[1,1'-biphenyl]-4-ylcarboxamido)benzoic acid (33) was prepared according to method C. For purification the remaining solid was washed with MeOH to provide the pure compound; yield: 77 %. Mp: 223–227 °C. ^{1}H NMR (500 MHz, DMSO-d_6) δ = 12.45 (br. s, 1 H, NH), 8.50 (dd, *J* = 12.1, 2.6 Hz, 1 H), 8.14–8.09 (m, 1 H), 7.84–7.80 (m, 1 H), 7.73 (d, *J* = 8.2 Hz, 1 H), 7.62–7.59 (m, 2 H), 7.52 (d, *J* = 1.9 Hz, 1 H), 7.46–7.42 (m, 2 H), 7.41–7.34 (m, 3 H), 7.12 (tt, *J* = 7.3, 1.2 Hz, 1 H), 7.07–7.03 (m, 1 H), 7.03–6.99 (m, 2 H) ppm.
^{13}C NMR (125 MHz, DMSO-d_6) δ = 169.4, 165.0 (d, *J* = 249.0 Hz), 163.9, 156.5, 153.5, 143.1 (d, *J* = 12.8 Hz), 136.7, 136.1, 134.7, 134.0 (d, J_{CF} = 11.0 Hz), 131.9, 130.2, 129.0, 128.4, 128.0, 123.5, 122.3, 118.5, 118.2, 113.0 (d, J_{CF} = 2.8 Hz), 110.1 (d, J_{CF} = 22.0 Hz), 106.4 (d, J_{CF} = 27.0 Hz) ppm.
LC/MS: m/z = 428 [M + H^+], 469 [M + H^+ CH_3CN], 855 [2M + H^+]; t_R = 15.13 min; 97.2 % pure (UV).

methyl 4-chloro-2-(2-phenoxy-[1,1'-biphenyl]-4-ylcarboxamido)benzoate (34a) was prepared according to method BIII. The product was purified by CC (*n*-hexane/EtOAc 9:1); yield: 22 %. ^{1}H NMR (500 MHz, $CDCl_3$) δ = 12.08 (br. s, 1 H, NH), 9.01 (d, *J* = 2.2 Hz, 1 H), 8.00 (d, *J* = 8.5 Hz, 1 H), 7.83 (dd, *J* = 7.9, 1.9 Hz, 1 H), 7.68 (d, *J* = 1.9 Hz, 1 H), 7.64–7.60 (m, 3 H), 7.44–7.40 (m, 2 H), 7.38–7.31 (m, 3 H), 7.11–7.07 (m, 2 H), 7.05–7.01 (m, 2 H), 3.95 (s, 3 H, OCH_3) ppm.
^{13}C NMR (125 MHz, $CDCl_3$) δ = 168.4, 164.9, 156.9, 154.6, 142.6, 141.2, 137.0, 136.8, 134.9, 132.0, 131.7, 129.9, 129.2, 128.3, 127.9, 123.4, 123.0, 121.9, 120.3, 118.9, 118.7, 113.3, 52.6 (OCH_3) ppm.
LC/MS: m/z = 458 and 460 [M + H^+], 915 and 917 [2M + H^+]; t_R = 17.56 min; 97.5 % pure (UV).

4-chloro-2-(2-phenoxy-[1,1'-biphenyl]-4-ylcarboxamido)benzoic acid (34) was prepared according to method C. For purification the remaining solid was washed with MeOH to provide the pure compound; yield: 92 %. Mp: 230–234 °C. ^{1}H NMR (500 MHz, DMSO-d_6) δ = 12.31 (br. s, 1 H, OCH_3), 8.75 (d, *J* = 2.2 Hz, 1 H), 8.04 (d, *J* = 8.5 Hz, 1 H), 7.82 (dd, *J* = 7.9, 1.9 Hz, 1 H), 7.73 (d, *J* = 7.9 Hz, 1 H), 7.63–7.59 (m, 2 H), 7.52 (d, *J* = 1.9 Hz, 1 H), 7.46–7.42 (m, 2 H), 7.40–7.34 (m, 3 H), 7.27 (dd, *J* = 8.5, 2.2 Hz, 1 H), 7.16–7.09 (m, 1 H), 7.03–6.99 (m, 2 H) ppm.
^{13}C NMR (125 MHz, DMSO-d_6) δ = 169.3, 163.8, 156.5, 153.5, 141.9, 138.6, 136.7, 136.1, 134.7, 132.9, 131.9, 130.2, 129.0, 128.4, 128.0, 123.5, 123.0, 122.4, 119.3, 118.5, 118.2, 115.4 ppm.
LC/MS: m/z = 444 [M + H^+], 485 [M + H^+ CH_3CN], 887 [2M + H^+]; t_R = 15.37 min; 97.3 % pure (UV).

6.1.3 Computational Chemistry

Pharmacophore modelling and virtual screening. The following compounds **I**–**VII** were retrieved from literature[1,6–9]:

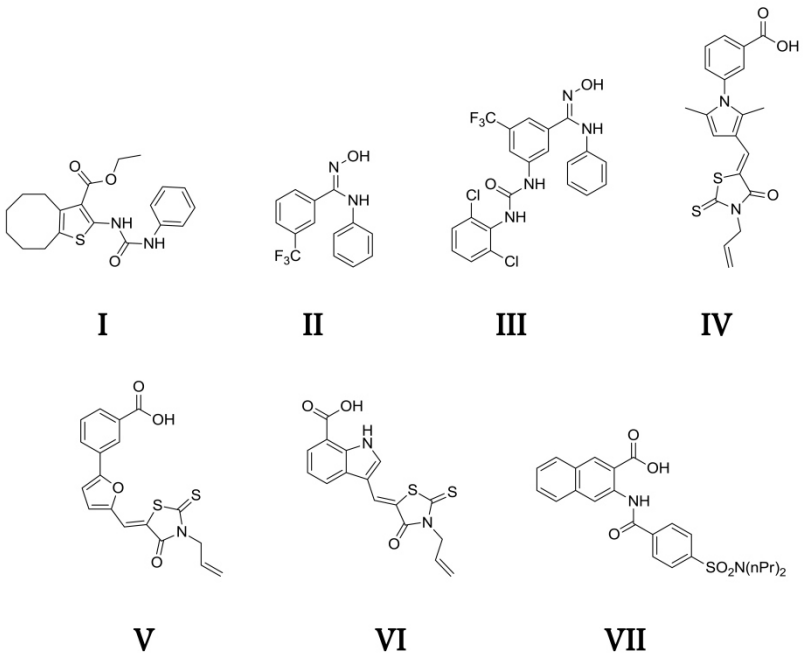

Figure S1. Compounds used for the flexible alignment

I: Published by Arhin et al.[6] ("compound 1") as inhibitor of *S. aureus* RNAP. It was shown that these compounds do not bind to the Rifamycin binding site, but the exact mode of action is not known.
II and **III**: Published by Artsimovitch et al.[7] ("CBR703 and CBR9379") as inhibitors of *E. coli* RNAP. They bind to a surface exposed groove at the junction of the β'-bridge helix and the β-subunit.
IV, **V** and **VI**: Published by André et al.[8] ("SB8 and SB2") and Villain-Guillot[9] ("compound 11b") as inhibitors of *E. coli* RNAP. The mode of action of these compounds is the prevention of the protein-protein interaction between σ^{70} and the RNAP core enzyme.
VII: Published by Larsen et al.[1] ("compound 1") as inhibitor of transcription/ translation in *S. aureus*. Resynthesis and testing in our *E. coli* RNAP *in vitro* inhibition assay revealed **VII** as a potent inhibitor of *E. coli* RNAP (IC_{50} 42 µM).

Compounds **I**–**VII** (Fig. S1) were aligned using the flexible alignment module of MOE (*Molecular Operating Environment*)[10] with the stochastic search option turned on. We modified the default flexible alignment settings; the Aromaticity and CO_2-type centroid weights were set at 2 – strikingly these two chemical moieties are present in most of the initial seven template compounds. Weights on volume and acceptor/donor projection features were switched on. Further, we set the configuration limit to 100 and conjugate gradient minimization steps to 1000. The alignment with the best similarity score was retained and refined within MOE.

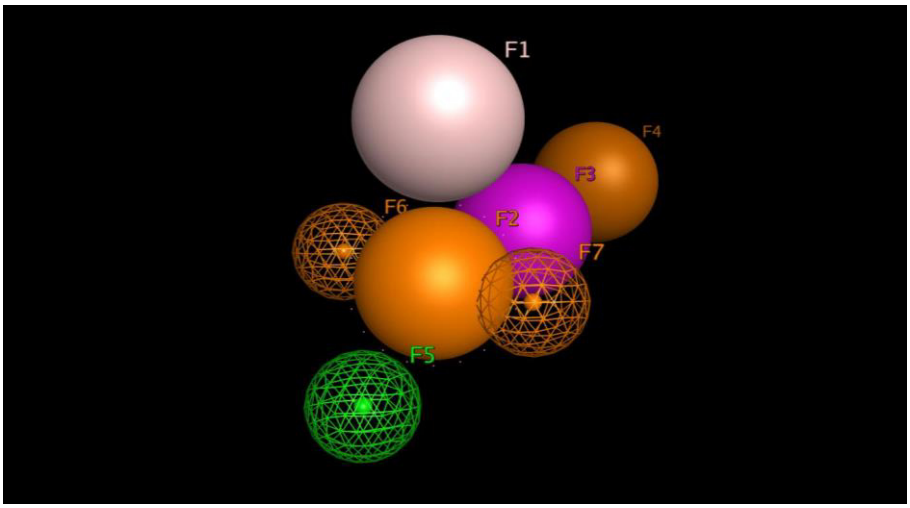

Figure S2. Final pharmacophore model used for virtual screening

This alignment was used to identify common features within the seven superimposed ligands via the Pharmacophore Consensus utility (tolerance of 1.2 and threshold value of 50% (ligands that match one feature)). The resulting pharmacophore model (consisting of 9 features) was manually refined and reduced to 7 features with 6 needed partial matches. The final pharmacophore model (Fig. S2) consisted of following features (F1-F4 - feature radius of 1.5 Å, F5-F7 - feature radius of 1 Å):

Feature F1 (rose): O2|Ani|N[O,o]|(O(C=O)C (this includes CO_2-like centroids (both acids and ester), anionic atoms as well as N.sp^2-O moieties (i.e. oximes, nitro)

Feature F2 (orange): Aro (all aromatic systems)

Feature F3 (violet): HBD/HBA/Aro (this feature can be matched by either a hydrogen-bond donor or acceptor or by an aromatic system)

Feature F4: Aro/Hyd/pi (in this position aromatic, hydrophobic or planar-conjugated pi systems are requested)

Feature F5 (green): Hydrophobic

Features F6+F7 (hatched orange): Aromatic ring projections

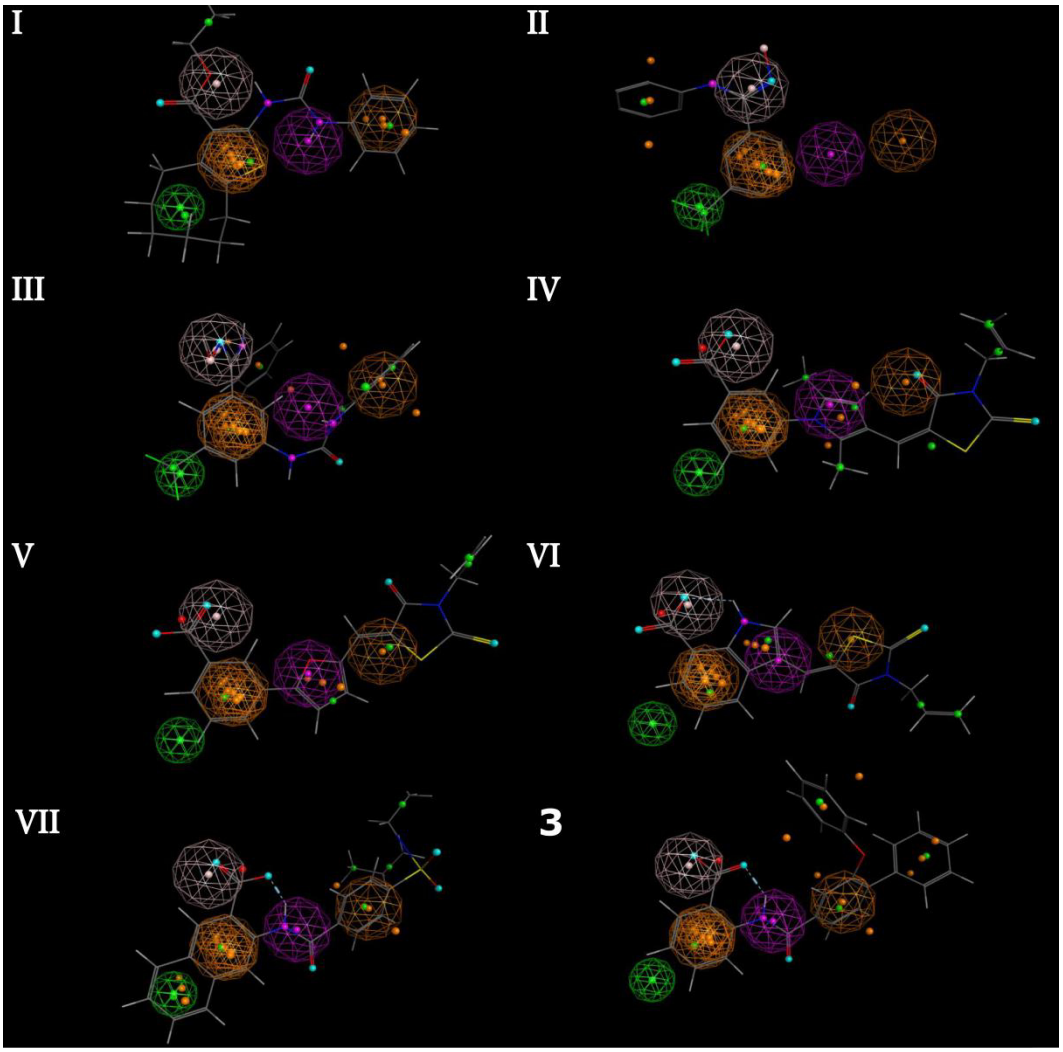

Figure S3. Overlay of the resulting pharmacophore model with inhibitors **I**–**VII** and **3**

A virtual library was built including approximately 2000 synthetic *in-house* compounds that had been developed as aromatase, CYP17, CYP11B1, CYP11B2, thromboxane A2, 5α reductase, 17β HSD1, 17β HSD2, FabH and PqsD inhibitors. For each compound a conformational search was performed using the default parameters of the conformational search module of MOE2010. Conformers were energy minimized using MMFF94xs forcefield and the Generalized Born implicit solvent model. The obtained multiple-conformer database was now used in the pharmacophore search.

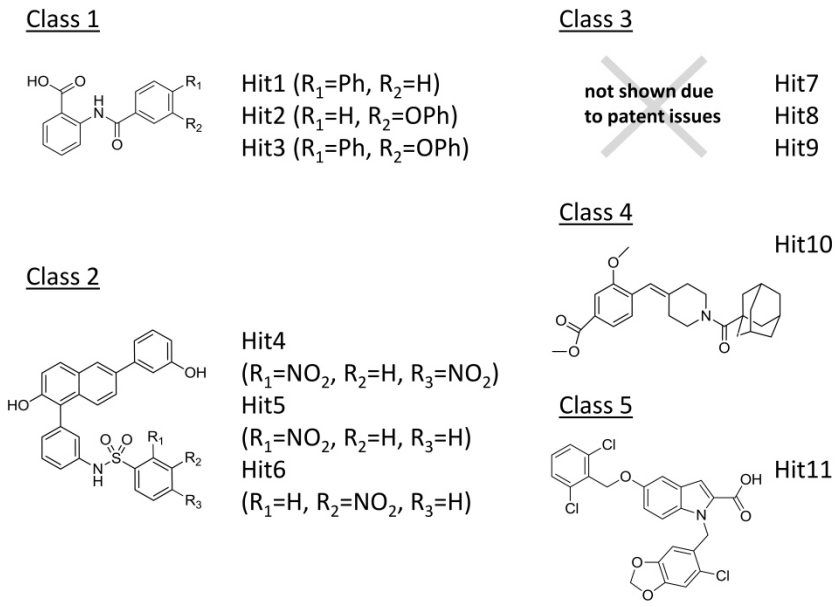

Figure S4. Experimentally validated virtual hit compounds

In total 64 hits were found matching at least the four core features and the two aromatic projections, while the presence of the accessory feature was not mandatory. All hit compounds were tested on inhibitory potency, for eleven of them (comprising five different structural classes) an inhibition >20% was measured at 200 µM (Fig. S4).

Based on the activities of **1**–**4**, the seven-feature pharmacophore model (Fig. S2) was extended by two additional features (F8 and F9):

Features F8+F9 (hatched yellow): Aro/Hyd (feature radius of 1.5 Å)

Using this model (Fig. S5) in further screenings, a compound will be defined as a hit if, beside the 4 core features, at least one of the new accessory features is present.

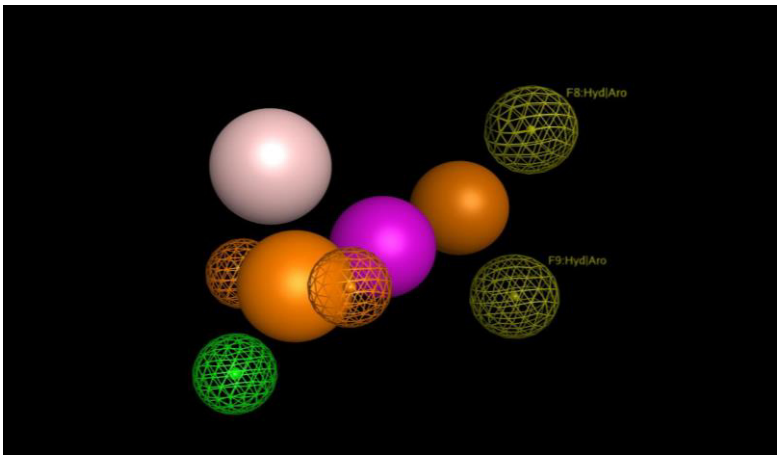

Figure S5. Extended pharmacophore model

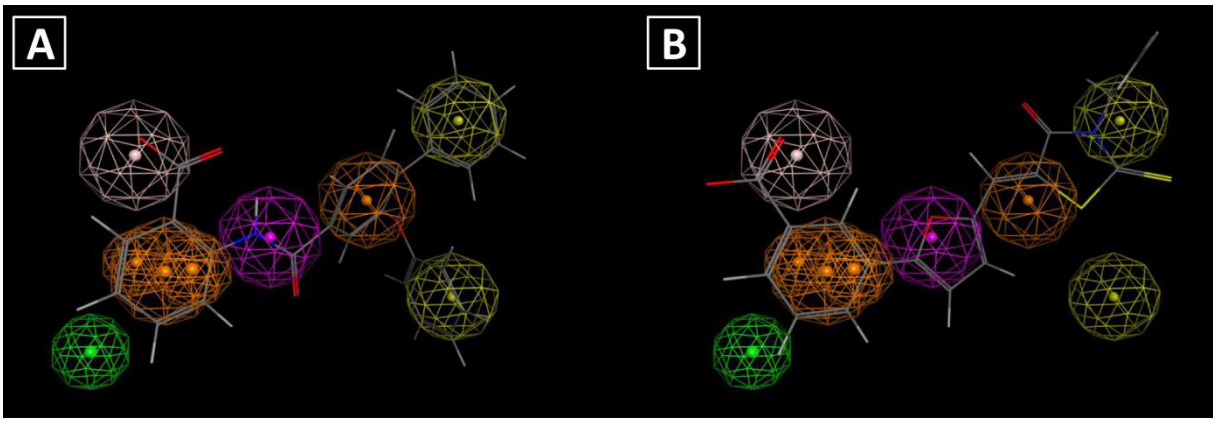

Figure S6. Overlay of the extended pharmacophore model with
A) most potent hit compound **3**
B) described inhibitor **V**

6.1.4 References

(1) Larsen, S. D.; Hester, M. R.; Craig Ruble, J.; Kamilar, G. M.; Romero, D. L.; Wakefield, B.; Melchior, E. P.; Sweeney, M. T.; Marotti, K. R. Discovery and initial development of a novel class of antibacterials: Inhibitors of Staphylococcus aureus transcription/translation. *Bioorg. Med. Chem. Lett.* 2006, *16*, 6173–6177.

(2) Heikkilä, T.; Thirumalairajan, S.; Davies, M.; Parsons, M. R.; McConkey, A. G.; Fishwick, C. W. G.; Johnson, A. P. The first de novo designed inhibitors of Plasmodium falciparum dihydroorotate dehydrogenase. *Bioorg. Med. Chem. Lett.* 2006, *16*, 88–92.

(3) Nie, Z.; Perretta, C.; Lu, J.; Su, Y.; Margosiak, S.; Gajiwala, K. S.; Cortez, J.; Nikulin, V.; Yager, K. M.; Appelt, K.; Chu, S. Structure-based design, synthesis, and study of potent inhibitors of ß-ketoacyl-acyl carrier protein synthase III as potential antimicrobial agents. *J. Med. Chem.* 2005, *48*, 1596–1609.

(4) Meyer, H. The linking of aromatic amino acids. *Liebigs Ann. Chem.* 1907, *351*, 267–282.

(5) Thorarensen, A.; Ruble, C. J.; Romero, D. L. Preparation of aminoarylbenzoic acid derivatives as antibacterial agents for use as disinfectants and therapeutic agents. *PCT Int. Appl. (2004), WO 2004018414 A2 20040304.* 2004.

(6) Arhin, F.; Bélanger, O.; Ciblat, S.; Dehbi, M.; Delorme, D.; Dietrich, E.; Dixit, D.; Lafontaine, Y.; Lehoux, D.; Liu, J.; McKay, G. A.; Moeck, G.; Reddy, R.; Rose, Y.; Srikumar, R.; Tanaka, K. S. E.; Williams, D. M.; Gros, P.; Pelletier, J.; Parr Jr, T. R.; Far, A. R. A new class of small molecule RNA polymerase inhibitors with activity against rifampicin-resistant Staphylococcus aureus. *Bioorgan. Med. Chem.* 2006, *14*, 5812–5832.

(7) Artsimovitch, I.; Chu, C.; Lynch, A. S.; Landick, R. A New class of bacterial RNA polymerase inhibitor affects nucleotide addition. *Science* 2003, *302*, 650–654.

(8) André, E.; Bastide, L.; Michaux-Charachon, S.; Gouby, A.; Villain-Guillot, P.; Latouche, J.; Bouchet, A.; Gualtiéri, M.; Leonetti, J.-P. Novel synthetic molecules targeting the bacterial RNA polymerase assembly. *J. Antimicrob. Chemoth.* 2006, *57*, 245–251.

(9) Villain-Guillot, P.; Gualtieri, M.; Bastide, L.; Roquet, F. O.; Martinez, J.; Amblard, M.; Pugniere, M.; Leonetti, J.-P. Structure-activity relationships of phenyl-furanyl-rhodanines as inhibitors of RNA polymerase with antibacterial activity on biofilms. *J. Med. Chem.* 2007, *50*, 4195–4204.

(10) *Molecular Operating Environment*, 2010.10; Chemical Computing Group Inc., 1010 Sherbooke St. West, Suite #910, Montreal, QC, Canada, H3A 2R7, 2010.

6.2 Supporting Information for Publication II

Full supporting information is available online:
http://www.future-science.com/doi/suppl/10.4155/fmc.14.105

6.3 Supporting Information for Publication III

Full supporting information is available online:
http://www.sciencedirect.com/science/MiamiMultiMediaURL/1-s2.0-S0223523414001342/1-s2.0-S0223523414001342-mmc1.docx/271932/FULL/S0223523414001342/c59ab0eabb97965487b6b7f58683ce1b/mmc1.docx

Table S1. RNAP and PqsD inhibition values for 51–86

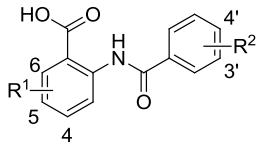

51–73, 78–86

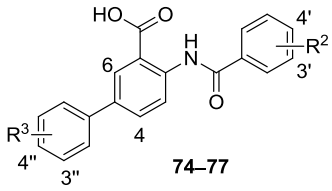

74–77

Cmpd	*(Cmpd no. of Weidel et al.[a])*	R^1	R^2	R^3	PqsD inhibition[b,c]	RNAP inhibition[d]
51	***(2)***	H	3'-SO_2NEt_2	–	19.8 µM	n.i.
52	***(9)***	H	4'-SO_2NEt_2	–	44%	n.i.
53	***(34)***	H	4'-Br, 3'-SO_2NEt_2	–	6.9 µM	n.i.
54	***(35)***	H	4'-Me, 3'-SO_2NEt_2	–	27.3 µM	n.i.
55	***(36)***	H	4'-Et, 3'-SO_2NEt_2	–	39%	n.i.
56	***(37)***	4-Cl	3'-SO_2NEt_2	–	9.4 µM	n.i. @ 100 µM
57	***(38)***	4-F	3'-SO_2NEt_2	–	8.0 µM	n.i.
58	***(39)***	4-NO_2	3'-SO_2NEt_2	–	6.3 µM	n.i.
59	***(40)***	5-Me	3'-SO_2NEt_2	–	18.4 µM	n.i.
60	***(41)***	5-CF_3	3'-SO_2NEt_2	–	12.4 µM	n.i. @ 50 µM
61	***(42)***	5-F	3'-SO_2NEt_2	–	11.4 µM	n.i. @ 100 µM
62	***(43)***	5-Br	3'-SO_2NEt_2	–	9.9 µM	n.i. @ 50 µM
63	***(44)***	5-CN	3'-SO_2NEt_2	–	26.2 µM	n.i.
64	***(45)***	5-NO_2	3'-SO_2NEt_2	–	8.9 µM	30% @ 100 µM
65	***(10)***	5-Br	4'-SO_2NEt_2	–	13.0 µM	28 %

Cmpd	*(Cmpd no. of Weidel et al.[a])*	R^1	R^2	R^3	PqsD inhibition[b,c]	RNAP inhibition[d]
66	***(14)***	5-Br	3'-$C(O)NEt_2$	–	25.5 µM	n.i.
67	***(46)***	5-F	4'-Br, 3'-SO_2NEt_2	–	6.6 µM	n.i. @ 100 µM
68	***(47)***	5-Br	4'-Br, 3'-SO_2NEt_2	–	3.8 µM	n.i. @ 50 µM
69	***(48)***	5-Ph	3'-SO_2NEt_2	–	3.0 µM	n.i. @ 100 µM
70	***(49)***	6-OMe	3'-SO_2NEt_2	–	44%	n.i.
71	***(50)***	6-Cl	3'-SO_2NEt_2	–	39.0 µM	n.i.
72	***(51)***	6-F	3'-SO_2NEt_2	–	24.9 µM	n.i.
73	***(52)***	6-OH	3'-SO_2NEt_2	–	1.2 µM	n.i.
74	***(53)***	–	3'-SO_2NEt_2	3''-$C(O)NH_2$	3.8 µM	45%
75	***(54)***	–	3'-SO_2NEt_2	4''-$C(O)NH_2$	1.9 µM	78 µM
76	***(55)***	–	3'-SO_2NEt_2	3''-CO_2H	1.5 µM	24%
77	***(56)***	–	3'-SO_2NEt_2	4''-CO_2H	2.7 µM	23% @ 50 µM
78	***(57)***	H	3'-SO_2NH_2	–	43.6 µM	n.i.
79	***(58)***	H	3'-SO_2NMe_2	–	35%	n.i.
80	***(59)***	H	3'-$SO_2N(n\text{-}Pr)_2$	–	5.4 µM	n.i.
81	***(13)***	H	3'-$CONEt_2$	–	n.i.	n.i.
82	***(60)***	H	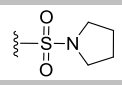	–	47%	n.i.
83	***(61)***	H	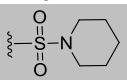	–	14.4 µM	n.i.
84	***(62)***	H	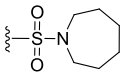	–	14.8 µM	n.i.
85	***(63)***	H	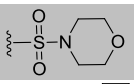	–	16%	n.i.
86	***(64)***	H	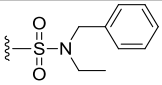	–	16.5 µM	29%

[a] Weidel, E.; de Jong, J.C.; Brengel, C.; Storz, M.P.; Braunshausen, A.; Negri, M.; Plaza, A.; Steinbach, A.; Müller, R.; Hartmann, R.W. Structure optimization of 2-benzamidobenzoic acids as PqsD inhibitors for *Pseudomonas aeruginosa* infections and elucidation of binding mode by SPR, STD NMR, and molecular docking. *J. Med. Chem.* **2013**, *56*, 6146–6155.
[b] IC_{50} value (SD <25%, except for **63** (40%)) or percentage inhibition at 50 µM (SD <40%); Data represent the mean values of at least three experiments.
[c] PqsD inhibition values originally published by Weidel et al.[1]
[d] IC_{50} value (SD <20%) or percentage inhibition at 200 µM (SD <40%) for *E. coli* RNAP; Data represent the mean values of at least two experiments.
n.i.: no inhibition

7. Appendix

7.1 Publications

Hinsberger, S.; de Jong, J.; Groh, M.; Haupenthal, J.; Hartmann, R.W. Benzamidobenzoic acids as potent PqsD inhibitors for the treatment of *Pseudomonas aeruginosa* infections. *Eur. J. Med. Chem.* **2014**, *76*, 343–351.

Hüsecken, K.; Hinsberger, S.; Elgaher, W.A.M.; Haupenthal, J.; Hartmann, R.W. Surface plasmon resonance – more than a screening technology: Insights in the binding mode of σ^{70}:core RNAP inhibitors. *Future Med. Chem.* **2014**, *6*, 1551–1565.

Fruth, M.; Plaza, A.; Hinsberger, S.; Sahner, J.H.; Haupenthal, J.; Bischoff, M.; Jansen, R.; Müller, R.; Hartmann, R.W. Binding mode characterization of novel RNA polymerase inhibitors using a combined biochemical and NMR approach. *ACS Chem. Biol.* **2014**, *9*, 2656–2663.

Weidel, E.; Negri, M.; Empting, M.; Hinsberger, S.; Hartmann, R.W. Composing compound libraries for hit discovery – Rationality-driven preselection or random choice aiming at structural diversity? *Future Med. Chem.* **2014** accepted.

Hinsberger, S.; Hüsecken, K.; Groh, M.; Negri, M.; Haupenthal, J.; Hartmann, R.W. Discovery of novel bacterial RNA polymerase inhibitors: Pharmacophore-based virtual screening and hit optimization. *J. Med. Chem.* **2013**, *56*, 8332–8338.

Wetzel, M.; Gargano, E.M.; Hinsberger, S.; Marchais-Oberwinkler, S.; Hartmann, R.W. Discovery of a new class of bicyclic substituted hydroxyphenylmethanones as 17β-hydroxysteroid dehydrogenase type 2 (17β-HSD2) inhibitors for the treatment of osteoporosis. *Eur. J. Med. Chem.* **2012**, *47*, 1–17.

Oster, A.; Hinsberger, S.; Werth, R.; Marchais-Oberwinkler, S.; Frotscher, M.; Hartmann, R.W. Bicyclic substituted hydroxyphenylmethanones as novel inhibitors of 17β-hydroxysteroid dehydrogenase type 1 (17β-HSD1) for the treatment of estrogen-dependent diseases. *J. Med. Chem.* **2010**, *53*, 8176–8186.

7.2 Conference contributions

Hinsberger, S.; Hüsecken, K.; Groh, M.; Negri, M.; Haupenthal, J.; Hartmann, R.W. Discovery of novel bacterial RNA polymerase inhibitors: Pharmacophore-based virtual screening and hit optimization. *4th International HIPS-Symposium* June **2014** Saarbrücken, Germany.

Hinsberger, S.; Hüsecken, K.; Groh, M.; Negri, M.; Haupenthal, J.; Hartmann, R.W. Discovery of novel bacterial RNA polymerase inhibitors: Pharmacophore-based virtual screening and hit optimization. *Discovery Chemistry Congress* February **2014** Barcelona, Spain.

Hinsberger, S.; Hüsecken, K.; Groh, M.; Negri, M.; Haupenthal, J.; Hartmann, R.W. Discovery of novel bacterial RNA polymerase inhibitors: Pharmacophore-based virtual screening and hit optimization. *Novel Agents against Infectious Diseases - An Interdisciplinary Approach* November **2013** Würzburg, Germany.

Hinsberger, S.; Negri, M.; Groh, M.; Haupenthal, J.; Hartmann, R.W. Development of new, potent bacterial RNA polymerase inhibitors with anthranilate core. *6th Summer School Medicinal Chemistry* September **2012** Regensburg, Germany.

Hinsberger, S.; Negri, M.; Groh, M.; Haupenthal, J.; Fruth, M.; Hartmann, R.W. Development of new, potent bacterial RNA polymerase inhibitors with anthranilate core. *2nd International HIPS-Symposium* June **2012** Saarbrücken, Germany.

Negri, M.; Haupenthal, J.; Hinsberger, S.; Zhu, W.; de Jong, J.; Hartmann R.W. Development of inhibitors of bacterial RNA polymerase with novel modes of action. *1st International HIPS-Symposium* June **2011** Saarbrücken, Germany.